AD NUMBER
AD392716
CLASSIFICATION CHANGES
TO: **UNCLASSIFIED**
FROM: **CONFIDENTIAL**
LIMITATION CHANGES
TO: **Approved for public release; distribution is unlimited.**
FROM: **Distribution authorized to U.S. Gov't. agencies and their contractors; Administrative/Operational Use; JUN 1968. Other requests shall be referred to Air Force Rocket Propulsion Lab., Edwards AFB, CA.**
AUTHORITY
30 Jun 1980, DoDD 5200.10 ; AFRPL ltr 16 Mar 1982

SECURITY MARKING

The classified or limited status of this report applies to each page, unless otherwise marked.
Separate page printouts MUST be marked accordingly.

THIS DOCUMENT CONTAINS INFORMATION AFFECTING THE NATIONAL DEFENSE OF THE UNITED STATES WITHIN THE MEANING OF THE ESPIONAGE LAWS, TITLE 18, U.S.C., SECTIONS 793 AND 794. THE TRANSMISSION OR THE REVELATION OF ITS CONTENTS IN ANY MANNER TO AN UNAUTHORIZED PERSON IS PROHIBITED BY LAW.

NOTICE: When government or other drawings, specifications or other data are used for any purpose other than in connection with a definitely related government procurement operation, the U. S. Government thereby incurs no responsibility, nor any obligation whatsoever; and the fact that the Government may have formulated, furnished, or in any way supplied the said drawings, specifications, or other data is not to be regarded by implication or otherwise as in any manner licensing the holder or any other person or corporation, or conveying any rights or permission to manufacture, use or sell any patented invention that may in any way be related thereto.

AFRPL-TR-68-98

(Unclassified Title)
SECONDARY COMBUSTION OF PENTABORANE-HYDRAZINE EXHAUST IN AIR

TECHNICAL REPORT AFRPL-TR-68-98

June 1968

S. D. Rosenberg, R. E. Yates, and R. C. Adrian
Aerojet-General Corporation

AIR FORCE ROCKET PROPULSION LABORATORY
Research and Technology Division
Air Force Systems Command
United States Air Force
Edwards, California

(1134)

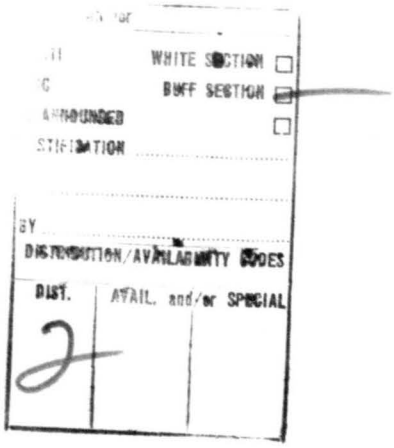

NOTICES

When US Government drawings, specifications, or other data are used for any purpose other than a definitely related government procurement operation, the government thereby incurs no responsibility nor any obligation whatsoever; and the fact that the government may have formulated, furnished, or in any way supplied the said drawings, specifications, or other data is not to be regarded by implication or otherwise, as in any manner licensing the holder or any other person or corporation, or conveying any rights or permission to manufacture, use, or sell any patented invention that may in any way be related thereto.

Do not return this copy when not needed. Destroy in accordance with pertinent security regulations.

Qualified users may obtain copies of this report from the Defense Documentation Center (DDC), (formerly ASTIA), Cameron Station, Bldg. 5, 5010 Duke Street, Alexandria, Virginia 22314.

(18) AFRPL (19) TR-68-98

CONFIDENTIAL

(6) (Unclassified Title)

SECONDARY COMBUSTION OF PENTABORANE-HYDRAZINE EXHAUST IN AIR (U). (8)

TECHNICAL REPORT AFRPL-TR-68-98

(11) Jun[redacted]68 (12) 111 p.

(9) Final rept. 1 May 67 - 30 Apr 68,

(10) Sanders D. /Rosenberg, Robert E. /Yates, [redacted] Robert C. /Adrian
Aerojet-General Corporation

(15) F04611-67-C-0106

(14) AGC-1134-81-F

AIR FORCE ROCKET PROPULSION LABORATORY
Research and Technology Division
Air Force Systems Command
United States Air Force
Edwards, California

1473

(403 364)

CONFIDENTIAL

FOREWORD

This Final Report (Aerojet Report No. 1134-81-F), covering the period from 1 May 1967 through 30 April 1968, is submitted in partial fulfillment of Contract F04611-67-C-0106.

This investigation was conducted by the Fuels and Combustion Research Section of Advanced Propulsion Research, Research and Technology Department, Aerojet-General Corporation, Sacramento, California. The Air Force monitor for the program is A. McPeak, Lt., AFRPL/RPCL.

The work described herein was performed by S. D. Rosenberg, R. E. Yates and R. C. Adrian. This report was written by the program staff, and was submitted 28 June 1968.

This report contains no classified information extracted from other classified documents.

This technical report has been reviewed and approved.

William H. Ebelke, Colonel, USAF
Chief, Propellant Division
Air Force Rocket Propulsion Laboratory

CONFIDENTIAL ABSTRACT

(U) The determination of c* performance of the air-augmented hydrazine/pentaborane system was conducted in a permanent micromotor test facility. The newly-constructed facility employs electrically-heated, clean secondary air and includes equipment for collection of solid and gaseous secondary exhaust products.

(C) The c* performance of the air-augmentation stage was determined in two flight simulation regimes. In the sea level/Mach 2.5 regime (200 psia chamber pressure/800°F air-temperature), the c* performance efficiencies were 96-99% of theoretical at air-to-propellant ratios of 8:1, 16:1, and 50:1. Chemical analysis indicated complete combustion of all primary exhaust products, including boron nitride and elemental boron. In the 40,000 ft/Mach 4.0 regime (50 psia chamber pressure/1500°F air-temperature), the c* performance was 91-92% of theoretical at air-to-propellant ratios of 8:1 and 16:1. Chemical analysis indicated high boron nitride combustion efficiency but very low elemental boron combustion efficiency. Low chamber pressure and low residence time were concluded to be major contributing factors to the low elemental boron combustion efficiency and reduced c* performance efficiency. A high water concentration in the secondary chamber, resulting from secondary hydrogen combustion, appears to contribute significantly to the high combustion efficiency of the boron and boron nitride. In addition, chamber pressures in excess of 50-75 psia appear to be required to ensure efficient elemental boron combustion.

(C) A model describing the secondary combustion process has been developed. The model reflects the importance of water vapor and high chamber pressure in promoting high combustion efficiency and high performance efficiency of boron-containing propellants.

TABLE OF CONTENTS

TABLE OF CONTENTS (cont.)

TABLE OF CONTENTS (cont.)

TABLE OF CONTENTS (cont.)

TABLE OF CONTENTS (cont.)

SECTION I

INTRODUCTION

(U) Air-augmented rockets offer significant improvement in specific impulse over conventional rockets. The improvement is realized through two important mechanisms: First, by addition of the air mass to the exhaust stream and, second, by achieving additional combustion of the primary rocket exhaust when the primary rocket is operated in an under-oxidized condition. Therefore, primary propellant systems which produce exhaust products that may be oxidized further in air are attractive for air-augmentation applications.

(U) The pentaborane/hydrazine propellant system is especially attractive in that the exhaust of this system consists chiefly of hydrogen, boron nitride, and boron. If significant combustion of these exhaust products can be achieved in air, a system of exceptional performance may be realized.

(U) The objective of this program was to establish the combustion characteristics in air of the exhaust products of the pentaborane/hydrazine system. A study of the combustion was conducted using a specially designed liquid micromotor. The test variables which were investigated included the following:

1. Temperature and pressure of the secondary air, simulating both low altitude/moderate Mach number, 2.5, and high altitude/high Mach number, 4.0.

2. Air-to-propellant-weight flow ratios in the range 8:1 to 50:1.

3. Primary propellant mixture ratio (N_2H_4/B_5H_9) of 1.27.

4. Composition of secondary air, i.e., air or nitrogen.

(U) Test measurements which were required included the following:

1. Propellant and air flow rates.

2. Air inlet temperature and pressure.

3. Primary and secondary chamber pressures.

4. The extent of conversion of the boron nitride and boron to boron oxides, by collection and analysis of the exhaust products.

Characteristic velocity and chamber temperature were calculated based on these test measurements and a combustion model has been developed to describe the secondary combustion phenomena.

SECTION II

SUMMARY

(U) The technical effort on this program was divided into three phases. The work performed and the results and their significance are summarized below, as are recommendations for future work.

1. PHASE I, DESIGN, FABRICATION AND INSTALLATION OF MICROMOTOR TEST FACILITIES

a. Design Requirements and Test Site Preparation

(U) A permanent air-augmentation facility was designed and installed in the Research Physics Laboratory of the Propulsion Division. Several equipment additions and modifications were made to provide the necessary services for the establishment of the micromotor facilities and for the execution of the experimental program.

(U) An air-handling system was designed and installed to provide electrically-heated air for the experimental study. These facilities consisted of an air compressor, storage tank, and an air-heater, employing a 425 KW power supply. Propellant storage tanks and cooling-water supply tanks were also installed.

b. The Liquid Micromotor

(U) The various components of the liquid micromotor were designed, fabricated and installed in the test area. These components included the primary bipropellant and igniter injectors, the water-cooled primary combustion chamber, the secondary air-injector, and the water-cooled secondary combustion chamber and replaceable nozzles. A second water-cooled secondary combustion chamber with provision for the installation of thermocouples was fabricated.

c. Exhaust Handling and Sampling System

(U) A water-cooled duct was installed to conduct the exhaust products from the exit of the secondary nozzle to a bag filter for separation and collection of the solid exhaust products. In addition, Pitot-type sampling assemblies were installed in the exhaust duct to permit acquisition of auxillary samples of both solid and gaseous exhaust products for chemical analysis.

d. System Calibration and Preliminary Tests

(U) Critical instrumentation was calibrated prior to and during the test program. These calibrations were required to assure the accurate measurement of the test variables. Preliminary tests were conducted to develop operating procedures and to establish precise control of test variables.

2. PHASE II, DETERMINATION OF COMBUSTION CHARACTERISTICS IN AIR OF THE EXHAUST PRODUCTS OF THE HYDRAZINE/PENTABORANE SYSTEM

a. Performance of the Hydrazine/Pentaborane Bipropellant System

(C) The test apparatus was designed to permit the simultaneous study of the performance of the primary bipropellant system and the air-augmented propellant system. A total of 17 tests was made in this portion of the study. The data showed that, under the test conditions, c* performance efficiencies of about 85% of theoretical were realized. These results, consistent with similar studies of the bipropellant system, indicated that the primary combustion process is kinetically limited through the incomplete conversion of the available boron to boron nitride. Thermal decomposition of pentaborane and monopropellant decomposition of hydrazine also decreased the combustion efficiency significantly.

(U) The performance efficiencies determined from measurements in the primary combustion chamber were verified in the secondary performance efficiencies determined from tests wherein nitrogen was used as the augmenting gas. The excellent agreement of these results attest the ability of the test equipment to yield reliable data and the reliability of all of the performance data.

b. Performance of the Secondary Combustion of the Hydrazine/Pentaborane Exhaust

(C) Tests were conducted under conditions which simulated two flight regions: (1) Mach 2.5 at sea level, using 800°F inlet air at 200 psia chamber pressure; and (2) Mach 4.0 at 40,000 ft, using 1500°F inlet air at 50 psia chamber pressure. Characteristic velocity, c*, efficiencies of 96-99% prevailed in the tests simulating sea level/Mach 2.5. Although air-to-propellant ratios of 8:1, 16:1 and 50:1 were employed in these tests, no significant change in c* efficiency was observed; c* efficiencies of about 85% were obtained in corresponding nitrogen tests. These results indicated that very nearly complete combustion of all exhaust products, including the solid boron and boron nitride, occurred in the secondary combustion chamber Furthermore, the severe reduction in chamber temperature resulting from high air flow rates did not adversely affect the combustion efficiency significantly.

(C) The c* efficiencies obtained in the tests simulating 40,000 ft/Mach 4.0 flight were somewhat lower, i.e., 91-92%. No noticeable change in c* efficiency was observed to result from changing air-to-propellant ratio from 8:1 to 16:1. The c* efficiency for the corresponding nitrogen run was 86%. The lower performance efficiencies obtained in these tests indicated poor combustion efficiency of one or more of the solid components of the hydrazine-pentaborane exhaust.

c. Chemical Analysis of Exhaust Products

(U) Samples of both solid and gaseous products of the secondary combustion were collected in several tests. The tests selected were representative of all three levels of air-to-propellant ratios in both flight simulation regimes. Chemical analyses were conducted according to a procedure which was developed specifically for these types of samples.

(C) The chemical analyses of the solid exhaust products in the 200 psia/800°F air tests showed only very small amounts of boron and boron nitride to be present. In tests at air-to-propellant ratios of 8:1 and 16:1, 96-99% of the available boron (B and BN) in the primary exhaust was burned in air. However, in the 50:1 air-to-propellant ratio test, only 80% of the available boron was burned.

(C) Analyses of the solid products from the 50 psia/1500°F-air tests showed a high elemental boron content and extremely low boron nitride content. At air-to-propellant ratios of 8:1 and 16:1, in the low chamber pressure regime, only about 55% of the available boron was burned.

(C) These analytical data indicated that high performance efficiencies were obtained in the high pressure regime because of complete combustion of the available hydrogen, boron, and boron nitride. In the low pressure regime, the performance of the secondary combustion system suffers from the inhibition of elemental boron combustion.

(C) The results of the chemical analyses indicate that the overall combustion efficiency and the c* performance efficiency is affected by the chamber pressure. The combustion of elemental boron is very sensitive to the chamber pressure; incomplete combustion occurs at 50 psia and virtually complete combustion occurs at 200 psia. The presence of water vapor, resulting from hydrogen combustion in the secondary combustion chamber, also promotes the combustion of boron nitride and boron.

d. Temperature Profile Measurements in the Secondary Combustion Chamber

(U) Temperature profile measurements were made along the length of the secondary chamber to determine both the progress of mixing in the chamber and the progress of the combustion reactions. The measurements were made with two sets of four tungsten-rhenium thermocouples, one set in-line with the air-inlet ports, the other midway between air-inlet ports.

(U) The temperature profiles obtained from the two sets of thermocouples were substantially different in shape and demonstrated the nonhomogeneity of the temperatures at the various sections along the secondary chamber. Prefire profiles obtained with both nitrogen and air showed very similar mixing and cooling patterns.

(U) The steady-state profiles obtained at air-to-propellant ratios of 8:1 and 16:1, in both low altitude/Mach 2.5 and high altitude/Mach 4.0 tests, showed that mixing of the gases was completed at a point near Station 4, about 12 inches from the air inlet ports. In the 40:1 air-to-propellant ratio tests, the profiles show that mixing was not completed until well downstream of Station 4, and may not have been completed within the secondary chamber. The increased severity of the cooling effect of the augmenting gas at the higher air to propellant ratios was also observed.

(C) The temperature profiles also showed, in the low altitude/Mach 2.5 tests, that the initial combustion of hydrogen occurs very near the air inlet with the production of extremely high temperatures. The oxidation of the hydrogen and combustion of the solids continue as the plasma proceeds downstream. The entire process, both mixing and combustion, is nearly complete near Station 4.

(U) Temperature profiles in the high altitude/Mach 4.0 tests were substantially different from those in the low altitude/Mach 2.5 tests. In the former, the initial high temperatures near Station 1 were somewhat lower and the downstream temperatures somewhat higher. These profiles indicated that the higher linear velocity of the plasma and lower chamber pressure caused a downstream shift in the combustion temperature profile.

(U) The temperature profile measurements showed that the mixing process was virtually completed in the secondary chamber under all conditions studied, except the very high air-to-propellant ratios.

3. PHASE III, INTERPRETATION OF MICROMOTOR TEST RESULTS

a. Primary Combustion Process

(C) The results of the present investigation are consistent with the findings of an extensive study of the hydrazine/pentaborane bipropellant system made several years ago. In that study it was found that the reaction proceeds by the initial formation of one or more adducts, e.g., $B_5H_9 \cdot 2N_2H_4$. The highly exothermic decomposition of the adducts produces hydrogen, boron nitride, and elemental boron. Whereas thermochemical calulations predict that the elemental boron and nitrogen will react to form boron nitride, this reaction proceeds much too slowly to be of significance in the primary chamber. Also, pentaborane thermally decomposes to form elemental boron and hydrogen. Thus, any pentaborane decomposition of this type which occurs prior to the formation of an adduct results in a loss of efficiency.

b. Secondary Combustion Process

(U) A model of the secondary combustion process has been developed on the basis of the experimental data obtained in this study. The combustion model provides important information regarding the performance of the air-

augmented hydrazine/pentaborane system. However, its greater significance lies in its utility in identifying and emphasizing the more important parameters affecting the performance of boron-loaded propellants in air-augmented applications.

(C) The initial process, that of mixing of the primary exhaust and secondary air, occurs to a significant extent in the vicinity of the air-injector. The mixing is performed by the development of eddy currents and molecular diffusion as the gas streams impinge and move downstream. Thus, fuel-rich and oxidizer-rich regions of rapidly changing composition are formed within the initial mixing zone. Within these regions, expecially the oxygen-rich regions, ignition and combustion of hydrogen occurs. As the diffusion of the streams and combustion of hydrogen continue, the concentration of the water vapor increases, and the combustion of the boron nitride becomes more significant. As the particle temperatures increase, due to combustion with water and oxygen, the combustion of boron becomes significant. It is suggested that water vapor, or perhaps other hydrogen-oxygen species such as OH and HO_2, may serve as oxygen carriers for the combustion of the solid particles.

(C) Higher chamber pressures improve the kinetics of the solid combustion both by increasing the rate of adsorption of the oxygen bearing species on the particle surface and by increasing the residence time of the reacting plasma. The presence of water vapor in the system improves the kinetics of the solid combustion by providing the particles with an environment rich in reactive oxygen-bearing species.

4. RECOMMENDATIONS

(C) Based on the results obtained on the present program, it is recommended that a comprehensive study be made of several boron-containing, air-augmented propellant systems. Four systems which presently show merit from a theoretical performance standpoint and from their potential ability to shed more light upon the inherent nature of air-augmented boron combustion are: (1) the hydrazine/pentaborane system at low mixture ratios from 0.1 to 1.0 and at air-to-propellant ratios up to 50:1; (2) the hydrazine/boron-loaded pentaborane system at various primary mixture ratios, boron-loading levels and air-to-propellant ratios; (3) chlorine trifluoride/boron-loaded pentaborane system at several low-primary mixture ratios, boron-loading levels, and air-to-propellant ratios; and (4) the chlorine trifluoride/ATF-2 system at several low-primary-mixture ratios and air-to-propellant ratios.

(U) The research should include the determination of characteristic velocity, thrust, specific impulse, secondary chamber temperature profiles and secondary exhaust composition. Examination of the effects of chamber pressure, flight Mach number, and the catalytic action of combustion species on the combustion efficiency of boron should provide valuable information regarding the development of promising propellant systems for air-augmentation applications, be they based on liquid or solid primary propellant systems.

SECTION III

TECHNICAL DISCUSSION

(U) The program was divided into three phases: Phase I, Design, Fabrication, and Installation of Laboratory Micromotor Facilities; Phase II, Determination of the Combustion Characteristics in Air of the Exhaust Products from the Pentaborane/Hydrazine System; and Phase III, Interpretation of Micromotor Test Results. The work performed and the results and their significance are discussed in this section.

1. PHASE I, DESIGN, FABRICATION, AND INSTALLATION OF LABORATORY MICROMOTOR FACILITIES

(U) Phase I was concerned with the design, fabrication, and installation of the liquid micromotor. The micromotor was used for the determination of characteristic velocity, c*; for the determination of exhaust product composition, both gaseous and solid; and for the measurement of the temperature profiles in the seconday chamber.

(U) The test site for the experimental combustion studies was the Research Physics Laboratory of the Propulsion Division. Several additions to and modifications of the existing facilities were made to provide a permanent air-augmentation test facility.

a. Design Requirements and Test Site Preparation

(U) A schematic diagram of the mechanical system required for the execution of the experimental effort is shown in Figure 1. The mechanical facilities may be divided into 5 main sub-systems: (1) secondary air handling and heating; (2) primary propellant; (3) cooling water supply; (4) micromotor; and (5) exhaust handling and sampling.

(1) Secondary Air Handling and Heating Sub-System

(a) Air Storage and Compression

(U) Test firing durations of up to 60 sec were initially anticipated at low air-flow for the 8:1 air-to-propellant ratio and of 10-15 sec at high air-flow for the air-to-propellant ratio as high as 40:1. Supply air-pressure was established by the total of chamber pressure, injector pressure-drop, line frictional resistance, the large pressure-drop across an acoustic nozzle used to establish the air flow-rate, and the pressure-drop across the high pressure regulator supplying constant pressure to the acoustic nozzle.

(U) The air supply-vessel was required to be of this minimum capacity plus a sufficient excess to provide time for stabilization of air flow-rate and temperature. The vessel selected had a capacity of

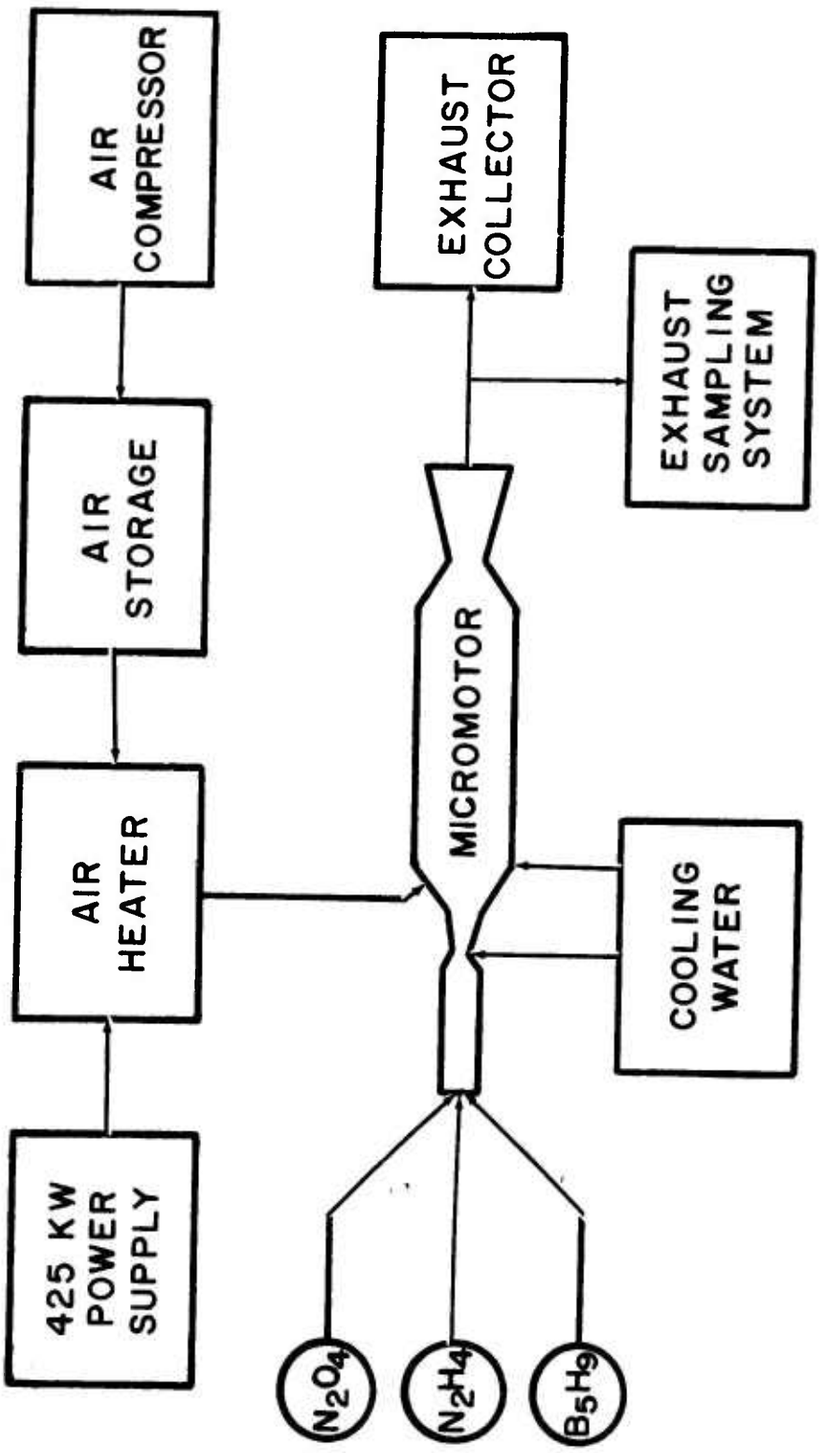

Figure 1. Mechanical Subsystem Diagram of Micromotor Facilities

15 cu ft and was capable of supplying clean air or nitrogen at 6000 psia. The excess capacity was desired in order to minimize variation in air flow-rate that would be caused by dropping supply-pressure to the controlling high-pressure regulator. By using this system, a drop in supply pressure from 3000 psia to 2400 psia resulted in essentially no change in air flow-rate to the heater.

(U) A choice was available for primary air supply. Dry air could be purchased in cylinders at 2200 psia, with the advantage of being readily available and of a given quality, or a compressor could be installed. The inherent disadvantages in the former approach were the considerable labor involved in changing cylinder banks, the probable time-loss in delivery, and the fixed low supply-pressure. Therefore, a 10 HP, three-stage compressor was installed, with a capability of 15 SCFM and a delivery pressure of 5000 psia. Because the presence of either water or oil in the delivered air would be detrimental to performance analysis, a series of condensers, knock-out traps, and a silica-gel drier were installed between the compressor and the supply vessel. With minimum service, these units supplied air of high purity and of fixed humidity. For those tests requiring nitrogen, a facility supply was available which insured a dew point of less than 200°R.

(U) A series of calibrated sonic nozzles was selected for measuring air flow-rate. Under suitably controlled conditions, these devices provided reliable and reproducible flow measurement, requiring only a pressure and temperature measurement to determine flow with an accuracy of 1%.

(b) Air Heater

(U) Three of the possible methods of heating the augmenting air were given careful consideration: A direct-fired pebble-bed, an electrically-heated pebble-bed, and a resistance-heated tubular system. The direct-fired bed would produce the maximum temperature but with the serious faults of a dropping run-temperature, possible bed attrition, and gas contamination. The electrically-heated bed would eliminate only the last fault. The potential problem areas for a resistance heated tube were temperature limitation, power requirements, mechanical limitations at high temperature, and the balance of electrical resistance with the heat transmission rate. Calculations showed that only a few alloys would provide adequate electrical resistivity and the high yield strength required under the projected temperature and pressure conditions.

(U) The resistance heating system was selected, primarily because a large power supply was available. The safety and working-comfort aspects of this system, although not overriding, were much superior to the existance of a very hot body in the test bay for a significant time period.

(U) The heater, as designed, consisted of two elements, each with a separate power source, The first element consisted of approximately 30 ft of 1" dia Type 316 stainless steel and the second consisted of a similar length of 1-1/2" dia Inconel tubing. Each section was thermally insulated with 1/4" of Fibrefrax felt paper and was covered with preformed 85%-magnesia insulation. Thermal integrity of the insulation under the conditions of operation was found to be good. Mechanical strength of the stainless steel section was adequate and no scaling was observed. The Inconel section showed no weakness.

(U) Joule-Thompson expansion effect across the air regulator was found to produce a relatively minor drop in gas temperature. Temperature, after expansion, varied from 0°F to 25°F with an initial air temperature slightly above ambient. Provisions were made to preheat the supplied air if necessary; however, this was not required for the tests described in this report.

(c) Air Heater Power Supply

(U) A heat-sink type of air heat-exchanger requires a substantially lower rate of electrical power input than the tubular resistance heater designed for this application, although total energy-input would be greater in the heat-sink because of losses. With a calculated maximum air flow-rate of 1.3 lb/sec, it was determined that an existing power source of 425 KW would nearly satisfy the instantaneous heat required if efficient heat-transfer were attained, An internally-extended surface exchanger would permit a closer approach to complete heat utilization, but at a greatly increased cost because of the refractory metals required in the operating temperature range.

(U) The first zone (stainless steel) of the heater was energized by four 50 KW, 15 Volt DC, 3000 ampere units with 480 V, 3 phase primary. These are of the saturable core reactor type and were designed by Aerojet. The second zone (Inconel) was heated by a Ling Model RVS-75/3000 power supply of the SCR type. This is of 225 KW capacity with a 75 volt, 3000 ampere secondary. Both units are voltage regulated and can be adjusted in operation from a remote location in the test bay control-room on the same console that housed the balance of the firing controls.

(2) Primary Propellant Sub-System

(U) A significant advantage of micromotor testing is the small quantity of propellant expended. For stable and relatively non-hazardous propellants such as N_2O_4 and N_2H_4, run vessels may be large enough to permit a long series of test firings without additional propellant transfer. In the case of pentaborane, it was considered safer to use a relatively large run-tank rather than make repeated propellant transfers and a vessel was selected to hold three pounds of fuel.

(U) The N_2O_4 and N_2H_4 systems were cleaned according to standard practice and assembled with flared tube or AND 10050 fittings. Both propellants were pressurized with a facility nitrogen supply using a common electrically-actuated loader with each system isolated by two check valves.

(U) The B_5H_9 system was thoroughly cleaned and assembled using minimally applied petrolatum as lubricant where required. Pentaborane may ignite upon exposure to air; therefore, this system was made as leaktight as practical, utilizing either welded connections or flared tube connections with tube seals. After assembly the fuel system was filled with hexane and thorougly cleaned, with actuation of all remote and hand valves, by flowing the hexane through the propellant circuit. It was then evacuated and backfilled with helium before receiving the fuel. Previous experience has shown that small quantities of moisture will react with pentaborane to form solids that tend to clog orifices, valves, and other small openings. To prevent this, the pentaborane was filtered through a 10 micron and a 5 micron filter in series during transfer to the run vessel. Helium was used as the pressurizing gas. During the series of test firings, no problem was encountered due to solids in the system. Flowmeters and pressure transducers removed from the system after the test series showed no indication of solids buildup. The injector was removed for cleaning after each firing and it is significant that the line and a check valve immediately upstream of the injector developed solids which caused complete clogging of the check valve on several occasions, notwithstanding a long purge following each shutdown.

(3) Cooling Water Supply

(U) Both chambers of the combustor were water cooled. The exhaust gases from the secondary chamber were to be filtered through a glass fiber bag system that had a temperature limitation of approximately 600°F; therefore, a cooling section was required between the secondary nozzle and the filter. To obtain high heat transfer rates in these sections, a high annular velocity was required in the jacket which introduced a high pressure-drop through the water system. Water was supplied at 750 psi from a vessel located in the test bay. Each of the three cooling zones was separately regulated to provide approximately a 500 psi pressure-drop through the jackets and valving. Deionized water was used to minimize scale formation and interference with thermocouples located at four points in the water circuit. A total water flow-rate in excess of 10 gal/min was used for all firings.

b. Instrumentation Requirements

(U) A relatively complex instrumentation facility was employed for data acquisition in this study. A schematic diagram of the instrumentation is shown in Figure 2. Ten pressure channels were employed and records were made of run tank pressures, injector pressures, venturi, and chamber pressures. As many as 45 thermocouples were monitored simultaneously,

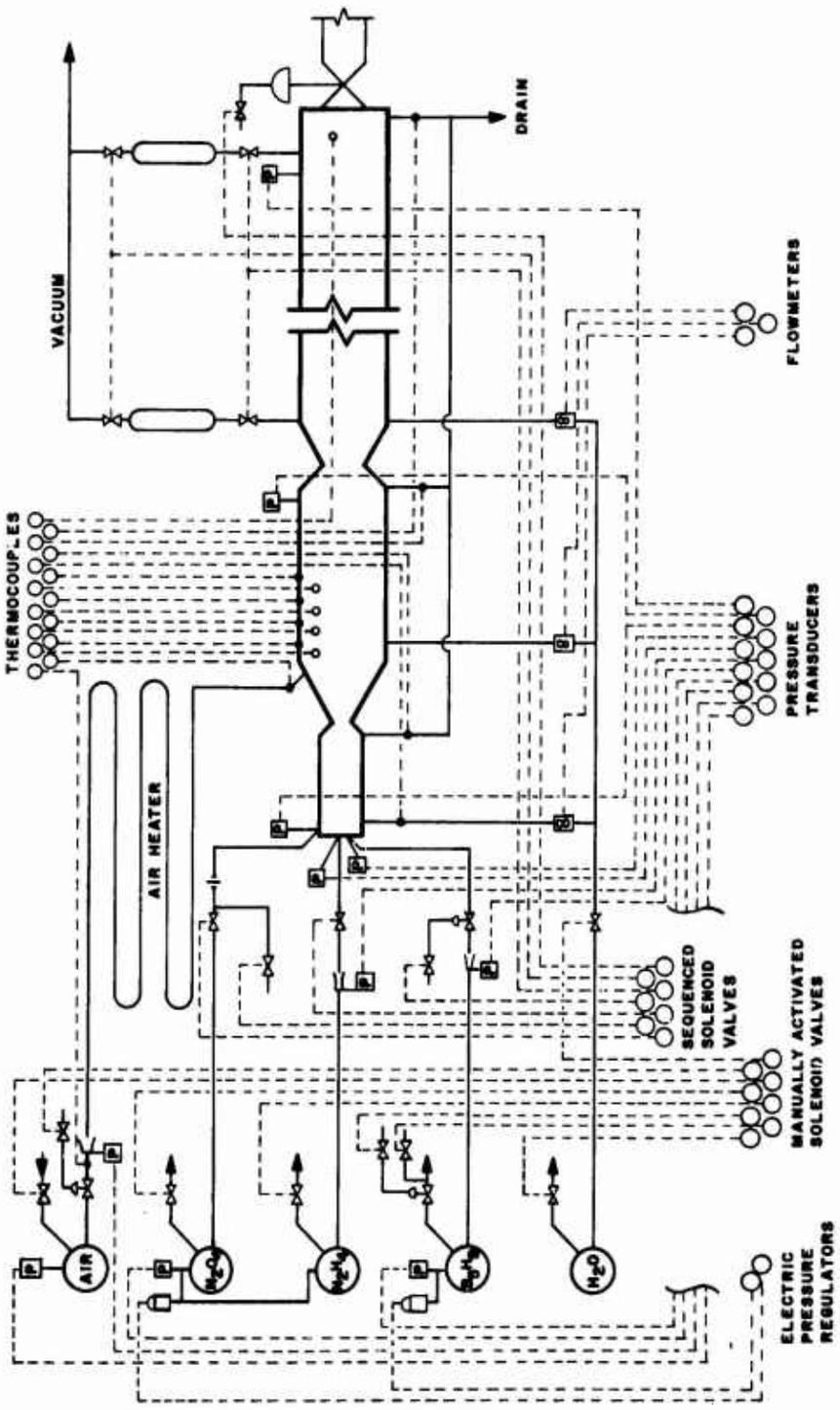

Figure 2. Micromotor Instrumentation and Process Control Diagram

including secondary chamber temperature profile measurements. Three turbine meters were used throughout the program. Current and voltage for the two sections of the air-heater were also recorded. In addition, several valve and switch traces were employed and a solid-state malfunction shutdown system was adapted for use.

(1) Instrumentation, General Description

(U) A comprehensive block diagram of the instrumentation and data acquisition system in use in the Research Physics Laboratory is shown in Figure 3. Cables from transducers located on the experimental apparatus in the test bay are routed to a central data patch system via instrumentation drop boxes and shielded transmission lines. The inputs and outputs of signal conditioning and calibration equipment, as well as the end recording devices, also appear on this patch board.

(U) Forty-eight wideband differential instrumentation amplifiers are used throughout to convert low level data to the high signal levels required for the digital recorder and oscillograph galvanometers. Continuous signal shields and a single point ground system are employed to maintain signal integrity exclusive of environmental conditions.

(U) Test parameters are recorded on a Consolidated Electrodynamics Corporation direct writing oscillograph and on a Consolidated Systems Corporation analog-to-digital data conversion system. The digitized test data is recorded on magnetic tape recorders in a format suitable for computer processing.

(2) Static Pressure Measurement

(U) A six-wire pressure measurement system utilizing strain gage pressure transducers was used. The transducers have 350-ohm bonded strain gages in a fully-active, four-arm bridge configuration.

(U) The transducers were calibrated and standardized in the Propellant Division's Transducer Laboratory for unipolar single arm shunt calibration. A twenty-four channel bridge balance and shunt calibration unit located in the control room provided simulated pressure calibration steps of 0, 10, 25, 50 and 75 percent of transducer full scale. All channels were calibrated simultaneously through this sequence of steps upon command from an external master calibration control unit.

(U) Bridge excitation voltage was obtained from individual precision strain gage power supplies. These units were guarded and isolated from the power line to preclude noise introduction into the system.

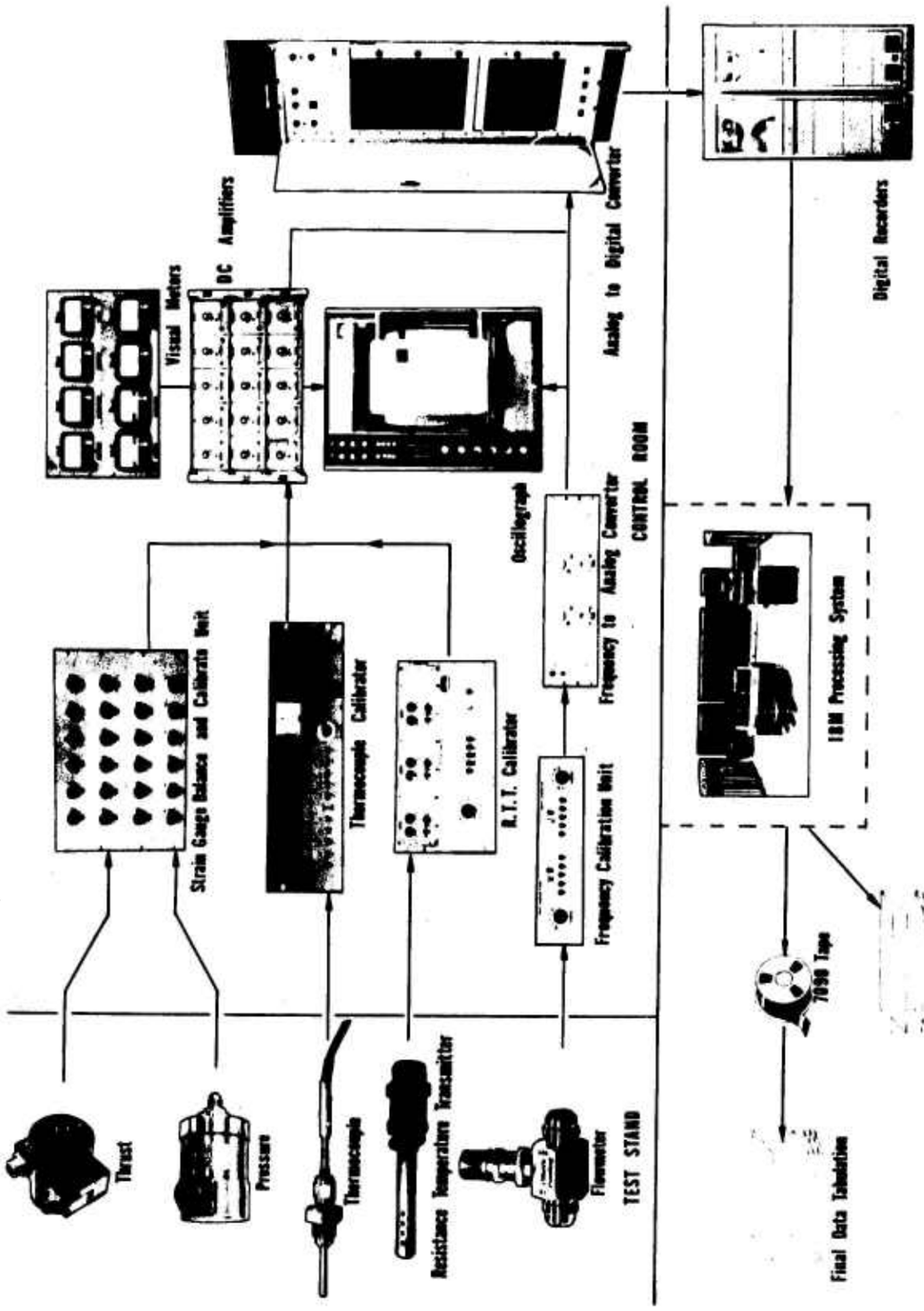

Figure 3. Research Physics Laboratory Instrumentation and Data Processing System

(3) Thermocouple Temperature Measurement

(U) For this program three types of thermocouples were used. Cooling-water temperatures were measured with iron-constantan thermocouples and normal gas temperatures from ambient to 1600°F were measured with chromel-alumel thermocouples. The secondary chamber temperatures were, in some tests, in excess of 4000°F; special tungsten-rhenium thermocouples were used for these measurements.

(U) Reference junctions were immersed in water and ice baths located at the experimental site. Transmission lines to the data patch were shielded, twisted copper pairs.

(U) Temperature system calibrations were derived from a twenty-channel precision voltage substitution unit. Standard calibration steps of 0, 5, 10, 25 and 50 millivolts with a 1.0 or 0.1 multiplier option were automatically selected by the master calibration unit during pre- and post-test calibrations. The temperature calibrator was standardized daily against an internal Epply Standard Cell.

(4) Flow Measurement

(U) Two methods of flow rate measurement were used. Conventional differential pressure devices such as sharp edged orifices, venturis or flow nozzles were employed where suitable. Pressure drops were derived from measurements made with the aforementioned pressure and thermocouple systems. Cooling water flow rates were metered with turbine flowmeters.

(5) Data Recording

(U) A digital data conversion system is the basic source of data in the Research Physics Laboratory. This completely solid-state unit sequentially multiplexes up to forty-eight (48) analog data channels and digitizes them in a gapless BCD tape format. The 17 bit BCD output is serialized and transmitted over coaxial cables to the Propellant Division's Central Data Recording area. The data are reconverted to a parallel format and reduced on Ampex digital tape recorders. Pre- and post-firing system calibrations are recorded on the same tape just prior to and immediately after each test. Upon completion of the recording, the raw tape is rerun to achieve a gapped format suitable for direct entry into the IBM System 360 data processing unit.

(U) An IBM punched card deck was made up from the instrumentation data-sheet submitted to the data processing group prior to testing. This deck and the recorded data, complete with firing calibrations, were then processed. The data processing unit derived offset, range and scale factors from the calibrations and converted the data to engineering units. Linearity and out-of-range checks were applied to the calibrations to ensure accurate, meaningful data. The test data were printed in tabular form along with the

appropriate parameter nomenclature, transducer ranges, calibrations and accumulated test time. Time interval data summaries were also used. The resultant data presentations were the basis for performance evaluations.

(U) A CEC Model 5-133 thirty-six channel direct recording oscillograph provided an immediately available recording suitable for rapid visual analysis in addition to providing accurate backup test data. Transient operating conditions were evaluated from this record. Twenty-four galvanometers were normally used for data recording on this machine, employing galvanometers with a nominal 600 Hz frequency response. In addition, 10 events-channel galvanometers were used for data correlation.

(6) Process Control

(U) Switch and lamp indicator control panels were used for manual operation of valves and equipment in the test bays. A 28 volt DC facility power supply provided operating voltage for this function. For electric loading manifolds used with dome loaded pressure regulators, multiple throw toggle switches were used. In addition, a variety of special control and functional panels were available for facility purposes and for specialized applications.

(U) A forty-nine channel patch board and relay controller or sequencer were used to provide automatic, preset programming for the wide variety of experimental apparatus employed. Twenty channels of solid-state timers provided the timing functions for this programmer. The unit, designed for flexible operation, was set up to provide automatic shutdown in the event of malfunction in the test apparatus.

c. Micromotor Design

(U) The construction of a test apparatus that would realistically simulate mission hardware and, simultaneously, provide all desired small-scale experimental information required a few approximations and several novel design features. The combustor components of the micromotor included the primary bipropellant injector, the igniter injector, the jacketed primary combustion chamber and nozzle, the secondary air injector, and the jacketed secondary combustion chamber and replaceable nozzles. A sketch of the assembled, two stage combustor is shown in Figure 4.

(1) Primary Bipropellant Injector

(U) The injector designed for these tests, shown in Figure 5, was a simple triplet configuration with two oxidizer streams impinging at 90° on a single fuel stream. At total propellant rates on the order of 15 gm/sec, orifice sizes of 0.018 in. (oxidizer) and 0.020 (fuel) were required. Impingement was checked before each test firing and excellent mixing and atomization were attained, as shown in Figure 6. With the propellant combination under study, no deterioration of the injector occurred after 22 test firings. This unit was fabricated from Type 347 stainless steel.

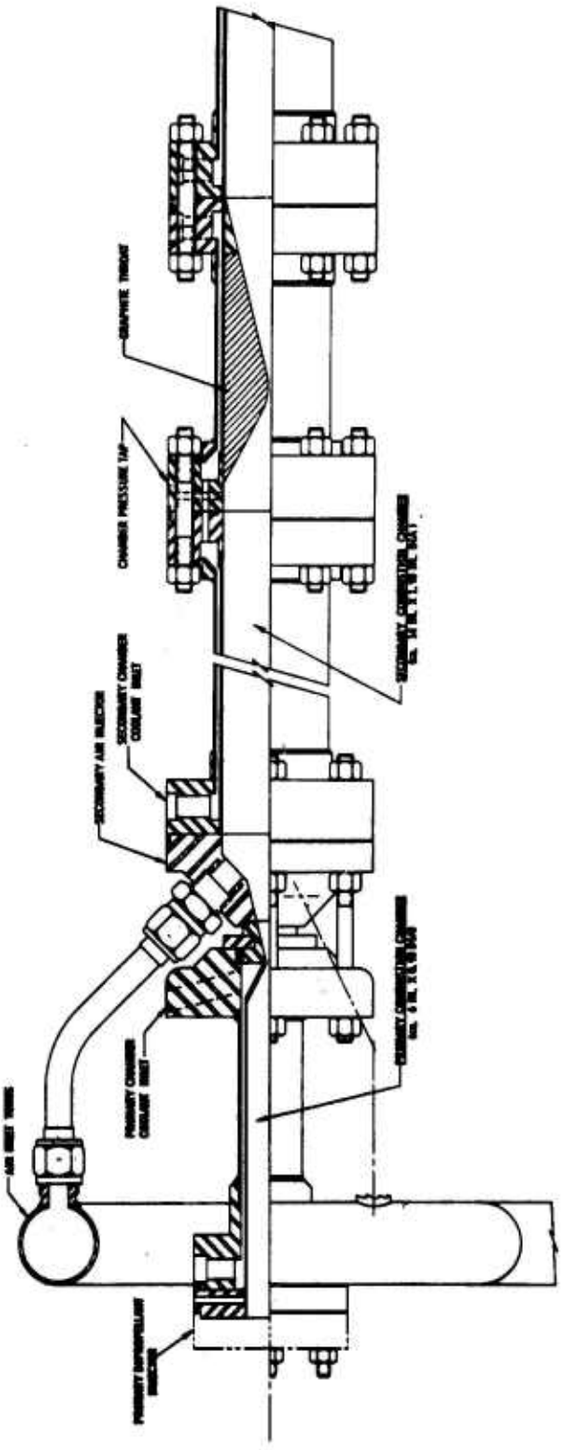

Figure 4. Micromotor Engine Assembly, AA Mod 1

Figure 5. Primary Bipropellant Injector (2 Ox on 1 Fuel Triplet)

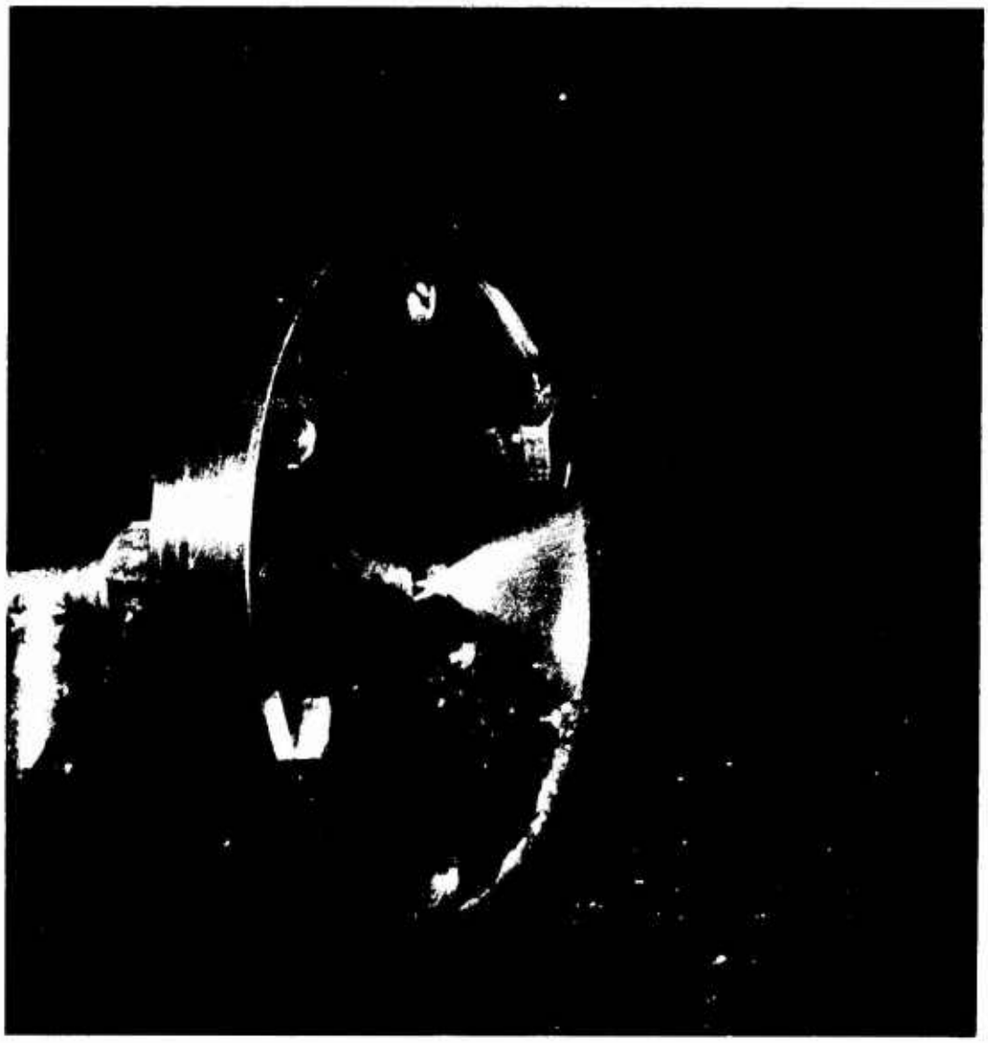

Figure 6. Hydrotest of Primary Bipropellant Injector

(C) Mixtures of pentaborane and hydrazine tend to detonate rather than to ignite smoothly; therefore, an auxiliary igniter was used. This consisted of a nitrogen tetroxide stream directed at the basic propellant impingement point. An N_2O_4 lead, followed by N_2H_4 at approximately 50 millisec, with subsequent B_5H_9 injection at 150 millisec, proved to supply positive ignition. With two exceptions, smooth basic propellant ignitions were obtained in the tests. In one of the two instances noted, a pressure spike occurred at the time of pentaborane injection, resulting in a bulged injector-connection and an over-ranged pressure transducer. No damage occurred in the second instance. This phenomenon did not recur although sequencing was not changed.

(U) With small flow-rates sequencing can only be approximated mathematically. Thus, several firings were made to establish correct timing for valve actuation. An Aerojet-designed electronic sequencing system, with malfunction shutdown control, was programmed for these tests.

(2) Primary Combustion Chamber

(U) The primary combustion chamber, shown in Figure 7 before assembly, was designed with a characteristic length (L*) of 312 in. Although an L* of 50 to 80 in. may have been more realistic, such a small length is inordinately difficult to use at low flow-rates. The primary chamber was approximately 6 in. long (injector-to-throat) and 0.90 in. in dia. A throat dia of 0.125 in. was used throughout, the convergent zone being 30° half-angle and the divergent zone 15°. Nominal primary chamber pressure was 425 psia.

(U) The primary combustion chamber was inserted into a cooling-water jacket, shown in Figure 8. Water cooling was employed to prevent primary chamber burnout and provided heat-rejection data for the measurement of heat-losses in the primary combustion process.

(3) Secondary Air Injector

(U) The air injector was fabricated in such a manner as to form a short portion of the expansion section of the primary nozzle. Figure 9 is a photograph of the assembled primary combustor and secondary air injector. The air was introduced into the secondary chamber at three locations at 45-degree angles to the axis of the secondary chamber at a position just aft of the exit plane of the primary nozzle. The velocity of the inlet air was adjusted to approximately Mach 0.4 by means of orifice inserts in the air inlet ports. Previous experimental work at Aerojet had shown that this condition provides near-optimum aerodynamic mixing.

(4) Secondary Combustion Chamber

(U) The wide variety of test conditions encountered in the test program required an unusually high degree of flexibility in the design

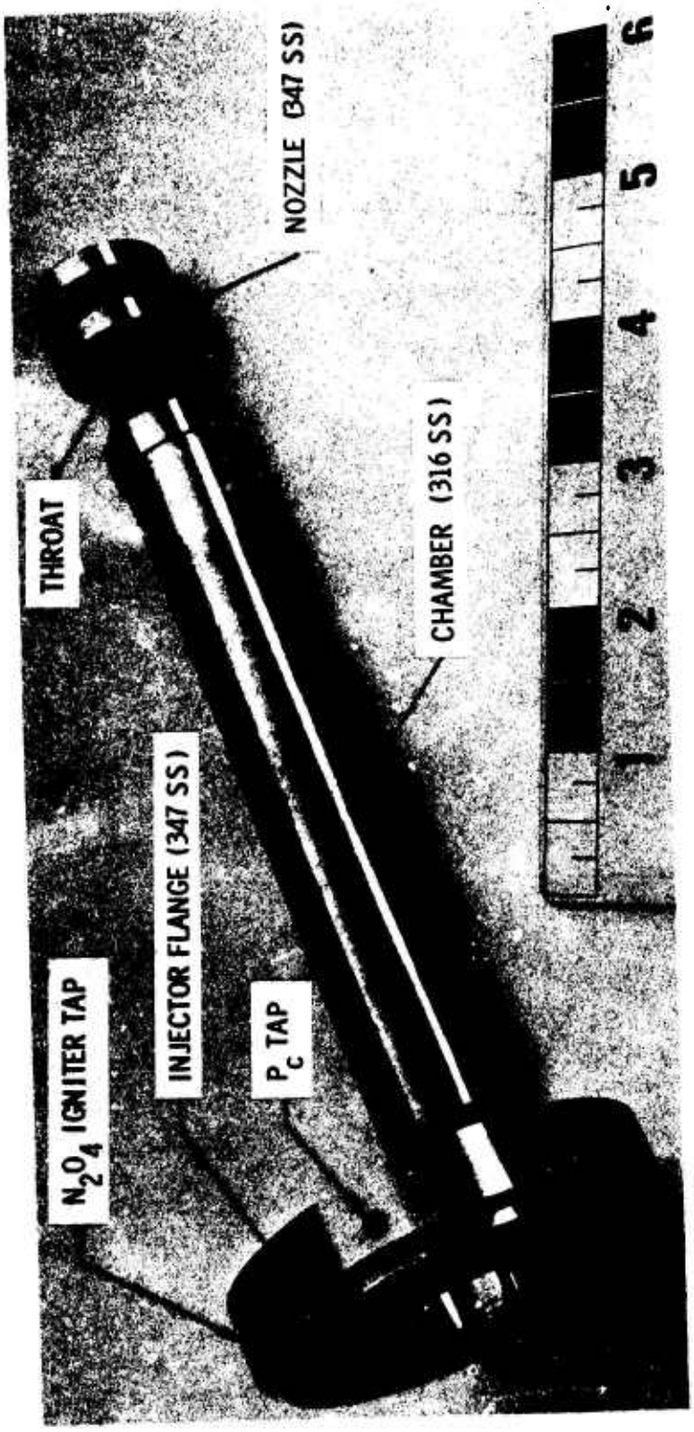

Figure 7. Primary Combustor Chamber and Nozzle

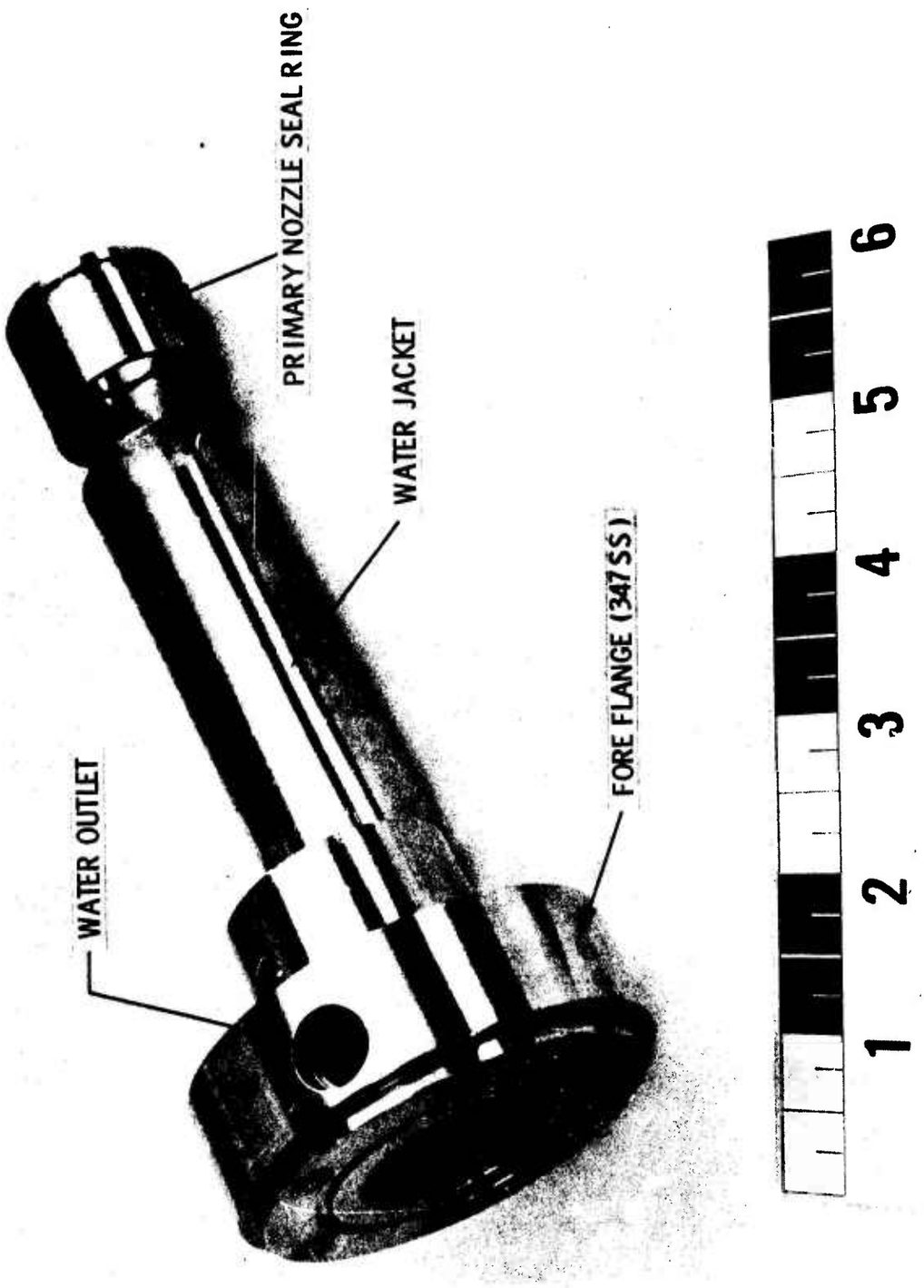

Figure 8. Primary Combustor Water Jacket Components

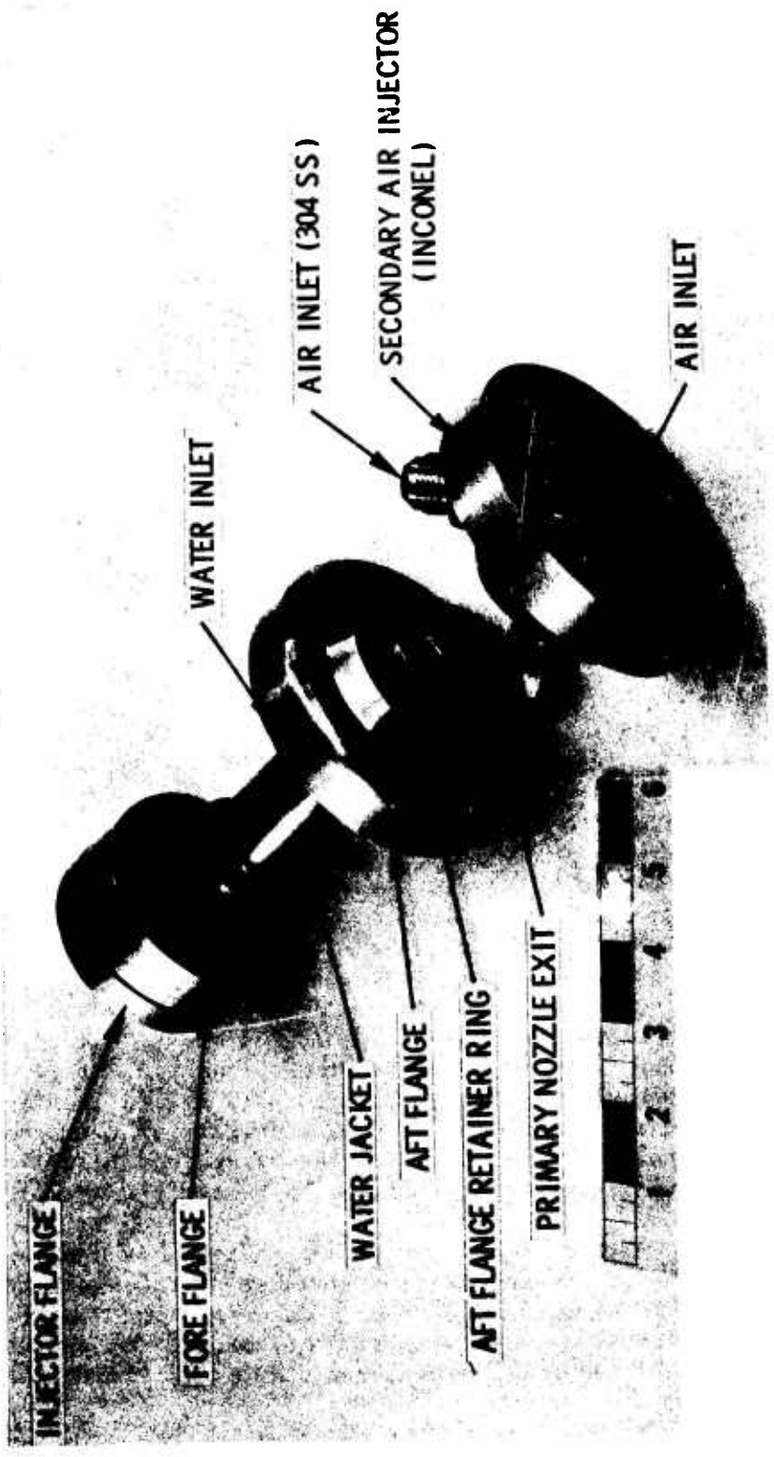

Figure 9. Assembled Primary Combustor and Secondary Air Injector

of the secondary combustion chamber. Nominal chamber pressures were 50 psia and 200 psia and nominal air-to-propellant ratios were in the range 8:1 to 40:1. These widely varied conditions necessitated frequent interchange of secondary nozzles. Fabrication of the secondary combustion chamber in two sections facilitated the interchange of nozzles and the measurement of post-test throat diameters.

(U) The secondary combustion chamber, shown in Figure 10 before assembly, consisted of a 1.87-in. ID, jacketed tube flanged at both ends. The nozzle section of the secondary chamber is shown in Figure 11 before assembly. The graphite nozzles were inserted into the short jacketed tube and rested against the steel retaining ring. The mating flanges which joined the two sections were constructed so that the cooling water flowed uniformly throughout the secondary chamber, thereby preventing the development of hot spots.

(U) The overall length of the secondary combustion chamber varied somewhat with the secondary nozzle size. For the small-throated nozzle (0.315 in. dia throat) the secondary combustion chamber length was about 16 in. and for the large-throated nozzle (1.260 in. dia throat) the length was about 18 in. The L* values for these extremes were 585 and 43 in., respectively.

(U) High density graphite (ATJ) was chosen for the nozzle material because of its superior high-temperature qualities and because its inherent lubricity tends to resist the adhesion of liquid and solid combustion products. In the high air-to-propellant regime, erosive oxidation of the nozzle was expected; however, post-firing inspection indicated that the nozzles were in excellent condition and no perceptible erosion had occurred. Figure 12 is a photograph of several of the nozzles used and illustrates their excellent condition after several tests with each.

(U) Temperature profile measurements in the secondary combustion chamber were also made during the test program. In order to accomplish these measurements, another secondary chamber section was fabricated with the same overall dimensions as that described above, but with additional provision for inserting thermocouples into the combustion chamber. The thermocouple ports were placed in pairs at four equally spaced locations along the length of the secondary chamber. One of each pair of thermocouples was in line with one of the air inlet ports in the air injector, while the other thermocouple of each pair was located midway between air inlet ports.

(U) A third secondary combustion chamber was designed to permit the measurement of gas and particle cloud temperatures at three separate locations. These measurements were to employ the Spectral Comparison Pyrometer. A discussion of this portion of the program and the secondary combustion chamber designed for the measurements is contained in Appendix I of this report.

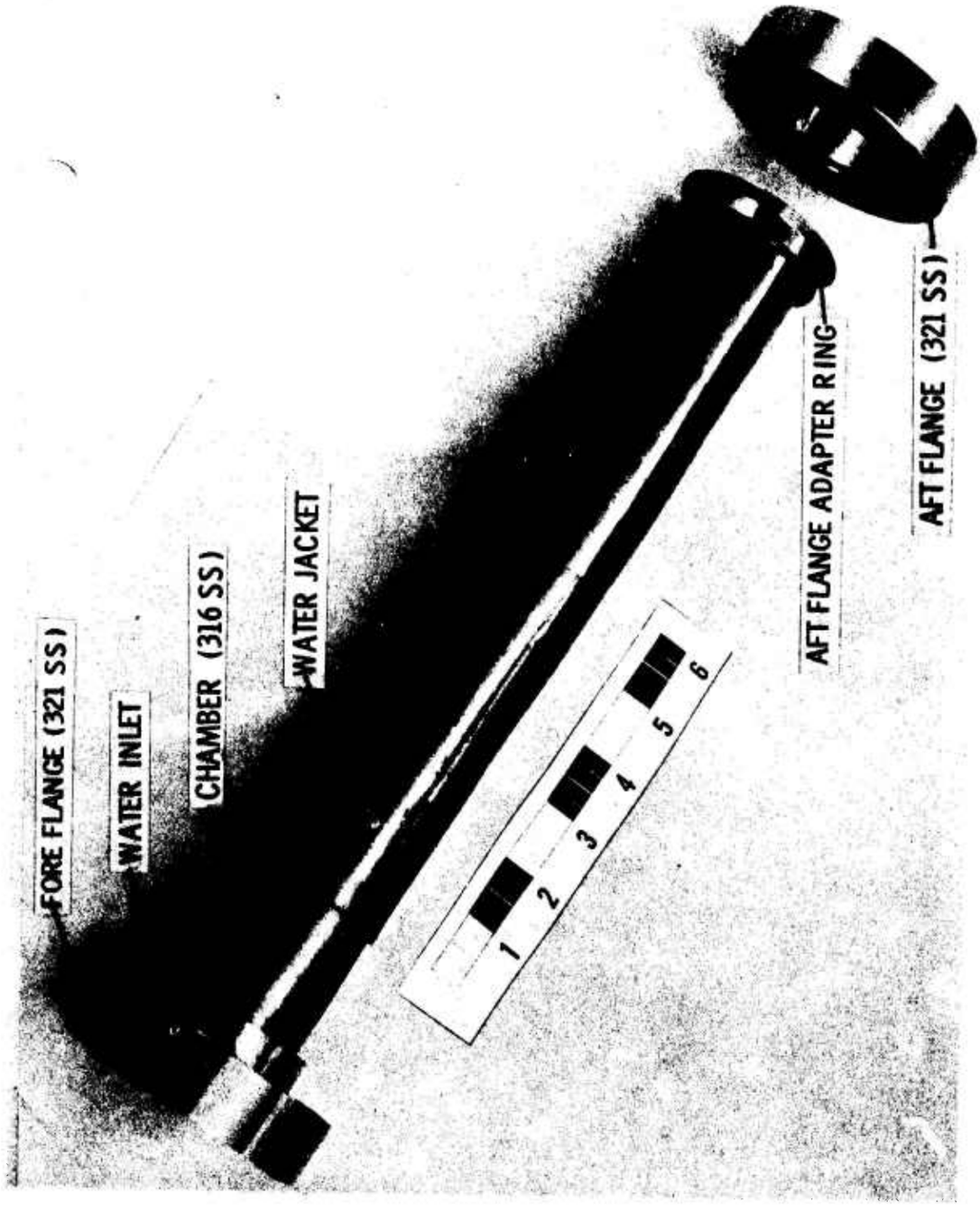

Figure 10. Secondary Combustor Chamber

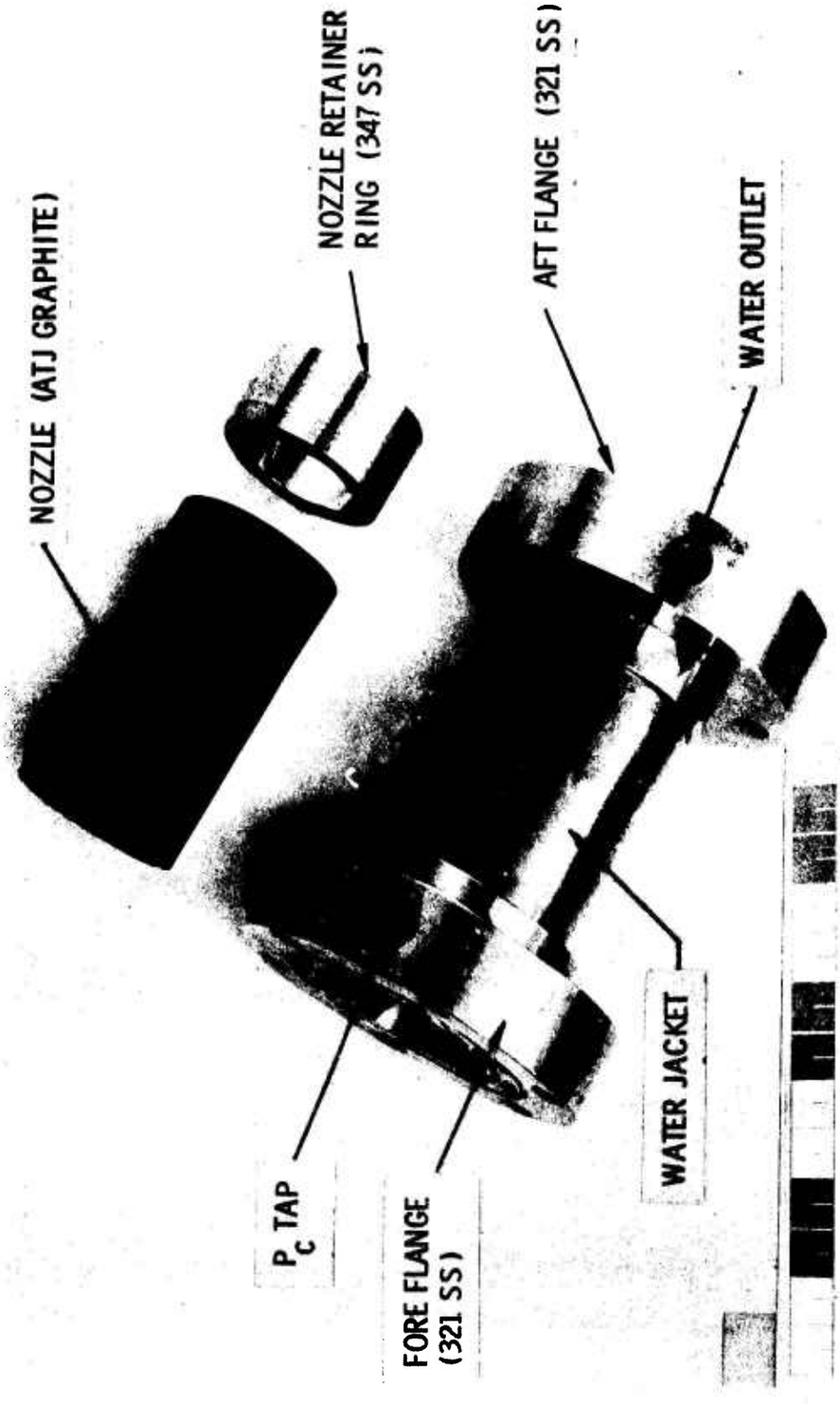

Figure 11. Secondary Nozzle Components

Figure 12. Secondary Nozzles (ATJ Graphite)

d. Exhaust Handling and Sampling Equipment

(U) An important part of the present study was the determination of the extent of combustion of the boron nitride and boron formed in the initial hydrazine/pentaborane combustion reaction. This determination was made by collection and analysis of the exhaust from the secondary combustor. The combustion products formed during the initial, transient portion of the test were exhausted to the atmosphere. When the steady-state condition was achieved in the combustor, the exhaust was diverted through the main filtration unit for collection of the solid products.

(U) In addition to the combustion of the boron nitride and boron in the secondary combustion chamber, further oxidation, i.e., post-oxidation, of these materials downstream of the nozzles was considered to be possible. The occurrence of post-oxidation would have affected the interpretation of the analytical data. Consequently, provision was made for determining the extent of post-oxidation, if any, in the system.

(U) The main exhaust filtration unit was used to collect the entire solid combustion product from the steady-state portions of the test firings. The high maximum exhaust rate, 29 cu ft/sec, necessitated a large filter area. Therefore, a significant reduction of the exhaust temperature was required to achieve a practical filter size. A section of water-cooled exhaust duct was fabricated for this purpose and consisted of 11 ft of 1.90 in. ID stainless-steel tubing enclosed in a cooling-water jacket. An additional 15 ft of air-cooled duct, 2 in. ID, was fabricated to provide additional cooling of the exhaust stream before filtration. The main exhaust diversion valve, a pneumatically-operated, 2 in. ball valve, was mounted between these two sections of exhaust duct.

(U) The main exhaust filtration unit was compartmented so that the wide range of exhaust flow rates could be accomodated. The unit was constructed to permit the use of three 12-in. dia by 6 ft long glass fiber filter bags or three 6-in. dia by 6 ft long filter bags or any combination thereof. The manifold ports leading to the bag mounting rings were provided with covers to permit the selection of the number of bags used.

(U) In addition to the solid exhaust samples collected in the main filtration unit, two auxiliary samples of both solid and gaseous products were taken at two locations along the exhaust duct. Pitot-type sampling flanges, shown in Figure 13, were placed just aft of the secondary nozzle and at the aft end of the water-cooled section of the exhaust duct. A sketch of the Pitot taps in this configuration is shown in Figure 14. During the steady state portion of the test firings, samples of the exhaust stream were drawn through the Pitot taps, passed through Millipore filters for collection of the solids and into gas sample cylinders.

Figure 13. Exhaust Sampling Flange

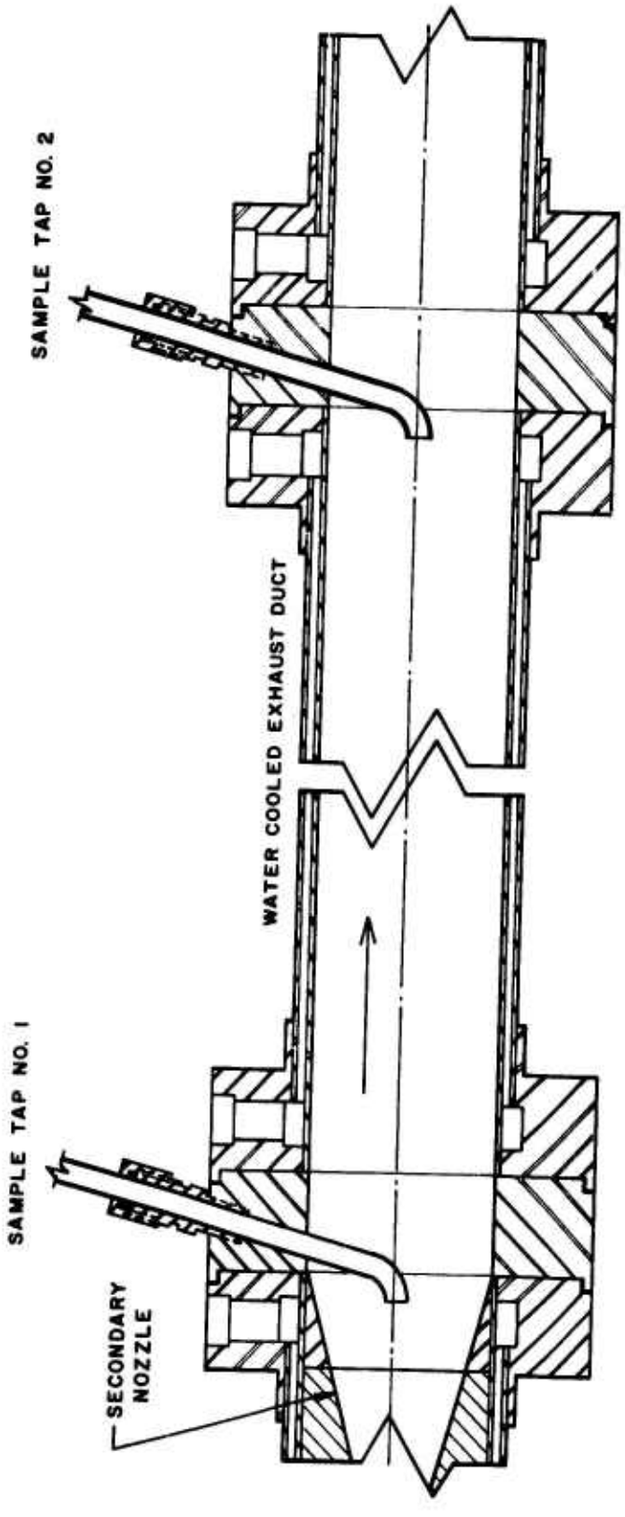

Figure 14. Water-Cooled Exhaust Duct with Sampling Flanges

e. Instrument Calibration

(U) The accurate determination of characteristic velocity from test data requires the careful calibration of the instrumentation. The three parameters of greatest significance are: (1) chamber pressure, (2) throat area, and (3) the mass flow rates of the propellants and air. The significance of errors in the measurement of these parameters has been examined and is presented in Appendix II of this report.

(U) The measurement of the mass flow rates of the primary propellants and air was given special attention, because of the very small flows used. The devices used for these measurements were calibrated at various times during the course of the test program to assure the accuracy and precision of the measurements.

(U) Throughout the test program the flow rate of pentaborane was measured by means of a paddle wheel flowmeter. However, because of the toxic and pyrophoric character of pentaborane, calibration of the flowmeter was conducted using hexane as the fluid. The choice of hexane as the substitute fluid was based on the fact that its physical properties are very nearly the same as those of pentaborane.

(U) In the early tests some difficulty was encountered in controlling the flow of pentaborane. The flow rate of pentaborane was dependent on the pressure drop in the propellant line to the injector and was subject to change as the primary chamber pressure changed. A cavitating venturi, introduced into the propellant line downstream of the flowmeter, eliminated the difficulty.

(U) Extensive calibration of the pentaborane flowmeter was conducted under a variety of conditions. The results of these calibrations are illustrated graphically in Figure 15. Two cavitating venturis were used to control the pentaborane flow. The flowmeter was calibrated with each of these venturis in the system to give the composite calibration shown in the figure.

(U) The flow rates of hydrazine were measured by means of cavitating venturis. Two venturis were used, thereby providing two ranges of flow rates. These devices were calibrated directly using hydrazine at several times during the test program. The results of these calibration experiments are presented in Figure 16.

(U) The secondary air and nitrogen flow rates were measured by means of sonic orifices located between the storage tank and air heater. The flow rate was controlled by regulating the pressure on the upstream side of the sonic orifice. Measurement of the air temperature and pressure upstream of the orifice along with the calibration data for the orifice permitted the determination of air flow rate. The orifices were calibrated against standard orifices using nitrogen in the pressure and temperature ranges employed in the test program. These calibration data are presented in Figure 17.

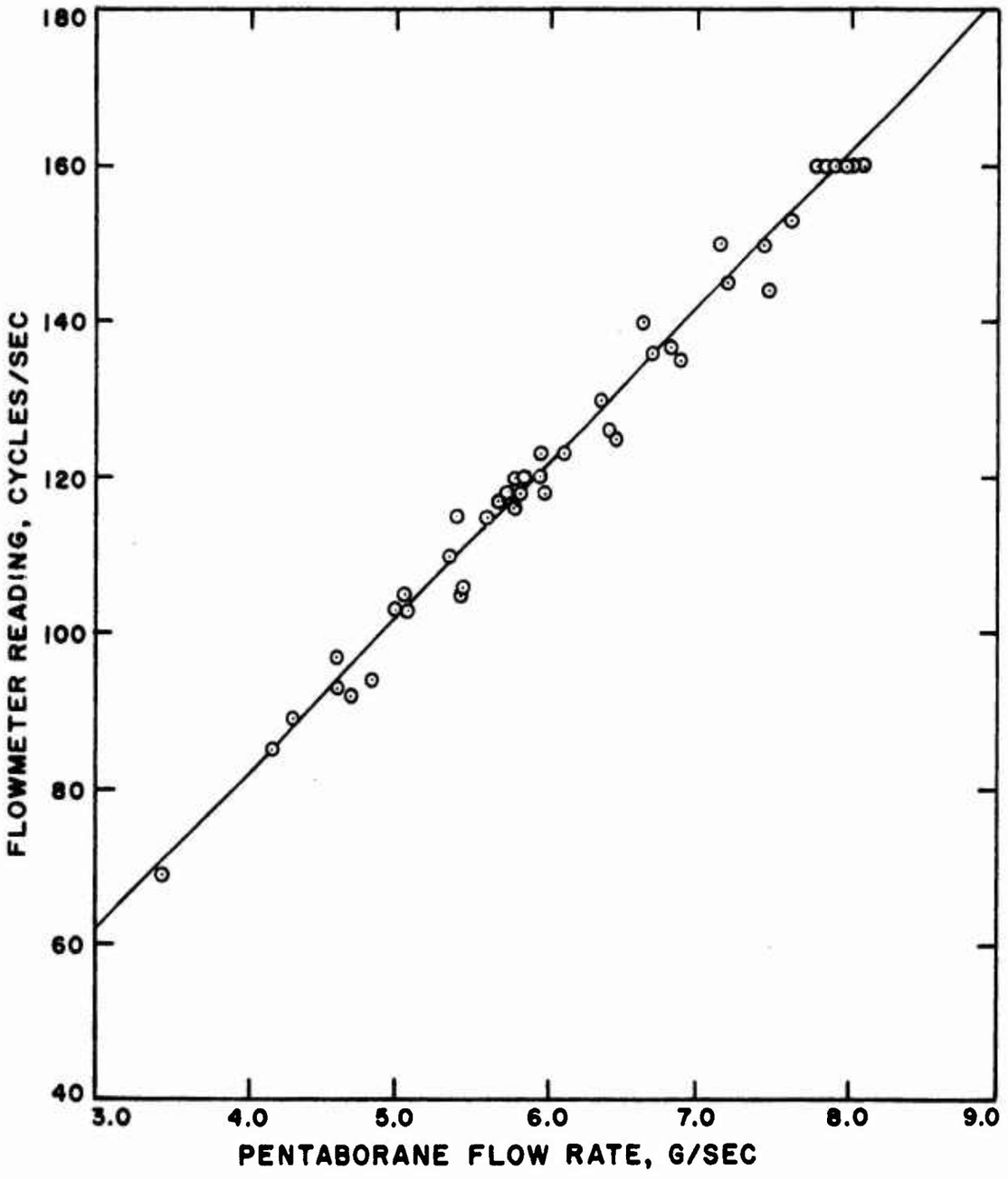

Figure 15. Pentaborane Flowmeter Calibration

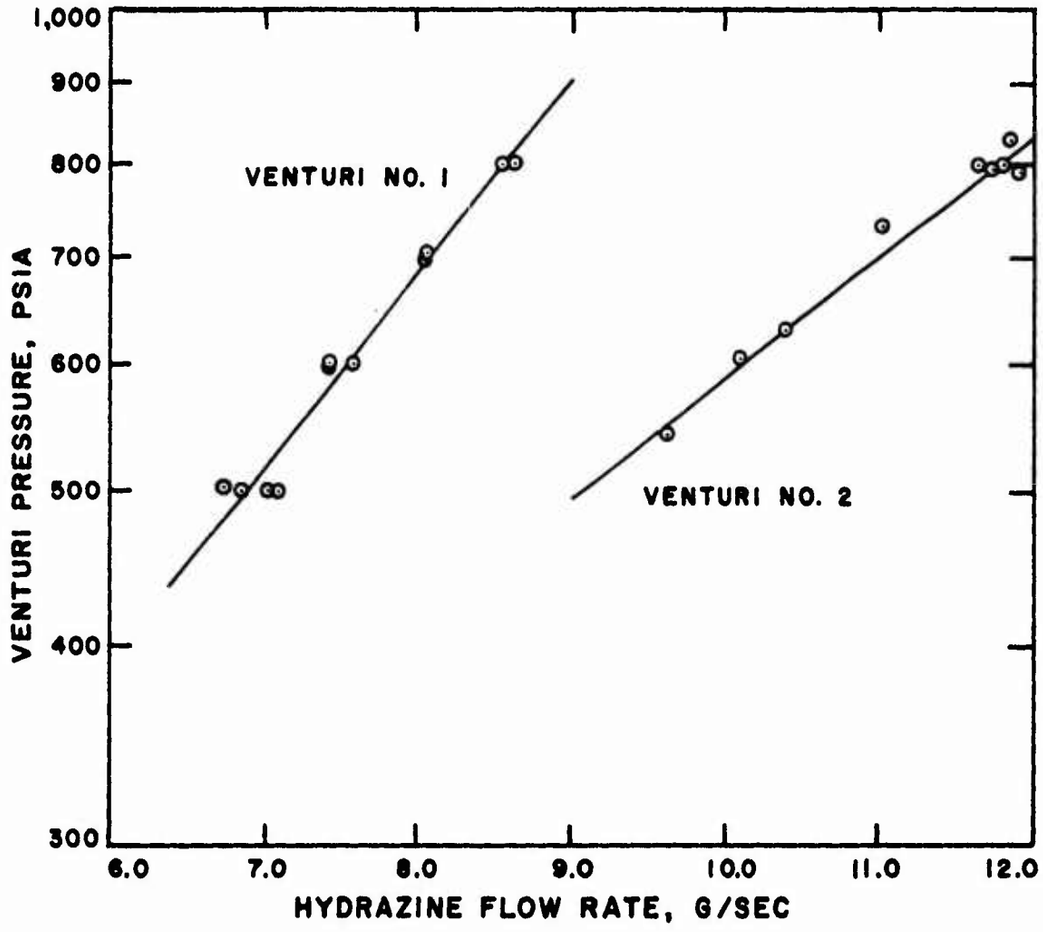

Figure 16. Hydrazine Venturi Calibration

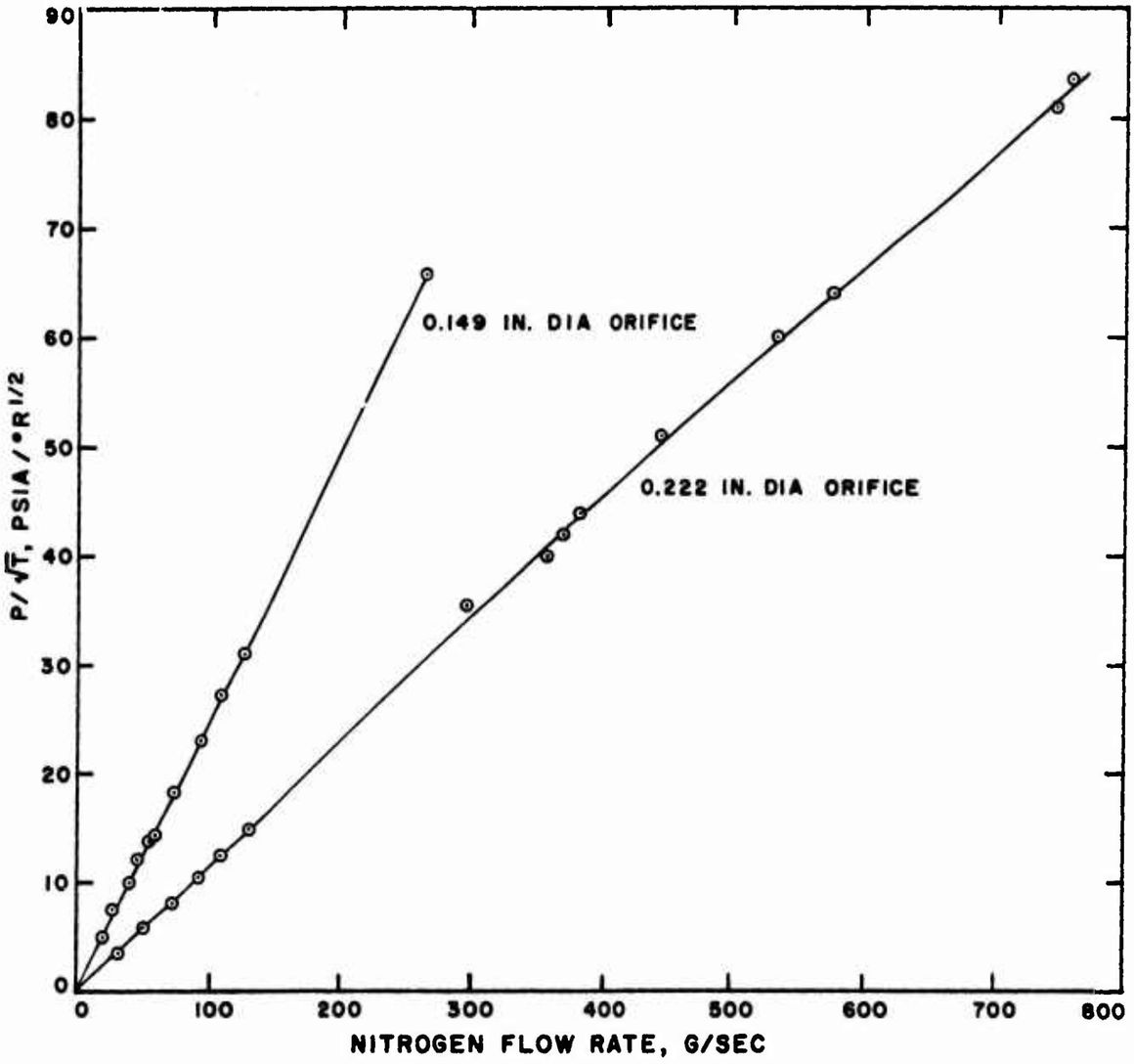

Figure 17. Air Orifice Calibration

f. Preliminary Facility Tests

(U) Several types of preliminary tests were conducted to determine suitable operating conditions. Air heater tests were conducted to establish the air-heater operating procedure and the specific power-supply control requirements. A series of tests was conducted to establish a suitable procedure for the operation of the primary ignition and combustion system. Two air-heater tests were conducted to determine a suitable operating procedure and power-supply requirements to assure the achievement of the desired gas inlet temperatures at the various desired flow rates. The procedure developed from these tests consisted of the following: (1) the power supplied to the air-heater was adjusted to preheat the heater wall to a predetermined temperature, (2) the desired mass flow of air (or nitrogen) was established, and (3) the power supplied to the heater was readjusted to a value which brought the air to the desired temperature (as measured at the secondary air-injector). The flow of water in the primary and secondary chamber cooling-jackets was started as the air flow was established.

(U) Six preliminary test firings of the primary ignition and combustion system were conducted with the following objectives: (1) to establish the sequence of propellant valve actuation which provided a smooth start-transient for the ignition system (N_2O_4-N_2H_4), (2) to establish the pentaborane injection time which provided a smooth transition from igniter combustion to the N_2H_4-B_5H_9 combustion, and (3) to achieve desirable propellant flow rates by establishing values of flow control parameters. The results of these initial tests are summarized in Table I.

2. PHASE II, DETERMINATION OF COMBUSTION CHARACTERISTICS IN AIR OF EXHAUST PRODUCTS OF THE PENTABORANE/HYDRAZINE SYSTEM

(U) This portion of the program was directed toward the experimental determination of the combustion efficiency in air-augmented hydrazine/pentaborane system. The tests were conducted under conditions designed to simulate certain flight conditions. The temperature and pressure of the secondary air were varied to simulate two flight conditions: (1) Mach 2.5 at sea level and (2) Mach 4.0 at 40,000 ft altitude. The air-to-propellant weight flow ratio was varied over the range 8:1 to 50:1. Tests were also conducted using nitrogen instead of air as the secondary gas to provide base-line data for comparison of the effect of air-augmentation.

(U) The program objectives were accomplished by the acquisition of three different types of experimental data: (1) the measurement of the parameters required for the determination of characteristic velocity, i.e., propellant and air flow rates, primary chamber pressure, secondary chamber pressure, primary and secondary nozzle throat areas; (2) the determination of the composition of the secondary exhaust by collection and analysis of both the solid and gaseous exhaust products; and (3) by measurement of the temperature profiles along the secondary combustion chamber.

TABLE I

SUMMARY OF PRELIMINARY IGNITION AND
COMBUSTION TESTS WITH THE PRIMARY PROPELLANT SYSTEM (U)

Test Number	Propellants	Mixture Ratio	$\dot{w}$ (g/sec)	P_{c-1} (psia)	Remarks
001	N_2O_4-N_2H_4	2.28	25.5	315	Smooth Start Transient
002	N_2O_4-N_2H_4	2.21	26.1	290	Smooth Start Transient
003	N_2O_4-N_2H_4-B_5H_9	----	----	---	Malfunction(a)
004	N_2O_4-N_2H_4	0.99	15.8	450	Smooth Start Transient
005	N_2O_4-N_2H_4	0.97	15.7	465	Smooth Start Transient
006(b)	N_2O_4-N_2H_4	0.98	15.7	---	Smooth Start and
	N_2H_4-B_5H_9	1.34	13.9	455	Smooth Transition

(a) Overpressure shutdown caused by B_5H_9 entering chamber before N_2H_4.

(b) Test 006 was conducted without secondary combustion chamber.

(U) The heat rejection rates were also determined in the tests to obtain more reliable correlations of the experimentally determined values of characteristic velocity with the theoretical values. These data were determined from the measured flow rates of cooling water and the measured temperature rises of the water streams in the primary combustion chamber cooling jacket and the secondary combustion chamber cooling jacket.

(U) A total of seventeen tests were conducted under the variety of conditions outlined above. The results of these tests are presented and discussed in the following sections.

a. Performance of the Hydrazine/Pentaborane Bipropellant System

(U) The chief objective of the program, as stated earlier, was to study the combustion characteristics of the air-augmented hydrazine/pentaborane system. However, the experimental test apparatus was designed and constructed in such a manner that the performance of the primary bipropellant system could be studied simultaneously. The results of that portion of the study are presented in this section.

(U) The experimental test data obtained in the primary system during the test program are presented in Table II, along with the experimentally determined values of characteristic velocity. Heat-rejection rates in the primary combustion chamber were also determined and were used for making heat-loss corrections in the calculation of the theoretical values of c*.

(C) Theoretical thermochemical evaluation of the N_2H_4/B_5H_9 bipropellant system predicts that the only exhaust products are boron nitride and hydrogen at the stoichiometric mixture ratio 1.27, utilizing the combustion reaction represented by Equation (1):

$$2.5\ N_2H_4 + B_5H_9 \rightarrow 5\ BN + 9.5\ H_2 \qquad (1)$$

Optimum performance is also predicted to occur at this stoichiometric mixture ratio, as illustrated in Figure 18.

(C) An extensive investigation (References 1 and 2) of this system was conducted earlier, utilizing a variety of chemical and physical methods. The results of that investigation, which included micromotor tests with exhaust sampling and analysis, indicated that the combustion reaction does not occur in accordance with Equation (1). Instead, the evidence indicated that the combustion reaction actually occurring (at a mixture ratio of 1.27) could best be represented by Equation (2).

$$2.5\ N_2H_4 + B_5H_9 \rightarrow 4\ BN + B + 8.75\ H_2 + 0.5\ NH_3 + 0.25\ N_2 \qquad (2)$$

TABLE II

PERFORMANCE DATA ON THE HYDRAZINE/PENTABORANE SYSTEM IN THE PRIMARY COMBUSTION CHAMBER OF THE LABORATORY MICROMOTOR (U)

Test Number	Propellant Flow Rate (g/sec)	Mixture Ratio ($\dot{w}_o/\dot{w}_f$)	Primary Chamber Pressure (psia)	c*			c* efficiency	
				Expt'l. (ft/sec)	Theory 2[a] (ft/sec)	Theory 1[b] (ft/sec)	Theory 2[a] (%)	Theory 1[b] (%)
102[c]	14.37	1.16	428.7	5342	5992	6263	89.2	85.3
105	13.49	1.78	541.2	----[d]	5589	6112	----	----
106	14.81	1.23	378.7	4579	5949	6322	77.0	72.4
107	14.25	1.48	413.4	5195	5766	6257	90.1	83.0
108	11.59	2.79	540.8	----[d]	5303	5809	----	----
111	15.00	1.32	423.1	5051	5869	6328	86.1	79.8
112[c]	17.03	1.01	319.6	4710	6117	6117	77.0	77.0
113	15.88	1.21	342.0	5405	5961	6306	90.7	85.7
115	16.87	1.07	341.3	5078	6029	6153	84.2	82.5
116	14.94	1.25	302.5	5082	5896	6301	86.2	80.7
117	14.90	1.24	319.6	5384	5904	6296	91.1	85.5
118	14.97	1.25	294.4	4937	5976	6370	82.6	77.5
119	14.91	1.25	308.8	5198	5912	6318	87.9	82.3
120	20.80	1.34	402.6	4859	5859	6322	82.9	76.9
121	20.70	1.32	409.7	4967	5927	6384	83.8	77.8
122	20.78	1.33	422.1	5097	5893	6356	86.5	80.2

a - Theoretical c* values based on Kinetically-Limited Combustion Model, see Equation (2) of text.
b - Theoretical c* values based on Equilibrium Combustion Model, see Equation (1) of text.
c - Tests 102-111 were conducted using a 0.125 in. dia throat.
Tests 112-122 were conducted using a 0.148 in. dia throat.
d - Subsonic flow in primary nozzle resulted from high secondary chamber pressure.

CONFIDENTIAL

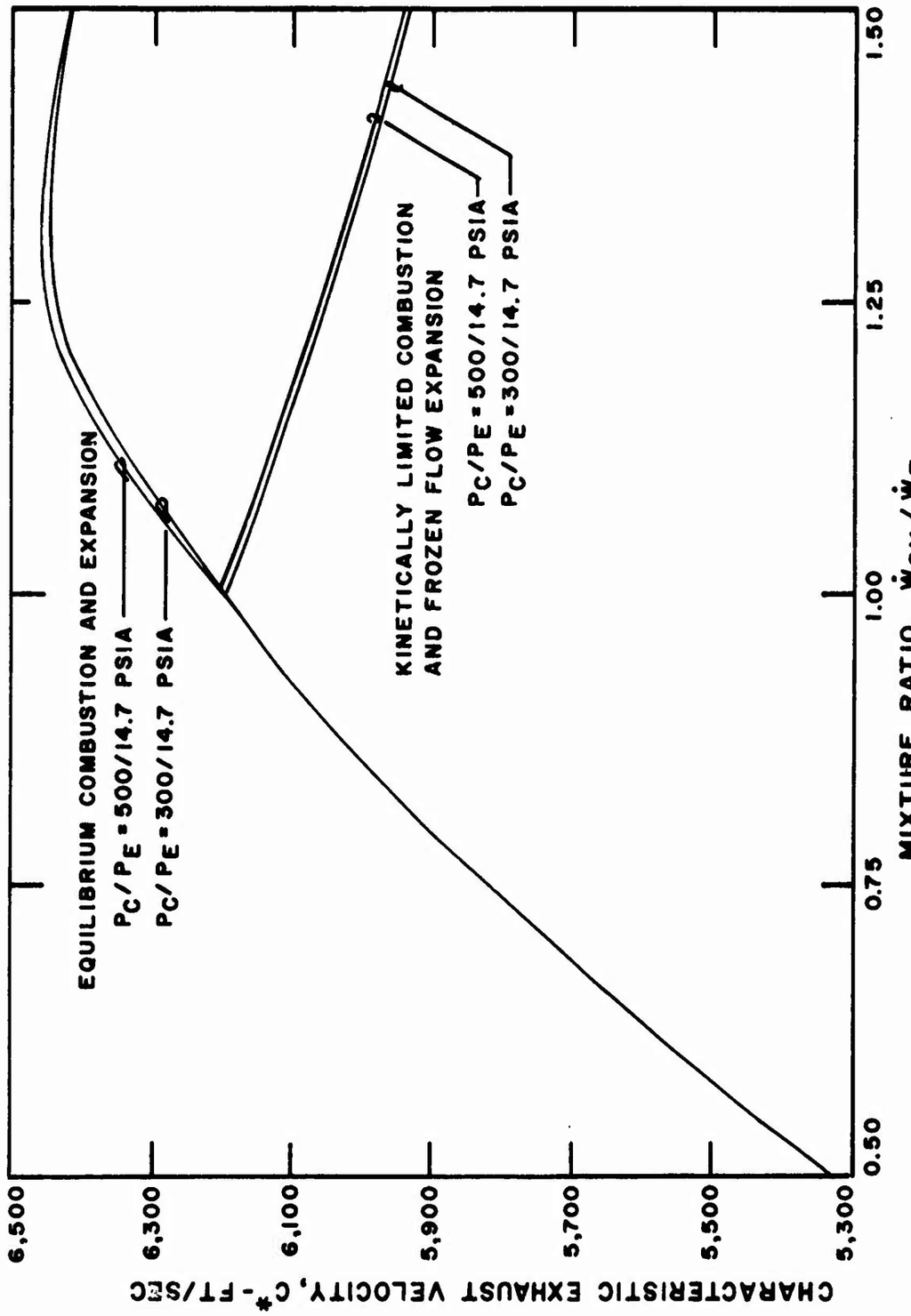

Figure 18. Theoretical c* Performance of the Hydrazine/Pentaborane System (u)

Equation (2) can be seen to be the resultant of Equations (3) and (4).

$$2.0\ N_2H_4 + B_5H_9 \rightarrow 4\ BN + B + 8.5\ H_2 \quad (3)$$

$$0.5\ N_2H_4 \rightarrow 0.25\ N_2 + 0.25\ H_2 + 0.5\ NH_3 \quad (4)$$

On the basis of these reactions, optimum performance is predicted to occur at the new stoichiometric mixture ratio, 1.01, as shown in Figure 18.

(U) In the present study, the experimentally determined values of the primary c* were compared with the theoretical values obtained on the basis of both combustion reactions. The theoretical values presented in Table II include the correction for the measured heat rejection rates in the primary chamber up to the nozzle throat.

(C) Examination of the data presented in Table II shows that primary combustion efficiencies, based on theoretical c* for Equation (2), are of the order of 80-90% with an average of 85.2%. These results are in agreement with the results obtained in the earlier study (Reference 2).

(U) Four tests were conducted using nitrogen instead of air as the secondary gas. The chief purpose of these tests was to provide base-line data for comparison with the c* performance obtained in the corresponding air-augmented tests. However, these tests also provide an independent check of the primary c* efficiencies obtained directly.

(C) Table III presents the primary c* efficiencies obtained in these tests along with the c* efficiencies determined in the secondary chamber. Comparison of these results indicates that the efficiency of the hydrazine/pentaborane combustion in this micromotor is on the order of 85%, in good agreement with the results obtained directly from the primary combustor data.

(U) These data also serve as a check on the reliability of the experimental test apparatus and the validity of calibration data. Inconsistencies in the results would indicate the existence of errors in the calibration data or measured parameters. The internal consistency of the data, therefore, indicates the absence of major errors.

(U) The minor variations in the c* efficiencies obtained by the two methods are random and suggest the existence of small random variations in the reproducibility of the measured variables. Comparison of the standard deviations of these two sets indicates that these small random variations have a greater impact on the results obtained from primary chamber measurements. However, inasmuch as the "true" combustion efficiencies may have varied within each set, the values of the standard deviations cannot be used as an index of the true precision of measurement. Appendix II of this report presents an error analysis which indicates the accuracy and precision of both the primary

TABLE III

CHARACTERISTIC VELOCITY EFFICIENCY OF THE HYDRAZINE/PENTABORANE SYSTEM IN THE LABORATORY MICROMOTOR USING NITROGEN AS THE SECONDARY GAS (U)

Test Number	c* Efficiency, %	
	Primary Chamber Data	Secondary Chamber Data
102	89.2	86.5
112	77.0	82.9
119	87.9	86.4
121	83.8	85.4
Average	84.5	85.3
Standard Deviation	±5.5	±1.7

and secondary c* measurements. The error analysis indicates that the probable error in the accuracy of the primary c* value is approximately 2%, while the probable error in the accuracy of the secondary c* value is approximately 1.5%. Therefore, the accuracy of the c* determinations is acceptable in both the primary and secondary systems.

(U) In several tests, notably Tests 105 and 108, the primary combustor operated in a subsonic mode because of high secondary chamber pressures. Inasmuch as the use of c* data as an index of performance is based on the assumption of sonic flow in the throat, values of c* which are calculated under subsonic throat conditions are invalid. The information required to determine whether sonic flow is obtained at the primary throat is provided in the computation of the theoretical c* performance. In the course of the computation, the primary throat pressure which corresponds to "choked" or sonic flow in the throat is calculated. Examination of the computed pressure data indicates that, in order for sonic flow to be achieved at the primary throat, the ratio of throat pressure to primary chamber pressure must be less than about 0.6. Therefore, if downstream pressures (secondary chamber pressures) are too high, then the primary throat pressure will be too high also, and the critical pressure ratio (throat-to-primary chamber) will be exceeded.

b. Performance of the Air-Augmented Hydrazine/Pentaborane System

(U) The principal effort on the test program was directed toward the determination of the characteristics of the secondary combustion in air of the exhaust of the hydrazine/pentaborane system. The test data obtained are presented in Table IV. These data were used to derive the values of the various parameters presented in Table V.

(U) The tests have been separated into two classes, based on the simulated flight regime. Thus, tests simulating Mach 2.5 flight at sea level utilized inlet air temperatures near 800°F and secondary combustion chamber pressures near 200 psia. Tests simulating Mach 4.0 flight at 40,000 ft altitude utilized inlet air temperatures near 1500°F and secondary chamber pressures near 50 psia.

(U) The characteristic velocity of the secondary combustion system was determined for each of the tests. Heat rejection rates in the secondary combustion chamber were also determined.

(U) The products resulting from the primary reaction include boron nitride, boron, hydrogen, ammonia, and nitrogen according to Equation (2).

TABLE IV

TEST DATA ON THE AIR-AUGMENTED HYDRAZINE/PENTABORANE SYSTEM IN THE LABORATORY MICROMOTOR (U)

Test[a] Number	Propellant Flow Rates N_2H_4 (g/sec)	B_5H_9 (g/sec)	Air (g/sec)	Air Temp. (°F)	Secondary Chamber Pressure (psia)	Secondary Nozzle Throat Area[b] (sq. in.)
102N	7.73	6.64	106.4	811.7	277.5	0.0779
105	8.64	4.85	126.5	811.3	485.6	0.0779
106	8.17	6.64	120.8	929.9	230.6	0.1684
107	8.50	5.75	256.9	668.2	286.1	0.2265
108	8.53	3.06	604.6	732.7	512.7	0.2165
111	8.56	6.44	609.3	752.3	176.9	0.7148
112N	8.56	8.47	117.3	837.3	142.5	0.1684
113	8.68	7.20	121.2	826.0	236.3	0.1619
115	8.73	8.14	247.9	828.9	201.7	0.3390
117	8.26	6.64	237.4	1354	63.5	1.0387
118	8.31	6.66	121.5	1545	49.6	0.7760
119N	8.28	6.63	117.9	1504	72.9	0.3526
120	11.90	8.90	168.6	815.8	180.1	0.3088
121N	11.80	8.90	157.1	808.1	157.6	0.1964
122	11.85	8.93	358.8	1138	72.6	1.2469

a - Tests in which nitrogen was used as the secondary gas are identified by N following the Test Number.

b - Secondary nozzle throat area based on post-test measurement for each test.

TABLE V

TEST PARAMETERS DERIVED FROM TEST DATA (U)

Test[a] Number	Simulated Mach No. Sea Level	Simulated Mach No. 40,000 ft	Primary Mixture Ratio	Air-to-Propellant Ratio
102N	2.64		1.16	7.41
105	2.64		1.78	9.38
106	2.85		1.23	8.16
107	2.37		1.48	18.03
108	2.50		2.79	52.2
111	2.54		1.32	40.6
112N	2.69		1.01	6.89
113	2.67		1.21	7.63
115	2.68		1.07	14.69
120	2.65		1.34	8.11
121N	2.64		1.32	7.59
117		4.25	1.24	15.93
118		4.53	1.25	8.11
119N		4.47	1.25	7.91
122		3.95	1.33	17.27

a - Tests in which nitrogen was used as the secondary gas are identified by N following the Test Number.

Consequently, the secondary combustion of these exhaust products in air will proceed according to Equations (4) and (5).

$$4.0\ BN + B + 8.5\ H_2 + 8.0\ O_2 \begin{cases} \nearrow 2.5\ B_2O_3 + 8.5\ H_2O + 2.0\ N_2 \\ \searrow 5.0\ HBO_2 + 6.0\ H_2O + 2.0\ N_2 \end{cases} \qquad (4)$$

$$0.5\ NH_3 + 0.25\ N_2 + 0.25\ H_2 + 0.5\ O_2 \longrightarrow 1.0\ H_2O + 0.5\ N_2 \qquad (5)$$

(U) The theoretical values of c* were calculated on the basis of the achievement of chemical thermodynamic equilibrium of all species present in the secondary combustion chamber, in accordance with the reactions of Equations (4) and (5) and other equations of minor significance. Theoretical calculations were made both with and without the heat-loss correction, based on the measured heat rejection rates.

(U) The results of the tests in the sea level/Mach 2.5 regime are presented in Table VI along with the pertinent test parameters. The corresponding tests using nitrogen as the secondary gas are also presented.

(C) These results indicate that in the low altitude/moderate Mach number regime, the secondary combustion of the hydrazine/pentaborane exhaust products, including the solid boron nitride and boron, proceeds very nearly according to theory. Comparison of the secondary efficiencies in the tests using nitrogen with those obtained using air indicates that the boron and boron nitride are consumed. Whereas the primary performance, as reflected in the c* efficiencies of the nitrogen tests, is significantly less than theoretical, the secondary performance in the air tests is very high.

(C) These results also indicate that the secondary combustion efficiency remains high as the air-to-propellant ratio is increased. The theoretical chamber temperature is very significantly reduced as the air-to-propellant ratio is increased. If the high chamber temperatures were required for efficient combustion of the boron and boron nitride, then the quenching effect resulting from increasing the air-to-propellant ratio would be reflected in a loss of efficiency in the secondary chamber. As the experimental results do not indicate a significant reduction in efficiency, it can be concluded that the quenching effect of the incoming air does not significantly reduce efficiency at air-to-propellant ratios up to about 50 in the sea level simulation tests. However, see the chemical analytical data reported in the next section (Tables VIII and IX).

(U) The results of the tests in the Mach 4.0/high altitude tests are presented in Table VII along with the pertinent test parameters.

TABLE VI

PERFORMANCE DATA ON THE AIR-AUGMENTED HYDRAZINE/PENTABORANE SYSTEM FOR THE SEA LEVEL/MACH 2.5 TESTS (U)

Test Number	Primary Mixture Ratio	Air-to-Propellant Ratio	Theoretical Chamber Temp. (°R)	Characteristic Length (in.)	Characteristic Velocity		c* Efficiency (%)
					Experimental (ft/sec)	Theoretical (ft/sec)	
105	1.78	9.38	380[illegible]	585	3945	4041	97.6
106	1.23	8.16	4480	273	4177	4317	96.8
113	1.21	7.63	4361	273	4151	4264	97.3
120	1.34	8.11	4511	131	4258	4344	98.6
107	1.48	18.0	3184	188	3490	3580	97.5
115	1.07	14.7	3582	131	3722	3880	95.9
108	2.79	52.2	1891	188	2638	2705	97.5
111	1.32	40.6	2400	62	2955	3035	97.4
102N	1.16	7.41	2053	585	2613	3021	86.5
112N	1.01	6.89	2212	273	2607	3146	82.9
121N	1.34	7.59	1991	238	2539	2974	85.4

CONFIDENTIAL

TABLE VII

PERFORMANCE DATA ON THE AIR-AUGMENTED HYDRAZINE/PENTABORANE SYSTEM FOR THE 40,000 FT ALTITUDE/MACH 4.0 TESTS (U)

Test Number	Primary Mixture Ratio	Air-to-Propellant Ratio	Theoretical Chamber Temp. (°R)	Characteristic Length (in.)	Characteristic Velocity Experimental (ft/sec)	Characteristic Velocity Theoretical (ft/sec)	c* Efficiency (%)
118	1.25	8.11	4695	62	4113	4469	92.0
117	1.24	15.9	3695	50	----[a]	3852	----[a]
122	1.33	17.3	3504	43	3478	3815	91.2
119N	1.25	7.91	2399	131	2824	3267	86.4

a - Subsonic flow in secondary nozzle resulted from high exhaust duct pressure.

The results obtained in the corresponding nitrogen test are also included for comparison.

(C) Comparison of the data obtained using nitrogen with those obtained using air indicates that the combustion of the hydrazine/pentaborane exhaust products does occur. At the higher air-to-propellant ratio, 16:1, no significant change in efficiency is observed.

(C) A slightly lower combustion efficiency was achieved in the secondary combustion reaction in the high altitude/high Mach number regime than was obtained previously in the low altitude/moderate Mach number regime at comparable air-to-propellant ratios. This lower efficiency was observed to occur in spite of the slightly higher chamber temperature in the higher Mach number simulation.

(C) Simulation of low altitude/Mach 2.5 was accomplished in the test program by supplying air heated to approximately 800°F at a chamber pressure of about 200 psia. On the other hand, simulation of high altitude/Mach 4.0 was accomplished by supplying air at approximately 1500°F at a chamber pressure of about 50 psia. Two important parameters were varied simultaneously: (1) temperature of the secondary air and (2) secondary chamber pressure. Therefore, changes observed in the secondary combustion efficiency must be related (directly or indirectly) to changes in these two parameters. As mentioned previously, however, the effect of the increased chamber temperature has little effect on combustion efficiency in the low altitude tests. Consequently, the secondary chamber pressure and parameters directly related to secondary chamber pressure appear to be factors which determine the efficiency of the combustion reaction.

c. Chemical Analysis of Secondary Exhaust Products

(U) Samples of both the solid and gaseous exhaust products were collected in several of the tests. Two Pitot-type sample taps were inserted in the exhaust duct at widely separated locations; the first tap, Sampling Station 1, was located immediately downstream of the secondary nozzle while the second, Sampling Station 2, was located approximately eleven feet downstream of Sample Station 1, at the exhaust diversion valve at the end of the water cooled exhaust duct. In addition, the main body of the solid exhaust products were collected in a glass fiber bag filter, Sampling Station 3, located fifteen feet downstream of the exhaust diversion valve. The samples obtained from the Pitot taps consisted of solid exhaust products, collected on Millipore filters, and gaseous exhaust products, collected in evacuated cylinders. Figure 19 is a photograph of the micromotor in the exhaust sampling and collection configuration.

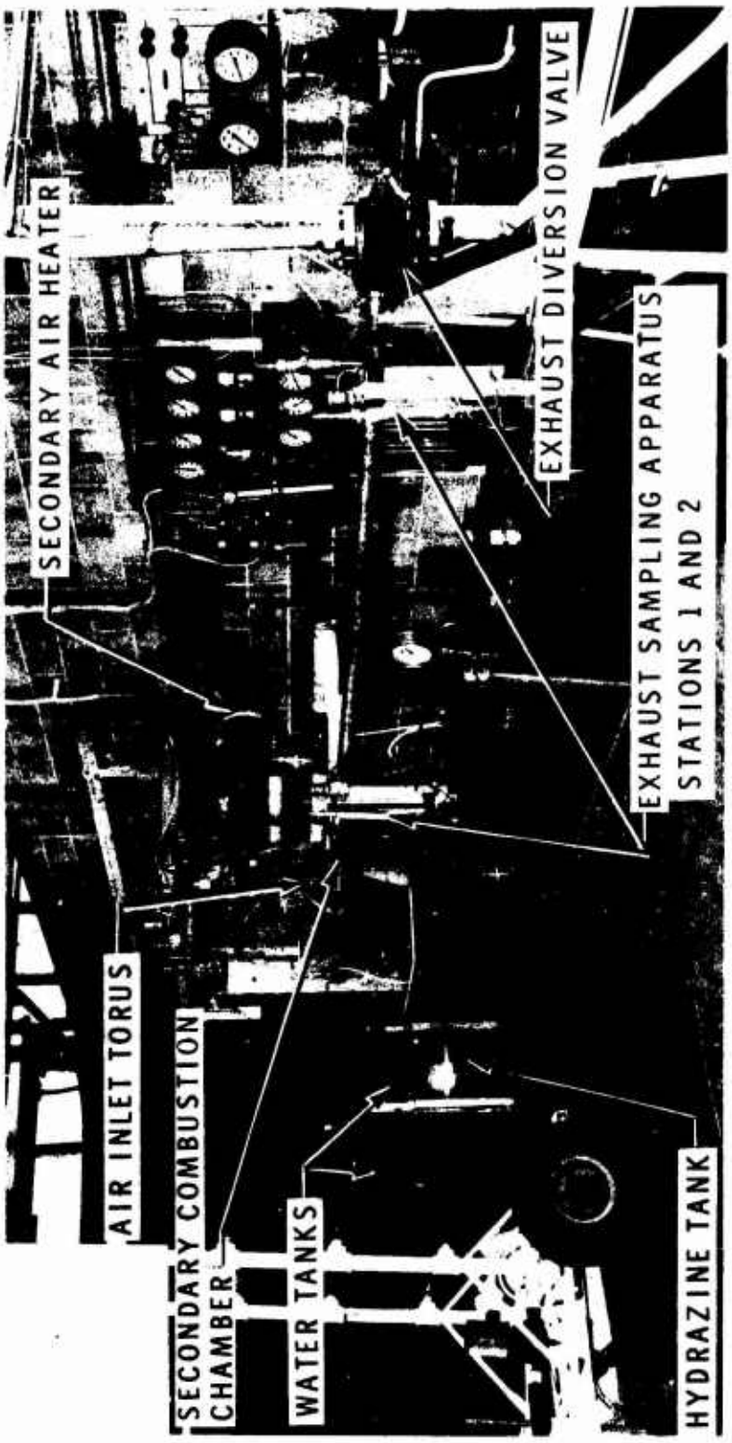

Figure 19. Micromotor in the Exhaust Sampling and Collection Configuration

(1) Analysis of the Solid Exhaust

(a) Background Information

(U) The solid exhaust products from the secondary chamber are boron and boron derivatives representing various stages of oxidation and hydration. These solids were expected to contain virtually any combination of the reactants and products shown in Equations (4) and (5). These include unreacted BN and B, and various boric acids and oxides. The presence of minor amounts of other species such as B-N-H polymers, higher boron hydrides and metal borides, was also expected.

(U) A flow diagram of the analytical procedure for determining the amounts of the major solid reaction products is presented in Figure 20. This approach will determine BN, B, H_3BO_3, HBO_2, $H_2B_4O_7$, B_2O_3, and various minor components. The determination of the various oxides and acids of boron is a major task of this analytical scheme which includes infrared analysis, emission spectroscopy, thermal decomposition, elemental analysis, and several wet chemical analyses.

(U) Both elemental boron and boron nitride yield boric oxide upon combustion with oxygen. In the presence of water, B_2O_3 can be hydrated to yield various boric acids; e.g.,

$$4\ H_3BO_3 \xrightarrow[103°C]{-4\ H_2O} 4\ HBO_2 \xrightarrow[191°C]{-H_2O} H_2B_4O_7 \xrightarrow[600°C]{-H_2O} 2\ B_2O_3 \qquad (6)$$

Orthoboric acid — Metaboric acid — Pyroboric acid (tetraboric acid) — Boric oxide

(U) The overall combustion reaction produces a large excess of water; therefore, it was expected that mixtures of boric oxide, pyroboric acid, metaboric acid and boric acid would be formed. Because of the H_2O-B_2O_3 reactions, the apparent composition tends to shift to the more highly hydrated boric acids if the solids are allowed to cool in the sampling apparatus.

(b) Analytical Procedures

(U) As indicated in Figure 20, the original sample is heated stepwise at 103, 191, and 600°C to constant weights, and the ortho-, meta-, and pyro-boric acids are calculated from the weight losses of water. The residue at 600°C contains mainly B_2O_3, BN, and B, with possible traces of boron carbide, metal borides, and metal oxides. The B_2O_3 is dissolved

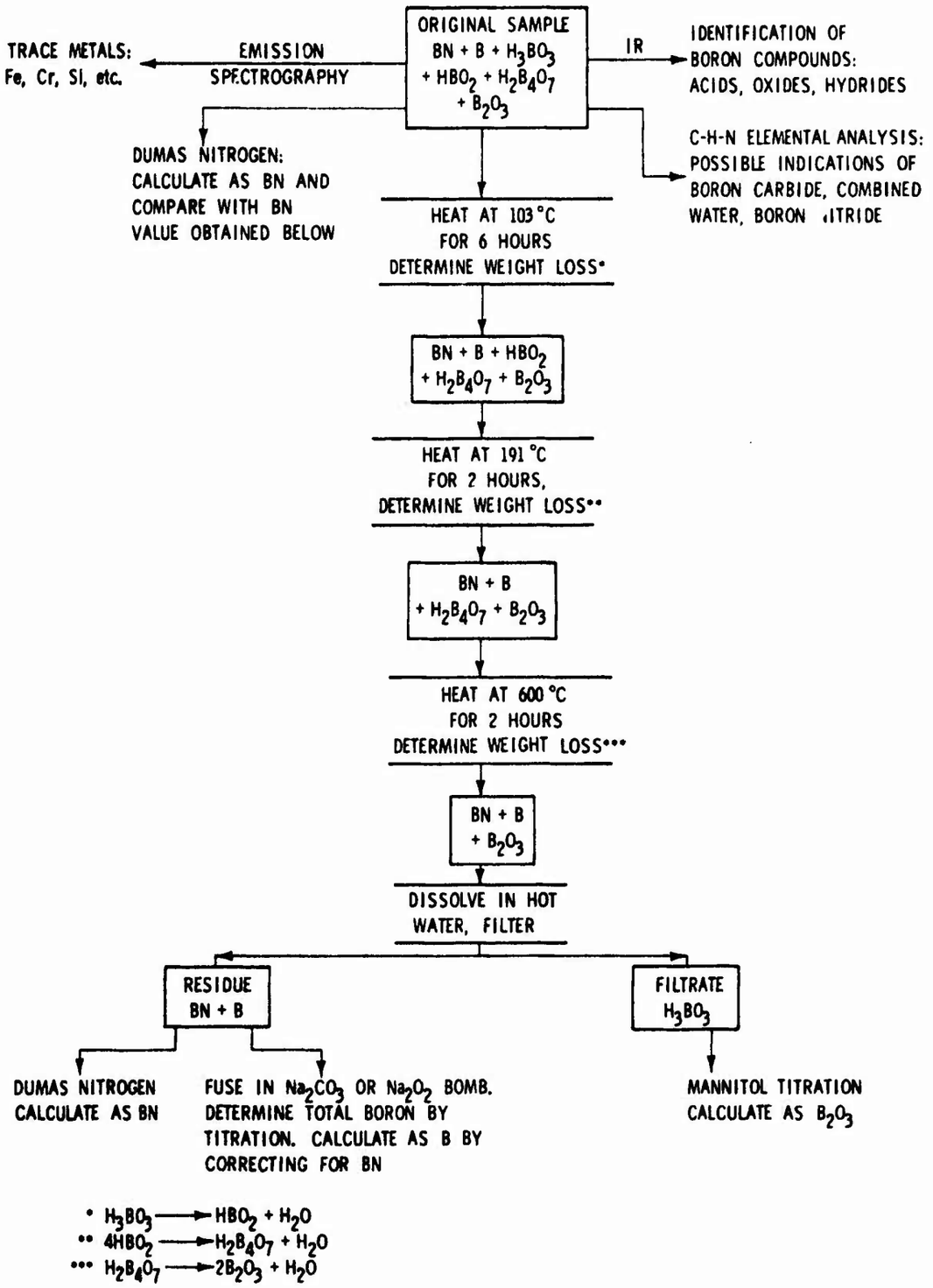

Figure 20. Systematic Chemical Analysis of Solid Exhaust Products

out in hot water and the total boron in the filtrate is determined and calculated as B_2O_3 by alkalimetric titration in the presence of mannitol. In addition, a direct check on this value is obtained from the weight of the residue after water leaching.

(U) The mannitol titrations are performed using a Metrohm automatic recording titrimeter in a procedure which is decidely superior and less subject to interferences than either the classical two-indicator method or the frequently recommended "idential-pH" procedure of Foote (Reference 3). Using the automatic recording titrimeter, the boron content is determined from actual inflections in a well defined titration curve to assure reliable results without interference. The response and plotting accuracy of this instrument is adequate, in fact, to provide useful inflections for boric acid ($pKa \simeq 9.2$) even without the addition of mannitol, which provides a complex of $pKa \simeq 5$. This provides added flexibility in cases of certain acidic interferences, as the boron can be titrated at either or both acid strengths to afford resolution from possible interferences.

(U) The residue of boron nitride plus elemental boron can be analyzed for BN by a modified Dumas method developed at Aerojet (Reference 4). This procedure, found superior to the Kjeldahl method, utilizes an especially effective silver vanadate/alumina catalyst with added cupric oxide to assure decomposition of the most refractory materials.

(U) An additional check of the nitride content can also be performed by analyzing the original sample of exhaust solids before the boric acids determinations. In the absence of any soluble nitrogen-bearing materials, the two analytical values should be identical.

(U) Elemental boron is finally determined by fusing the BN plus B residue with sodium carbonate in a platinum crucible, thus converting both compounds to soluble borates which can be readily determined by the mannitol titration. For added reliability, if the residue should prove exceptionally resistant to this treatment, the more vigorous sodium peroxide fusion can be used to bring the materials into solution. The elemental boron content is then calculated by subtracting the boron equivalent of the BN previously determined.

(c) Analytical Results

(U) Samples of the solid exhaust products were collected at all three stations during Tests 102, 105, 106, 107, and 108, which are representative of all air-to-propellant ratios in the low altitude/Mach 2.5 regime. In addition, solid samples were collected at Station 3 during Tests 117, 118, and 119, which are representative of air-to-propellant ratios of 8:1 and 16:1 in the high altitude/Mach 4.0 regime. Analyses of these solid samples were conducted as outlined in Figure 20. The results reported in weight percent, are presented in Table VIII.

TABLE VIII

ANALYSIS OF THE SOLID SECONDARY EXHAUST OF THE AIR-AUGMENTED HYDRAZINE/PENTABORANE SYSTEM (U)

Weight Percent

Test Number	102 (Nitrogen)			105 (A/P=9.38)			106 (A/P=8.16)			107 (A/P=18.0)		
Sampling Station	(1)	(2)	(3)	(1)	(2)	(3)	(1)	(2)	(3)	(1)	(2)	(3)
H_3BO_3	26.6	31.2	13.3	b	74.2	65.7	63.5	78.3	26.0	34.2	35.1	57.4
HBO_2	43.6	4.4	11.0		21.0	25.9	24.9	21.4	0.9	64.5	63.7	6.3
$H_2B_4O_7$	2.0	2.1	4.5		4.0	5.2	10.1	0.0	56.0	0.0	0.0	0.0
B_2O_3	0.0	0.0	0.0		0.0	0.0	0.0	0.0	15.9	0.0	0.0	35.2
B	13.1	34.1	30.1		0.0	0.0	0.0	0.0	0.2	0.0	0.0	0.3
BN	14.3	26.2	32.3		0.25	1.9	0.1	0.0	0.7	0.4	0.3	0.4
C	0.4	2.6	1.0		0.12	0.8	2.0	0.2	0.0	0.5	0.6	0.1
Total	100.0	100.6	92.2[a]		99.6	99.5	100.6	99.9	99.7	99.6	99.7	99.7

Test Number	108 (A/P=52.2)			117 (A/P=15.9)	118 (A/P=8.11)	119 (Nitrogen)
Sampling Station	(1)	(2)	(3)	(3)	(3)	(3)
H_3BO_3	98.0	88.9	33.4	6.81	32.4	12.7
HBO_2	0.0	0.0	20.8	25.8	25.2	2.09
$H_2B_4O_7$	0.0	0.0	11.3	34.0	11.3	1.29
B_2O_3	0.0	4.7	26.5	13.9	11.6	1.48
B	0.0	4.6	5.1	16.1	15.0	49.0
BN	0.0	1.2	1.0	1.25	1.09	17.4
C	0.11	0.11	0.1	<0.04	0.19	0.59
Total	98.1	99.5	98.2	97.9	96.8	99.5

a - Residual portion of sample consisted of metal particles.
b - Malfunction of sampling system prevented acquisition of sample.

CONFIDENTIAL

(U) Tests 102 and 119 were conducted using nitrogen as the secondary gas; therefore, the formation of boric oxide and boric acids was not expected. The analyses of the solid products from these tests showed oxides and acids were present. It is suggested that the nitrogen supply was contaminated with oxygen, probably as a result of residual air remaining in the storage tank after blow-down prior to filling the tank with nitrogen for the tests.

(U) These data indicate that water vapor in the secondary chamber, present as a contaminant or formed by the secondary combustion of hydrogen, is involved in the combustion of boron and boron nitride. This interpretation is discussed in a later section of this report.

(U) The purpose of the chemical analysis of the solid exhaust products from the secondary combustion chamber was to determine the completeness of combustion of the boron nitride and boron in the secondary chamber. The possibility existed that the continued oxidation of these materials downstream of the secondary nozzle but upstream of the bag filter could occur. Should this post-oxidation actually occur, then the analytical results obtained for samples collected at the bag filter would not be representative of the true secondary chamber exhaust species. Therefore, the collection and analyses of the exhaust species at Sampling Station 1 and 2 was undertaken to determine whether post-oxidation was occurring. The occurrence of post-oxidation in the exhaust duct would become apparent through differences in the boron and boron nitride content of the samples collected at the three sampling stations.

(U) Examination of the boron and boron nitride content of the samples collected at the three sampling stations during Tests 105, 106, 107, and 108 conclusively demonstrated the absence of post-oxidation in the system.

(U) The analytical data for the bag filter samples presented in Table VIII were used to determine the completeness of combustion of the boron and boron nitride in the secondary chamber under the varied test conditions. These results are summarized in Table IX.

(C) In the low altitude/Mach 2.5 regime, the combustion of the boron and boron nitride proceeds virtually to completion in the secondary combustion chamber at moderate air-to-propellant ratios. At the very high air-to-propellant ratios, the extent of combustion of these species is lower than at the moderate air-to-propellant ratios. These results suggest that the combustion reactions of the solid boron and boron nitride are too slow at the lower chamber temperature to achieve complete combustion. Residence time does not appear to be a significant factor in this instance, as will be discussed in a later section.

TABLE IX

EXTENT OF SECONDARY COMBUSTION OF BN AND B (U)

Simulated Flight Condition	Test Number	Air-to-Propellant Ratio	% of Available Boron Oxidized
Sea Level/Mach 2.5	105	9.38	95.6
	106	8.16	98.8
	107	18.0	98.0
	108	52.2	80.2
40,000 ft/Mach 4.0	118	8.11	54.6
	117	15.9	56.0

(C) In the high altitude/Mach 4.0 regime the combustion of the boron nitride proceeds virtually to completion, while the combustion of the elemental boron appears to occur to a very limited extent, if at all. Again, these results verify the earlier observation that the low chamber pressures involved in these tests produced a detrimental effect on the combustion efficiency through the inhibition of elemental boron combustion. On the other hand, the combustion of boron nitride is not inhibited and proceeds virtually to completion.

(2) Analysis of the Gaseous Exhaust

(a) Background Information

(U) A consideration of the reactants and products of Equations (4) and (5) indicated that the major gaseous exhaust species from the air augmentation stage are nitrogen and water, various proportions of the excess oxygen, and possibly minor amounts of unoxidized ammonia and hydrogen. Traces of pentaborane, hydrazine, other boron hydrides, nitrogen oxides, and various degradation or side reaction products were also considered to be present, but probably not in concentrations of practical significance.

(U) It should be noted that it was not expected that the gas analyses would be as useful as the solids data in appraising the combustion reaction characteristics. Nevertheless, the critical evaluation of subtle differences in gas compositions from combustion tests employing varied experimental parameters, in conjunction with the solids analyses, was expected to be of assistance in the development of combustion models. For example, correlation of the water analyses and the determined boric oxide-hydrate data could assist in reaching more definitive conclusions regarding the distribution of these species. In another case, the unburned boron, boron nitrides, ammonia, and hydrogen should correlate with the oxygen data and provide further evaluation of combustion efficiencies attainable under controlled experimental parameters. Minor amounts of nitrogen oxides, boron hydrides, etc., appearing in the exhaust gases would offer insight into adverse side-reactions that could be initiated under cetain conditions.

(U) In summary, the precise definition of combustion characteristics by gas analysis alone would be difficult, largely because of the large excess of air that was normally encountered. Nevertheless, these gas analyses were valuable as an adjunct to the more definitive solids examinations in providing the additional information required.

(b) Analytical Procedures

(U) Modern gas analysis is primarily accomplished through rapid instrumental techniques which have been developed to a high degree of perfection. The major tools commonly used in the analysis of gases are mass spectrometry, gas chromatography, and infrared absorption spectrophotometry. The gaseous exhaust compositions encountered in this program

posed no problems and the gas analyses were adequately performed by conventional mass spectrometry.

(c) Analytical Results

(U) The compositions, reported in mole percent, of the gas samples collected at Sample Stations 1 and 2, the Pitot sampling taps, are presented in Table X. In addition, the theoretical composition of the gas samples are presented. These theoretical values are based on complete oxidation of the boron nitride, boron, hydrogen, and ammonia in the secondary chamber and on the measured flow rates of the propellants and air.

(U) The analyses of the samples taken during Test 102 are of interest, particularly as they relate to the corresponding solid samples. The presence of relatively large amounts of water in the gas samples indicated that contamination of the secondary nitrogen had occurred.

(C) Comparison of the compositions of the gas samples as determined by mass spectrometry with the theoretical compositions based on the measured flow rates demonstrates the excellent agreement of experimentally determined values and theory. The absence of hydrogen and ammonia in the gaseous exhaust products from the air tests confirms the conclusion that the combustion of these species is complete. The absence of ammonia in secondary exhaust from the nitrogen tests indicates that the thermal degradation of the ammonia also occurs in the secondary chamber.

d. Temperature Profile Measurements in the Secondary Combustion Chamber

(U) The measurement of the temperature profiles in the secondary combustion chamber was undertaken to achieve two important objectives: (1) to obtain an indication of the progress of mixing of the primary exhaust and the secondary air and (2) to obtain an indication of the progress of the combustion reactions in the secondary combustion chamber.

(U) Protection of the thermocouples from complete destruction prior to the acquisition of the requisite data was of major concern. Therefore, the thermocouple junctions were inserted into the secondary chamber to a depth of one-sixteenth inch. It was recognized that the absolute values of recorded temperatures probably would not represent either main stream temperatures or the gas film temperatures; rather the recorded temperatures would be intermediate between these two zones and would reflect changes occurring in each. The order in which the tests were conducted was selected to prolong the life of the thermocouples as much as possible, consistent with making as few changes in the system as possible between tests.

(U) The micromotor configuration used in conducting these tests is shown in Figure 21. The chamber was fitted with eight tantalum-shielded tungsten-rhenium thermocouples. The thermocouples were placed in pairs at

TABLE X

ANALYSIS OF THE GASEOUS SECONDARY EXHAUST OF THE AIR-AUGMENTED HYDRAZINE/PENTABORANE SYSTEM (U)

Mole Percent

Test No.	102 (Nitrogen)			105 (A/P=9.38)			106 (A/P=8.16)			107 (A/P=18.0)			108 (A/P=52.2)		
Sampling Station	(1)	(2)	Theory[a]	(1)	(2)	Theory	(1)	(2)	Theory	(1)	(2)	Theory	(1)	(2)	Theory
N_2	83.7	78.4	80.0	b	91.6	87.4	92.5	97.22	93.8	86.3	82.6	83.8	80.5	80.4	79.0
O_2	0.0	0.5	0.0		4.9	4.4	5.99	1.20	0.0	12.6	15.6	12.2	18.1	18.4	18.2
A	0.13	0.13	0.0		1.13	0.96	0.92	1.09	1.04	0.98	0.98	0.96	0.93	0.93	0.92
CO_2	0.0	0.0			0.1		0.13	0.16		0.11	0.10		0.09	0.10	
H_2	6.4	18.7	20.0		0.00	0.00	0.13	0.03	0.54	0.00	0.00	0.00	0.00	0.00	0.00
H_2O	9.4	2.3	0.0		1.9	7.3	0.26	0.12	4.65	0.00	0.74	3.00	0.39	0.23	1.86
He	0.0	0.0			0.0		0.0	0.0		0.0	0.0		0.0	0.0	
NH_3	0.0	0.0			0.0		0.02	0.0		0.0	0.0		0.0	0.0	
NO	0.0	0.0			0.3		0.01	0.18		0.0	0.0		0.0	0.0	
N_2H_4	0.3	0.0			0.0		0.0	0.0		0.0	0.0		0.0	0.0	
B_5H_9	0.0	0.0			0.0		0.03	0.0		0.0	0.0		0.0	0.0	

a - Theoretical values are based on the following reaction sequence:

$$B_5H_9 + 2\ N_2H_4 = 4\ BN + B + 8.5\ H_2$$

$$N_2H_4 = N_2 + 2.0\ H_2$$

$$2\ H_2 + O_2 = 2\ H_2O$$

$$4\ BN + 6\ H_2O + 3\ O_2 = 4\ H_3BO_3 + 2\ N_2$$

$$B + 1.5\ H_2O + 0.75\ O_2 = H_3BO_3$$

b - Malfunction of Station 1 Sampling System.

CONFIDENTIAL

Figure 21. Micromotor in the Secondary Chamber Temperature Profile Configuration

four equally spaced locations along the length of the secondary chamber. One of each pair of thermocouples was in line with one of the air inlet ports in the air injector, while the other thermocouple of each pair was located midway between air inlet ports. Each thermocouple was inserted so that it penetrated the stream to a depth of 1/16 in.

(U) Temperature profile measurements were made at each of the test conditions studied. The results of these measurements are presented graphically in Figures 22, 23 and 24. Also included are several representative profiles resulting from the flow of the hot secondary air (or nitrogen) through the secondary combustion chamber prior to the ignition of the primary engine.

(U) Examination of the prefire profiles, shown in Figure 22, reveals that, as the secondary gas flows down the chamber, it is cooled to a greater or lesser extent depending on the gas flow rate; the greater the flow rate, the less cooling that is achieved by the cooling jacket. At the low flow rates both nitrogen and air show very nearly the same cooling rates, as expected.

(C) Consideration of the steady-state temperature profiles obtained in the low altitude/Mach 2.5 simulation tests, Figure 23, shows that, at the low air-to-propellant ratios, the in-line and not-in-line profiles converge to the same temperature very near Station 4. This convergence to a homogeneous temperature indicates that the mixing of the gas streams is complete and uniform temperatures prevail throughout the gas stream through the remaining portion of the chamber. In the case of the very high air-to-propellant ratio test, Test 111, the profiles appear to converge well downstream of Station 4. The mixing of the gas streams is not complete at Station 4 and may not be complete before reaching the secondary nozzle. These results provide evidence that the lower mixing efficiency, reduced residence time, and lower chamber temperature in the very high air-to-propellant ratio test are responsible for the presence of both boron and boron nitride in significant quantities in the exhaust products.

(U) The temperature profiles obtained in the high altitude/Mach 4.0 regime are shown in Figure 24. These profiles are somewhat different in appearance from those discussed above. It should be noted that part of this difference in appearance is the result of withdrawing the thermocouples to a depth of only about one-thirty-second of an inch. This change was made because the Station 1 thermocouples were burned out during the course of the 8:1 and 16:1 air-to-propellant ratio tests discussed above.

(C) The measurements shown in Figure 24 again demonstrate the convergence of the in-line and not-in-line profiles to a homogeneous temperature very near the Station 4 thermocouple; this indicates the mixing of the gas streams is complete at or near Station 4. However, in the high altitude/Mach 4.0 profiles the Station 1 and 2 thermocouples run somewhat cooler and

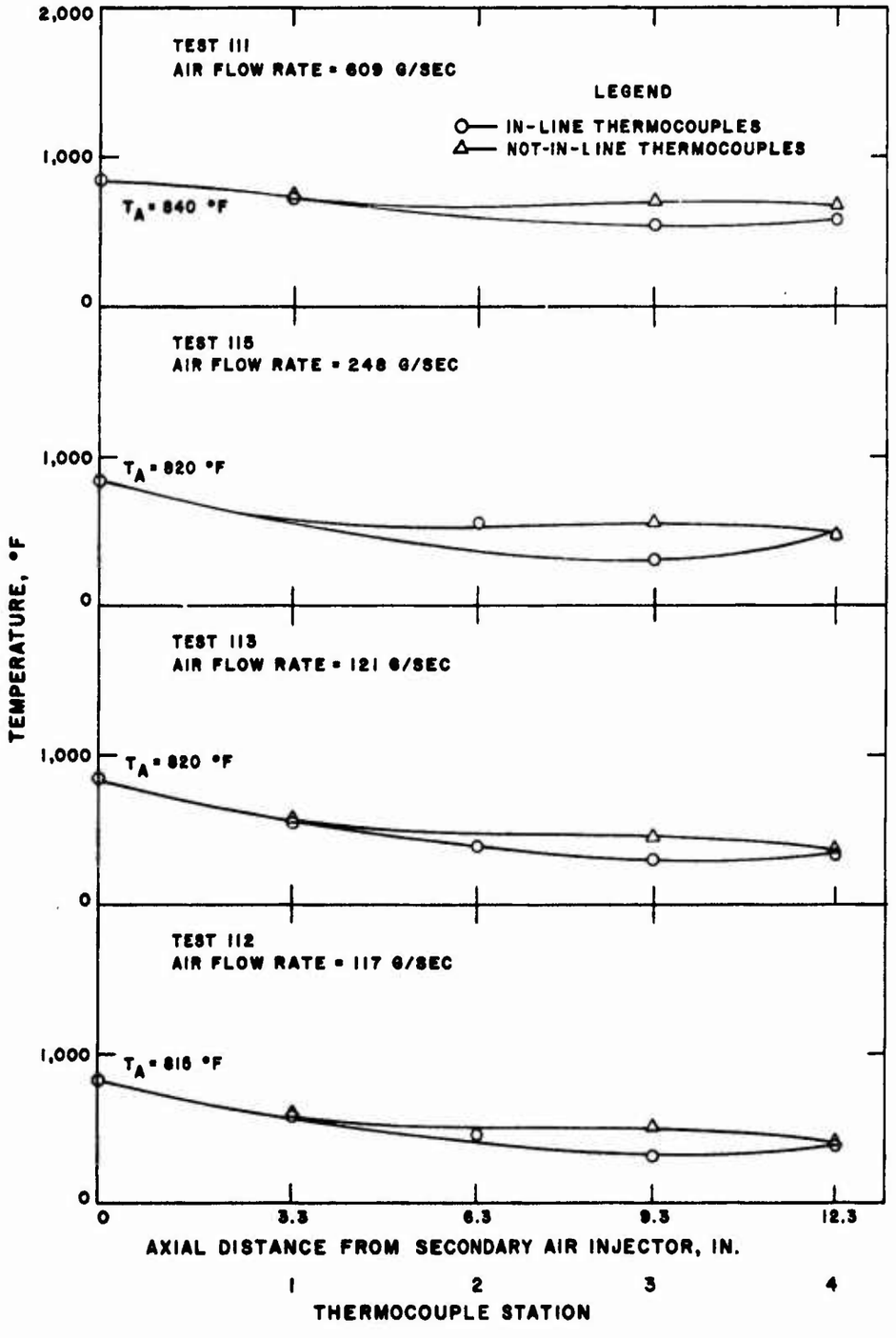

Figure 22. Prefire Temperature Profiles in Sea Level/Mach 2.5 Regime

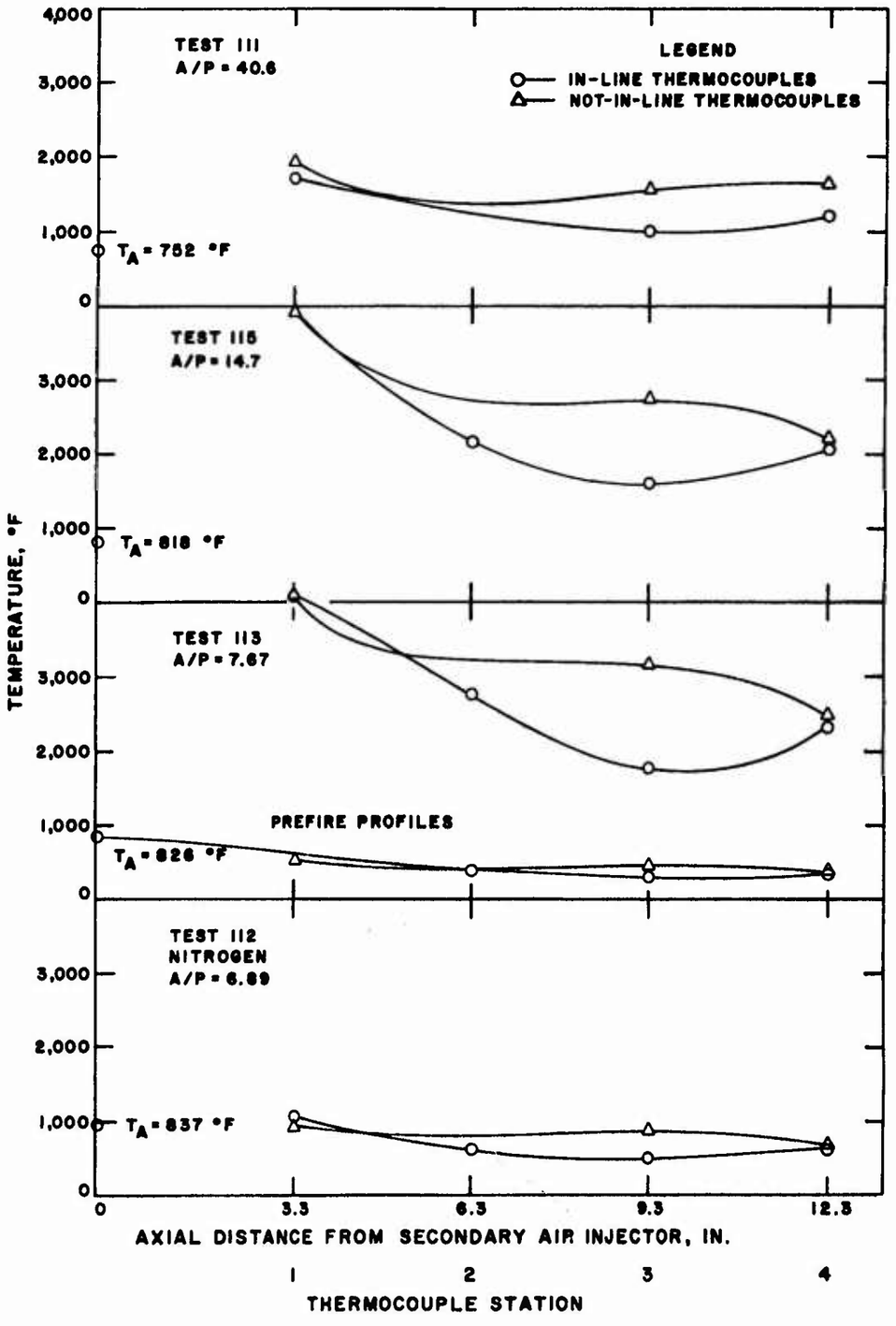

Figure 23. Steady-State Temperature Profiles in Sea Level/Mach 2.5 Regime

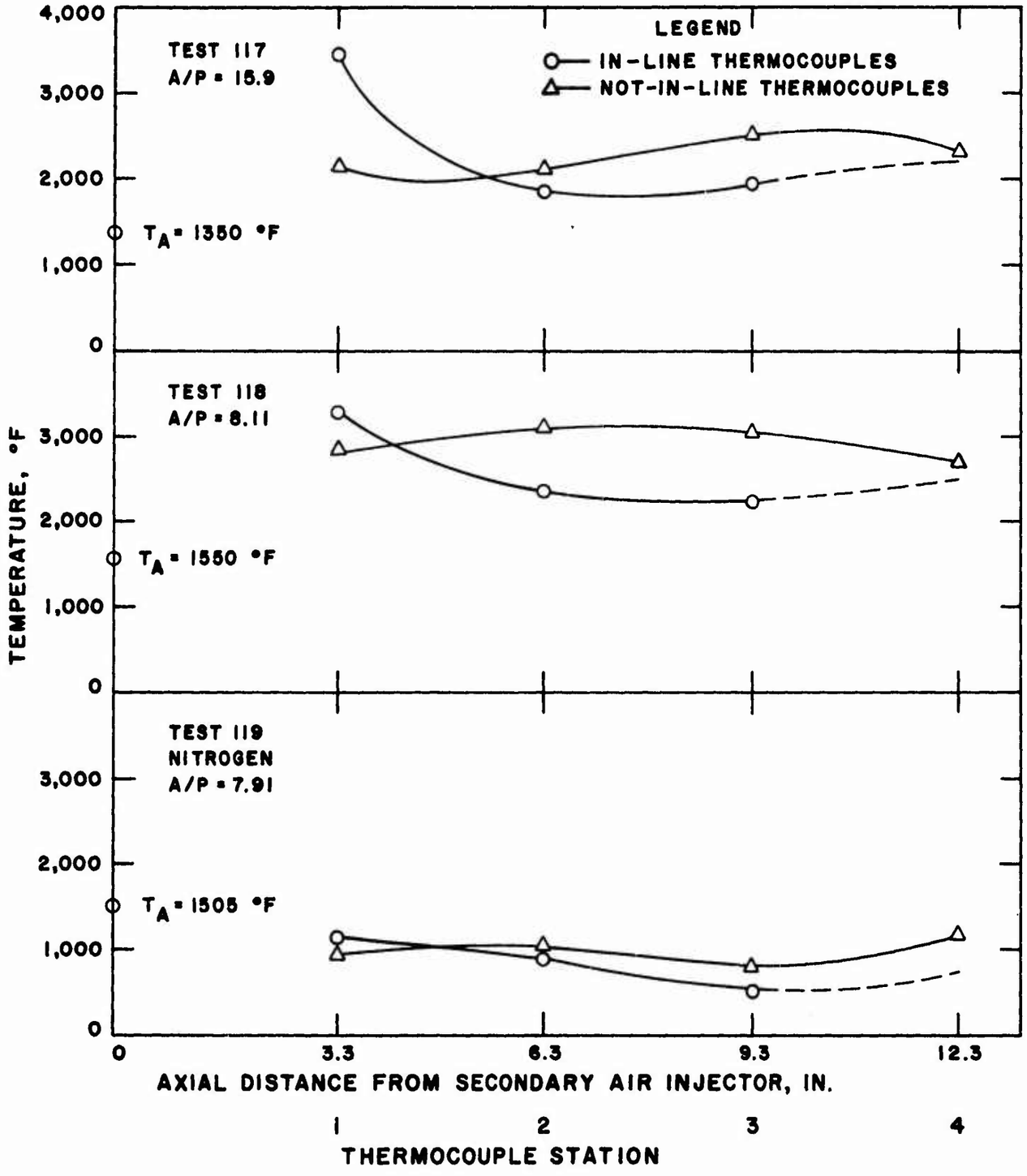

Figure 24. Steady-State Temperature Profiles in 40,000 ft/Mach 4.0 Regime

(This page is Unclass

the Station 3 and 4 thermocouples run somewhat hotter than the corresponding thermocouples under similar conditions in the low-altitude/Mach 2.5 profiles. This is believed to be brought about by the higher linear gas-velocity in the high altitude/Mach 4.0 tests. The lower chamber pressure and shorter reaction time tend to produce a more uniform linear distribution of temperatures.

(C) The temperature profiles observed in both the low altitude/Mach 2.5 and high altitude/Mach 4.0 regimes reflect similar patterns. The similarities of these patterns indicate that the mixing and combustion processes which occur in the secondary combustion chamber are reasonably consistent. The in-line profiles show a pattern characterized by a high Station 1 temperature, a rapid decrease to a minimum temperature at Station 2 or Station 3, and finally a slight rise at Station 4. The not-in-line profiles, on the other hand, show a high Station 1 temperature, a low Station 2 temperature, a second maximum in the vicinity of Station 3 and finally a decrease at Station 4.

(C) These patterns suggest a relatively consistent process of mixing and combustion under both simulated conditions. Changes in inlet air temperature, chamber pressure, and mass flow rate affect these mixing and combustion processes only slightly, except at the very high air-to-propellant ratios.

(C) The nature of the in-line temperature profiles suggests that the initial mixing and combustion of the primary exhaust and the secondary air streams are sufficient to produce the very high temperatures observed at Station 1. The major portion of the combustion process appears to occur just upstream of Station 1. As the gases proceed through the secondary chamber along the in-line streamline, heat is dissipated to the cooling jacket and only limited combustion occurs near Stations 2 and 3. Near Station 4 the gases along this streamline absorb heat from the main body of the plasma at a greater rate than it dissipates heat to the jacket, resulting in the observed temperature rise.

(C) The nature of the not-in-line profiles suggests that the initial mixing of the two gas streams along this streamline is sufficient to permit appreciable combustion at or near Station 1. Downstream at Station 2, continued mixing and combustion partly offset the dissipation of heat to the jacket while still further downstream at Station 3 mixing and combustion more than offset the cooling effect of the jacket, with an attendent rise in temperature. At Station 4 the mixing and combustion processes have been completed and the entire plasma is nearly homogeneous.

(C) The temperature profile data provide important information concerning the mixing and combustion phenomena occurring in the secondary combustion chamber. These data also support the conclusion that in both the low altitude/Mach 2.5 regime and the high altitude/Mach 4.0 regime, the air-augmented hydrazine/pentaborane system operates very efficiently up to air-to-propellant ratios approaching 40:1.

3. PHASE III, INTERPRETATION OF MICROMOTOR TEST RESULTS

(U) Phase III was concerned with the development of a theoretical model of the combustion process or processes. Correlation between the various experimental parameters was made through theoretical chemical and physical considerations.

a. Primary Combustion Process

(C) The combustion process which occurs in the primary chamber has been the subject of extensive study both at Aerojet and elsewhere (References 1 and 2). The theoretical reaction which yields the highest specific impulse and which is thermodynamically favored is represented by Equation (1).

$$B_5H_9 + 2.5\ N_2H_4 \rightarrow 5\ BN + 9.5\ H_2 \qquad (1)$$

However, analyses of the combustion products, both gaseous and solid, and experimental performance tests indicated that this optimum process does not occur. Rather, the reactions which most satisfactorily account for the observed combustion products and performance are shown in Equations (3) and (4).

$$B_5H_9 + 2\ N_2H_4 \rightarrow 4\ BN + B + 8.5\ H_2 \qquad (3)$$

$$0.5\ N_2H_4 \rightarrow 0.5\ NH_3 + 0.25\ N_2 + 0.25\ H_2 \qquad (4)$$

(C) The performance measurements made during the course of the present study confirm these earlier results. Furthermore, these results suggest that the performance of the primary system suffers significantly as the result of the decomposition of both propellants. The monopropellant decomposition of hydrazine follows Equation (4), while the pyrolytic decomposition of pentaborane follows Equation (7).

$$B_5H_9 \rightarrow 5\ B + 4.5\ H_2 \qquad (7)$$

(C) The theoretical thermochemical calculations indicate that boron should be converted to boron nitride in the presence of nitrogen under the conditions of the primary chamber. This reaction does not occur, however, as has been thoroughly demonstrated both in the earlier study and in the present study. A high boron content of the solid exhaust products was observed in the tests in which nitrogen was employed as the secondary gas. The thermochemical calculations indicate that the boron should be converted to boron nitride under these conditions also. Therefore, it is again concluded that the conversion of the boron to boron nitride is kinetically limited and does not occur under these conditions. Therefore, the loss of performance attendent with the thermal decomposition of pentaborane is not recoverable in the primary combustion chamber.

(C) The earlier study led to the postulate that the combustion of the pentaborane/hydrazine system involves the initial formation of an underoxidized adduct, i.e., $B_5H_9 \cdot 2\ N_2H_4$, with subsequent decomposition to boron nitride. Thus, for maximum performance to be achieved, the adduct must be formed before pentaborane decomposition occurs. Any method of assuring intimate mixing of the propellants, and hence the formation of the adduct, before monopropellant and pyrolytic decomposition sets in will have a modest beneficial effect on the primary combustion process and the performance of this bipropellant system.

b. Secondary Combustion Process

(C) The performance of an air-augmented rocket is primarily dependent on the efficiency of the secondary combustion process that takes place with the fuel-rich primary exhaust and air. A thorough understanding of the secondary combustion mechanism and the parameters that affect it are required to permit the selection of appropriate propellant formulations. Propellants for air-augmentation applications are characterized by high metal content (e.g., boron slurries, pentaborane, and boron-loaded solid propellants). Because of the high metal content of these propellants, the combustion in air of unburned metal particles or of intermediate metal compounds formed in the primary rocket chamber becomes the controlling factor in determining secondary combustion efficiency.

(C) In the present study, the products from the primary combustion reaction consist of both gases and solids. These species include hydrogen, ammonia, and nitrogen gases and solid boron and boron nitride. This system, therefore, offered an excellent opportunity to study the combustion processes involved in the combustion of boron-loaded fuels for air-augmentation application.

(C) The combustible gases in the primary exhaust ignite as they mix with the air. Hydrogen and ammonia have relatively wide flammability limits and low ignition temperatures. Hence the combustion of these gases was expected and, in fact, was found to occur rapidly and completely in the secondary combustion chamber. However, the extent to which combustion of the solid exhaust products occurred in the secondary chamber was questionable, prior to the acquisition of the data reported here.

(C) Several factors contributed to the uncertainty of whether combustion of the solid exhaust products, boron nitride and boron, would occur. One important parameter was the fact that the combustion of the hydrogen-rich, gaseous exhaust products in air generates substantial heat; however, the effective transfer of this energy to the particulate material and subsequent ignition thereof could not be assured. Secondly, because the incoming air temperature was substantially lower than the temperature of the hydrogen-air flame, the quenching effect could also have been sufficiently great to prevent the combustion of the solid products.

(C) The experimental data obtained in the low altitude/Mach 2.5 regime offers strong evidence that the solid exhaust products, as well as the gaseous exhaust products, are completely consumed. The high c* efficiencies and the chemical composition of the solid samples collected at the various stations indicate that the boron nitride and boron are very nearly completely burned in the secondary chamber in the lower air-to-propellant ratio tests (8:1 and 16:1). In the case of the high air-to-propellant ratio tests (50:1), the combustion of the BN and B is 80% complete.

(C) The performance and chemical analytical data were substantiated by the temperature profile measurements. In the 8:1 and 16:1 tests, the temperature profile measurements indicated that a homogeneous gas temperature is achieved just downstream of the Station 4 thermocouple, while the chemical analyses indicated nearly complete combustion of the solids had occurred. In the 50:1 tests, the profiles indicate that a substantial temperature differential still existed in the secondary chamber well downstream of Station 4; these data substantiate the slightly lower combustion efficiency of boron and boron nitride as indicated by the analytical data.

(C) The incomplete combustion of the boron and boron nitride at the very high air-to-propellant ratios suggests that the quenching effect of the secondary air, combined with the reduced residence time of the components, tends to reduce the combustion efficiency in this regime.

(C) In the high altitude/Mach 4.0 regime, on the other hand, the experimental evidence indicates that, in addition to the combustion of the gaseous products, only the combustion of boron nitride occurs in the secondary chamber. The analytical data show that only small amounts of boron nitride remain in the secondary exhaust, while relatively large amounts of elemental boron remain. Also, the slightly lower c* efficiencies obtained under these conditions suggests incomplete combustion.

(C) The two flight simulation conditions differ in four important parameters: (1) secondary air temperature, (2) secondary combustion chamber pressure, (3) chamber residence time, and (4) secondary chamber temperature. Thus, the incomplete combustion of elemental boron in the high altitude/Mach 4.0 regime must be related to one or more of these parameters.

(C) It is doubtful that the increased air inlet temperature, per se, would inhibit the elemental boron combustion; on the contrary, increased air temperature should improve combustion. Similarly, the slightly higher secondary chamber temperature in the high altitude/Mach 4.0 regime should improve combustion. Therefore, these factors may be considered to be beneficial to the combustion of boron, rather than detrimental.

(C) The chamber residence time is directly related to both chamber pressure and chamber temperature. To a first approximation, the relationship of residence time, t, to other parameters is:

$$t = (V_c M/R)(P_c/T_c \dot{w})$$

where V_c = volume of the secondary chamber

M = average molecular weight of gaseous plasma

R = gas constant

P_c = secondary chamber pressure

T_c = secondary chamber temperature

$\dot{w}$ = total mass flow-rate

This equation was employed to calculate the approximate stay times for the tests in which solid secondary exhaust products were analyzed. The quantity $V_c M/R$ remained nearly constant throughout the tests. Table XI summarizes the results of these calculations for the pertinent air tests. Thus, it is apparent that the slightly higher chamber temperature and much lower chamber pressure in the high altitude/Mach 4.0 regime significantly lower the residence time.

(C) If one assumes that boron nitride and elemental boron have approximately equal reaction rates, then the shorter residence time in the high altitude/Mach 4.0 regime would be expected to reduce the combustion efficiency of boron nitride as well as the elemental boron. On the other hand, if the boron nitride reaction rate is an order of magnitude greater than that of elemental boron, then the shorter residence time may have a significant effect on elemental boron combustion but not on the boron nitride. Thus, the chamber residence time may not be ruled out as a significant factor in the boron combustion efficiency.

(C) The secondary chamber pressure, per se, may also be a very important factor in the efficiency in the boron combustion. The chemical equations for the combustion reactions may be written as follows.

$$B + 0.75\ O_2 \rightarrow 0.5\ B_2O_3 \quad (8)$$

$$B + 0.75\ O_2 + 0.5\ H_2O \rightarrow HBO_2 \quad (9)$$

$$B + 1.5\ H_2O \rightarrow 0.5\ B_2O_3 + 1.5\ H_2 \quad (10)$$

$$B + 2\ H_2O \rightarrow HBO_2 + 1.5\ H_2 \quad (11)$$

Examination of these equations from a kinetic standpoint reveals that the higher chamber pressure would increase significantly the reaction rate of

TABLE XI

SECONDARY COMBUSTION CHAMBER STAY-TIME (U)

Test Number	Chamber Pressure (psia)	Chamber Temperature[a] (°R)	Total Mass Flow-Rate (g/sec)	Secondary Stay-Time (msec)	% Available Boron Oxidized
105	485.6	3802	140.0	28.3	95.6
106	230.6	4480	135.6	11.8	98.8
107	286.1	3184	271.1	10.3	98.0
108	512.7	1891	616.2	13.6	80.2
117	63.5	3695	252.3	2.11	54.6
118	49.6	4695	236.5	1.39	56.0

a - Theoretical Chamber Temperature with heat-loss correction.

the boron. In each of these reactions, as in most heterogeneous reactions (Reference 5), the rate-controlling step is very likely to be the adsorption of the gaseous reactant (water vapor, oxygen, or both) on the surface of the boron particle. This process is highly dependent on the partial pressure of the reactant gas. As examples, the reaction rate for Equation (8) would be proportional to the 0.75 power of the partial pressure of oxygen whereas the reaction rate for Equation (11) would be proportional to the square of the partial pressure of water vapor.

(C) The importance of the effect of chamber pressure in promoting the combustion of the boron and boron nitride is well illustrated in the results of Test 108. The combustion of these solids proceded to the extent of 80% of the available boron in this high pressure test in spite of the drastic reduction in chamber temperature resulting from the high air flow rate.

(C) On the basis of these considerations, the secondary chamber pressure has a very profound effect on the efficiency of boron combustion. The lower chamber pressure produces two adverse affects: (1) it materially reduces the residence time of the combustion mixture and (2) reduces the adsorption rate of reactant gases on the solid surface and, hence, reduces the reaction rate. Therefore, if one assumes that the rate of combustion of boron is directly proportional to the secondary chamber pressure, then the overall effect of reducing the secondary chamber pressure from 200 psia to 50 psia would be to reduce the elemental boron combustion efficiency by a factor of about 16.

(C) The combustion of the boron nitride appears to be unaffected by the changes in the flight simulation conditions. Therefore, it may be concluded that the rate of combustion of boron nitride is sufficiently great that a shorter residence time does not prevent virtually complete combustion and that the reaction rate of boron nitride is much greater than that of boron.

(C) In addition to the various factors which have been discussed above, the water vapor produced in the secondary combustion chamber very probably has a beneficial effect on the combustion efficiency of both the boron and boron nitride. Studies (Reference 6) of the oxidation of massive boron nitride in air at 3500°F have shown that the rate of oxidation is increased 25-fold in the presence of water vapor. Furthermore, thermochemical calculations indicate that the reactions of boron nitride with water vapor, represented by Equations (12) and (13), will occur. Similarly, the reactions

$$BN + 1.5\ H_2O \rightarrow 0.5\ B_2O_3 + 1.5\ H_2 + 0.5\ N_2 \qquad (12)$$

$$BN + 2.0\ H_2O \rightarrow HBO_2 + 1.5\ H_2 + 0.5\ N_2 \qquad (13)$$

represented by Equations (9), (10), and (11) suggest that water vapor may improve the combustion efficiency of elemental boron in a completely analogous manner.

(C) Careful evaluation of the chemical analytical data of tests in which nitrogen was used as the secondary gas shows that water vapor does indeed improve combustion of both boron and boron nitride. In the primary exhaust, the concentration of hydrogen is far greater than the concentration of either solid material, because the "effective" concentration of the boron and boron nitride is limited to the surface of the particles. Simultaneously, the oxygen concentration in the nitrogen supply* is very low. Therefore, the probability of the hydrogen-oxygen reaction occurring is many times greater than the probability of the boron nitride-oxygen or boron-oxygen reactions occurring. Notwithstanding this difference in probability, the oxidation of both boron nitride and boron did occur in the 200 psia test, whereas only the oxidation of boron nitride occurred to an observable extent in the 50 psia test. Therefore, the evidence indicates that water vapor improves the combustion of boron as well as boron nitride.

(C) Another important factor involved in the consideration of combustion efficiency of the boron nitride and boron is particle size. The earlier study (References 1 and 2) of the hydrazine/pentaborane bipropellant system showed that the solid boron nitride and boron of the primary exhaust was amorphous and had an average particle size less than 1 micron. The large surface area which results from small particle size has the effect of providing a high population of solid reactant sites with an attendant high reaction rate.

(C) The small particle size, in combination with a high particle number concentration, has another beneficial effect on the combustion efficiency: That of providing an adequate internal energy-transfer balance. The heat transferred from the energetic oxygen-hydrogen reaction to the particles is effectively utilized to raise the particle temperature because of the very high surface area available for the absorption of the radiant energy. In a similar way, relatively little of the heat radiated within the particle cloud is lost to the surroundings and the temperature of the particles remains high. In this manner the ignition temperature of the particles is reached and combustion may proceed.

(U) A combustion model has been developed, substantially based on the experimental observations, to describe the various physical and chemical processes which occur in the secondary combustion chamber. Whereas the combustion model has been used to explain the experimental results obtained in this investigation, the greater value of the model lies in its impact on the development of other boron containing propellant systems for air-augmentation application.

(C) The initial process which occurs in the secondary chamber is the mixing of the primary exhaust stream with the augmenting air. The mixing of these streams is not instantaneous, but is controlled by the development of eddy currents followed by molecular diffusion as the gases proceed downstream. Thus, within the initial mixing zone, fuel-rich and air-rich regions of varying composition are formed. Within these regions,

*Oxygen is present as a contaminant in the nitrogen; see text, p. 54.

especially the air-rich region, ignition and combustion of the hydrogen occur. Diffusion and combustion of the hydrogen continue to occur in the air-rich regions as the gases proceed down the secondary chamber. The combustion of the boron nitride probably begins soon after the initial hydrogen combustion reaction, in the air- and water-rich zones. As the particle temperatures increase, due to combustion, the combustion of the elemental boron becomes more significant.

(C) It is suggested that the high combustion efficiency of the boron nitride and boron may be the result of the hydrogen acting as a carrier for the oxygen. The precise mechanism through which water vapor enters the combustion reaction may be difficult to discern. However, one mechanism by which its entry may occur is as follows: (1) water vapor reacts with the boron or boron nitride surface with the liberation of hydrogen, (2) the hydrogen thus formed recombines with oxygen very near the particle surface, and (3) the reformed water vapor returns to further oxidize the surface. Whether the carrier species is the H_2O molecule, the diatomic OH species, or perhaps the HO_2 molecule (Reference 7) cannot be established on the basis of present data. However, such a mechanism would account for both a high heat-exchange efficiency and a high solid reaction efficiency.

(C) A consideration of these various factors which contribute to the combustion efficiency of boron is of importance in examining potential propellant systems for air-augmentation application. Optimum performance of the air-augmentation stage will require essentially complete combustion of the boron. In order to achieve efficient boron combustion, the chamber pressure must be maintained above some minimum level; the minimum level appears to be between 50 and 200 psia. The presence of water vapor in the combustion system also assures high boron combustion efficiency. The introduction of water vapor into the system may be accomplished by including a hydrogen-rich component in the primary propellant formulation, which produces water on combustion with the augmenting air. Care must also be taken to provide an air-inlet design which allows thorough mixing of the components and a secondary chamber design which allows the slower boron oxidation to occur. The experimental data obtained on this program indicate that this is feasible.

SECTION IV

CONCLUSIONS AND RECOMMENDATIONS

1. CONCLUSIONS

a. The Hydrazine/Pentaborane Bipropellant System

(C) The c* performance of the hydrazine/pentaborane bipropellant system was on the order of 85% of theoretical, based on the inhibited combustion model. These results are in agreement with earlier studies of this system.

(C) On the basis of these results and in accordance with the earlier findings, it has been concluded that optimum c* performance is obtained at a mixture ratio of 1.01 rather than 1.27 predicted on the basis of thermodynamic equilibrium calculations. The performance of this system is limited by the kinetics of the boron-nitrogen oxidation reaction. Monopropellant decomposition of hydrazine and pyrolytic decomposition of pentaborane lead to lower combustion efficiencies because of the poor efficiency of the kinetically-limited boron-nitrogen reaction.

b. Secondary Combustion in Air of Exhaust Products from the Hydrazine/Pentaborane System

(1) Sea Level/Mach 2.5 Regime

(C) The measured c* performance of the air-augmented hydrazine/pentaborane system was on the order of 96-99% of theoretical at chamber pressures near 200 psia. Chemical analytical data for tests at air-to-propellant ratios as high as 50:1 indicate the absence of hydrogen and ammonia, and the presence of a very low concentration of boron nitride and boron. At the very high air-to-propellant ratios, chemical analytical data indicate slightly higher boron nitride and elemental boron concentrations in the secondary exhaust than at low and moderate ratios.

(C) Temperature profile measurements in the secondary combustion chamber show that very high temperatures are achieved at about 3 in. downstream of the secondary air-injector at air-to-propellant ratios of 8:1 and 16:1. Very much lower temperatures are achieved at this location at an air-to-propellant ratio of 50:1. In the 8:1 and 16:1 air-to-propellant ratio tests, temperature profiles along the secondary chamber in-line with the air-inlet ports converge with those not-in-line at a point well upstream of the secondary nozzle. At a 50:1 air-to-propellant ratio, convergence appears to occur, if at all, much nearer the secondary nozzle.

(C) These experimental data lead to several conclusions: (1) the combustion of hydrogen and ammonia is complete and occurs very near

the secondary air injector; (2) virtually complete combustion (> 96%) of the solid boron nitride and boron occurs in the secondary chamber at air-to-propellant ratios of 18:1 and less and complete mixing and uniform gas temperature are achieved in the secondary chamber under these conditions; (3) combustion of these solid species occurs downstream of the hydrogen-oxygen combustion reaction; and (4) at an air-to-propellant ratio of 50:1, the quenching effect of the low air inlet temperature reduces the combustion efficiency of the boron and boron nitride and complete mixing and uniform gas temperature may not be achieved in the secondary chamber.

(C) In summary, the combustion efficiency of the exhaust is very near 100% and the measured c* performance of the air-augmented hydrazine/pentaborane system approaches the theoretical value.

(2) High Altitude/Mach 4.0 Regime

(C) The measured c* performance of the secondary combustion of the hydrazine/pentaborane exhaust was on the order of 92% of theoretical at chamber pressures near 50 psia. Chemical analytical data for tests at air-to-propellant ratios of 8:1 and 16:1 indicate the presence of appreciable amounts of elemental boron in the secondary exhaust but only very small amounts of boron nitride. Temperature profile data show lower temperatures near the air-injector than were observed in the corresponding low altitude/Mach 2.5 tests, but the downstream temperatures were higher. Convergence of the in-line and not-in-line temperature profiles was again observed, well upstream of the secondary nozzle.

(C) It has been concluded that: (1) the low secondary chamber pressures employed in the high altitude/Mach 4.0 regime results in lower reaction rates of all reactions; (2) the low secondary chamber pressure also results in lower residence times; and (3) the high air inlet temperature and chamber temperature increase reaction rates, but not sufficiently to offset the effects of low pressure. The net effect of these factors is to inhibit the combustion of elemental boron. Complete combustion of the hydrogen, ammonia, and boron nitride does occur within the secondary combustion chamber, although a greater length of the chamber is required to achieve complete combustion. The low combustion efficiency of the elemental boron causes the decrease in c* performance.

c. Combustion Model Development

(C) On the basis of these results, theoretical considerations, and the findings of other studies, it has been tentatively concluded that the combustion of the hydrazine/pentaborane exhaust proceeds in a stepwise process.

The chemical equations involved, in the order of decreasing reaction rates, are as follows:

$$2\ H_2 + O_2 \rightarrow 2\ H_2O$$

$$NH_3 + 1.5\ O_2 \rightarrow 1.5\ H_2O + 0.5\ N_2$$

$$BN + 2\ H_2O \rightarrow HBO_2 + 0.5\ N_2 + 1.5\ H_2$$

$$BN + 1.5\ O_2 \rightarrow 0.5\ B_2O_3 + 0.5\ N_2$$

$$B + 2\ H_2O \rightarrow HBO_2 + 1.5\ H_2$$

$$B + 1.5\ O_2 \rightarrow 0.5\ B_2O_3$$

A more definitive mechanism has been suggested, involving the transport of oxygen by hydrogen, atomic oxygen, hydroxyl radical or other energetic species which might be present in the water-rich plasma.

(C) The hydrogen and ammonia combustion reaction contribute the major portion of the high c* performances in the air-augmented hydrazine/pentaborane system. Thus, even with low combustion efficiencies for elemental boron under conditions of low pressure and residence time, the delivered performance efficiency of the air-augmented hydrazine/pentaborane system will remain high.

d. The Air-Augmented Micromotor Test Facility

(U) The air-augmented micromotor test facility was designed and constructed to provide accurate experimental verification of theoretical performance. The results of the present investigation of the hydrazine/pentaborane system clearly indicate that this small-scale test facility does indeed provide accurate experimental performance measurements and pertinent supporting data as well. The micromotor system is also readily adaptable to the study of other propellant systems for ducted-rocket application. With relatively minor modifications of the primary combustor, the system may be converted for use in testing a wide variety of propellant systems, including other liquid bipropellants, heterogeneous liquid propellants, hybrid propellants, and solid propellants.

(U) Numerous advantages accrue to the use of these small-scale test facilities. Electrical heating of the air, accomplished without the installation of expensive electrical components, permits the use of clean air for the realistic simulation of actual flight conditions on a small scale. Only moderate amounts of primary propellants are required for evaluation of the performance of candidate systems. Also, modification of the equipment for use with other primary propellant systems is relatively simple and can be accomplished inexpensively.

(U) It is concluded that this micromotor test-facility is especially well suited to the evaluation of candidate air-augmented propellant systems and for investigating the factors which affect the combustion and performance of these systems.

2. RECOMMENDATIONS

a. Continued Evaluation of the Air-Augmented Hydrazine/Pentaborane System in the Micromotor Test Facility

(C) The theoretical performance data for the air-augmented hydrazine/pentaborane system were compared at different primary mixture ratios at an air-to-propellant ratio of 50:1. The values of I_s (P_c/P_e, 1000/14.7) at 1.27, 0.6, and 0.1 are approximately 1740, 2050, and 2520 sec., respectively. The respective values of ρI_s are 1350, 1488, and 1620 g-sec/cc. Thus, a significant improvement in performance may be realized in the air-augmentation stage when the primary propellant system is operated at a highly under-oxidized condition.

(C) The results of the present study of the air-augmented hydrazine/pentaborane system demonstrate: (1) high performance efficiency in the air-augmentation stage at mixture ratios of 1.0 to 1.3; (2) the importance of maintaining the chamber pressure above a threshold value between 50 and 200 psia; and (3) the importance of water vapor in the combustion efficiency of boron and boron nitride.

(C) It is recommended that the air-augmented hydrazine/pentaborane system be subjected to further comprehensive and definitive study. The threshold values of the secondary chamber pressure should be determined under a variety of conditions to determine the effects of: (1) primary propellant mixture ratios (N_2H_4/B_5H_9) in the range from 0.1 to 1.0 and (2) air-to-propellant ratios in the range from 8:1 to 50:1. Several types of measurements should be made under these various conditions, including: (1) c* performance; (2) thrust; (3) I_s performance; (4) chemical analysis of the exhaust; and (5) secondary chamber temperature and temperature profiles, by both spectrometric and thermoelectric methods. Design parameters, such as primary nozzle expansion, air injector configuration, and minimum L* requirements should be considered also.

b. Evaluation of the Air-Augmented Hydrazine/Boron-Loaded Pentaborane System in the Micromotor Test Facility

(C) Theoretical calculations show that the hydrazine/boron-loaded pentaborane combination is an excellent primary propellant system for air-augmentation application. Specifically, the air-augmented system, hydrazine/73 wt% boron + 24 wt% pentaborane + 3 wt% gelant, operating at a mixture ratio of 2.0 and an air-to-propellant ratio of 30:1, has an I_s of about 1390 sec (P_c/P_e, 175/13.2). Under severly underoxidized conditions, i.e., a primary

mixture ratio of 0.2, and at an air-to-propellant ratio of 110, the I_s of the air-augmented system is 2320 sec. The ρI_s values for these primary mixture ratios, 2.0 and 0.2, are 1600 g-sec/cc and 3180 g-sec/cc, respectively.

(C) The results obtained on the present program showed that the boron combustion efficiency was significantly improved in the presence of water vapor. On this basis, the efficient combustion and high performance of boron-loaded propellants for air augmentation may depend on some minimum hydrogen content in the propellant. If this is the case, then the optimum level of boron-loading may be somewhat less than performance calculations would indicate, due to poor boron combustion efficiency.

(C) It is recommended that a study be conducted to examine the effect of hydrogen-content on the performance of the boron-loaded propellants, and simultaneously evaluate the performance of these systems. The hydrazine/boron-loaded pentaborane system represents a propellant system which has a high theoretical performance potential in both an air-augmented boost mode and cruise mode. In addition, a wide range of mixture ratios and boron-loading levels are made available for the evaluation of the effect of hydrogen content on boron combustion efficiency.

(C) The tests should be performed to assess the delivered performance efficiency under a variety of conditions: (1) Boron-loading levels in the range from 10 to 73 wt%, (2) primary mixture ratios in the range 0.2 to 2.0, (3) air-to-propellant ratios in the range from stoichometric for the mixture ratio to 50:1. Measurements should include: (1) c* performance, (2) thrust, (3) I_s performance, (4) chemical composition of the exhaust, and (5) secondary chamber temperatures.

c. Evaluation of the Air-Augmented Chlorine Trifluoride/Boron-Loaded Pentaborane System in The Micromotor Test Facility

(C) The chlorine trifluoride/73 wt% boron + 27 wt% pentaborane system has considerable merit as a potential primary bipropellant combination for air augmentation applications. Its moderate I_s of 249 sec (P_c/P_e, 500/14.7) and high ρI_s of 434 g-sec/cc at a mixture ratio of 8.0 make it attractive for initial boost at launch in a standard rocket operating mode. At a mixture ratio of 0.1; the high I_s of 2285 sec (sea level/Mach 2.5; P_c/P_e, 171/14.7) and high ρI_s of 3185 g-sec/cc make it attractive for air-augmented cruise at an air-to-propellant ratio of 64.

(C) The primary bipropellant combination is characterized by extremely high chamber and exhaust temperatures. Another characteristic of the system is that its exhaust is hydrogen-poor, because of the virtually complete removal of the hydrogen as hydrogen fluoride. Higher primary

exhaust temperatures would be beneficial to the secondary combustion of the elemental boron, whereas the absence or low concentration of hydrogen (and, hence, the low concentration of water vapor) would tend to inhibit the boron combustion. Therefore, it is suggested that, at some low primary mixture ratio, the temperature of the primary exhaust may remain sufficiently high to permit the efficient combustion of boron in air in spite of the low concentration of water vapor in the secondary combustion chamber. It is possible that improvement of boron combustion efficiency can also be brought about by exhaust species other than water, such as hydrogen fluoride. In the event that the hydrogen fluoride does promote boron-combustion, then high performance would still be assured.

(C) It is recommended that the air-augmented chlorine trifluoride/boron-loaded pentaborane system be evaluated under the following conditions: (1) boron-loading levels in the range from 10 to 73 wt%, (2) primary mixture ratios in the range from 0.1 to 8.0, emphasis being placed in the lower portion of the range (from 0.1 to 4.0), and (3) air-to-propellant ratios in the range from stoichiometric (for the primary exhaust) to 50:1 or greater. The types of measurements which should be made to assess the delivered performance efficiency include: (1) c* performance, (2) thrust, (3) I_s performance, (4) secondary exhaust composition, and (5) chamber temperature.

d. Evaluation of the Air-Augmented Chlorine Trifluoride/ ATF-2* System in the Micromotor Test Facility

(C) The chlorine trifluoride/ATF-2 system is similar in many respects to the boron-loaded pentaborane. The $^{\rho}I_s$ of the severly under-oxidized (mixture ratio of 0.1) system, operating in an air-augmented mode, is approximately the same as the 65 wt% boron-loaded pentaborane.

(C) It is recommended that this system be evaluated for air augmentation application at several mixture ratios. The system has an advantage over the boron-loaded pentaborane system in that the formulation of this material is more easily accomplished in the laboratory. The study of this air-augmented system should include tests at: (1) mixture ratios in the range from 0.1 to 5 and (2) air-to-propellant ratios in the range from stoichiometric for the primary exhaust to 50:1. The measurements should include: (1) c* performance, (2) thrust, (3) I_s performance, (4) exhaust composition, and (5) secondary combustion chamber temperature. In the event that hydrogen fluoride is found to have a beneficial effect on the combustion of boron, as has water vapor, then a system of considerable merit would become available for rapid development.

*ATF-2 is a gelled mixture of 73 wt% boron, 20 wt% ethanol, 7 wt% water, and 0.1 wt% gelant.

SECTION V

PROGRAM PERSONNEL

(U) Dr. S. D. Rosenberg served as Program Manager for the program. Lt. A. W. McPeak, USAF/RPCL, served as the Air Force monitor for the program. His valued assistance throughout the course of the program is sincerely appreciated.

(U) Dr. R. E. Yates served as Project Chemist for the program. Mr. H. C. Harper, Mr. K. Inouye, and Mr. L. A. Maucieri performed the chemical analyses. Mr. R. E. Anderson was responsible for the determination of theoretical performance data.

(U) Mr. R. C. Adrian served as Design and Test Engineer. Mr. J. R. Selby was the Instrumentation Test Engineer. Dr. J. M. Adams, who had previously designed and constructed the Spectral Comparison Pyrometer, assembled and prepared the spectral equipment for installation. Mr. R. C. Keith and Mr. A. Fink served as engineering consultants in the design and installation of the micromotor test facilities.

REFERENCES

1. Kinetics of Formation of Boron Nitride from Pentaborane and Hydrazine, Aerojet-General Reports 0635-01-2, September 1962; 0635-01-3, December 1962; 0635-01-4, March 1963.

2. Laboratory Investigation of the Hydrazine/Pentaborane Propellant System, Aerojet-General Report No. 1983, April 1961.

3. F. J. Foote, Ind. Eng. Chem., Anal. Ed., 4, 39 (1932).

4. K. Inouye, "Some Techniques for the Determination of Nitrogen in Fluoramine Compounds by the Dumas Method," Bull. 20th Meeting Interagency Chemical Rocket Propulsion Group, Working Group on Analytical Chemistry, CPIA Pub. No. 52, July 1964.

5. K. J. Laidler, Chemical Kinetics, McGraw-Hill Book Co., Inc., 1st Ed., 1950, p. 150 et seq.

6. S. Sklarew and M. J. Albom, "Plasma Torch Oxidation Resistance and Erosion Evaluation of Pyrolytic Materials," Sixth National SAMPE Symposium, Seattle, Washington, November 18-20, 1963.

7. N. R. Greiner, J. Phys. Chem., 72, 406 (1968).

APPENDIX I

SPECTROMETRIC MEASUREMENTS OF COMBUSTION PHENOMENA IN THE AIR-AUGMENTED HYDRAZINE/PENTABORANE SYSTEM

I. INTRODUCTION

(U) An important portion of the investigation of the air-augmented hydrazine/pentaborane system, as originally envisioned, was the spectrometric examination of the combustion phenomena occurring in the secondary combustion chamber. On this basis, the equipment required for the performance of these measurements was prepared for use and the necessary background information was developed. The fundamental components of the spectral equipment were available, but some additions and modifications were required to adapt these components for use in this application. These additions and modifications were made and the spectral equipment was assembled and prepared for installation. Unfortunately, because of unforeseen expenses and time delays in the progress of other phases of the program, the measurements could not be made. The background information developed to date and the work performed pertinent to the spectral measurements are presented in this Appendix.

II. BACKGROUND

(U) The principal objective of the spectrometric measurements is to obtain the static gas temperature and the optical depth of the particle cloud at three axial stations in the secondary combustion chamber. The ultimate objective of these measurements is to infer the extent of combustion of the primary exhaust occurring at each axial station, so that the effect of specific parameters on the overall performance of the system can be evaluated. The progression of combustion manifests itself as a decrease in the mass fraction of boron and boron nitride and as an increase in the static stream temperature, both of which can be determined from the measured values of spectral transmittance and radiance.

(U) The experimental program is directed toward obtaining (1) the spectral transmittance and radiance of the spectrum line center of the first line of the sodium-D, 5890 Å, and (2) the spectral transmission and radiance associated with the continuum emission of the particle cloud at a wavelength of 5880 Å. These measurements are taken at three axial stations in the secondary combustor, across the flow centerline.

(U) The principal variable of interest, the gas temperature and its estimate of variance, is calculated from the data taken at various times during the firing. The optical depth of the particle cloud is determined from the same data. The optical depth, combined with an estimate of the particle-size distribution in the cloud, serve to define the condensed-phase temperature and mass fraction. From a regression analysis, the uncertainty in both of these parameters are determined as well, based on the uncertainty in the particle size distribution.

III. SPECTRAL EQUIPMENT AND PROCEDURES

(U) The principle part of the apparatus is the Spectral Comparison Pyrometer which has been described in detail elsewhere (Reference 1 of Appendix I). The fundamental components of this device are shown in Figure 25. A reference light source (DC carbon arc), chopper and associated optics are used at each of the three axial positions under study. Each of the reference source beams pass through a set of diametrically opposed windows which are set into the wall of the combustor. The light from each station is picked up by an optical light guide and passed to an optical sampling scanner which sequentially samples the radiance from each station and focuses it on the entrance slit of the spectrometer.

(U) Placement of the apparatus is shown in Figure 26. Because of the hazards associated with any engine test experiments, the spectrometer and auxiliary equipment are protected by the steel wall shown in the figure. The light source assembly, which includes the support ring, brackets, three carbon arcs, and their optical acceptor assemblies is mounted around the secondary combustion chamber. Photographs of this assembly are shown in Figure 27 and 28. The source monitor, shown in Figure 29, continuously monitors the intensity of each of the sources. The optical sampling scanner and drive motor, developed under Contract AF 04(611)-10545, is shown in Figure 30. This unit is used to scan the optical sampling stations and dwells at each station for 0.48 sec.

(U) The success of the spectral measurements depends largely on the successful operation of the window protection system. Therefore, careful consideration was given to the design of windows with adequate surface purging to prevent condensation of boric acid or other chamber constituents. A photograph of the window components is shown in Figure 31. A sketch of a set of assembled windows, as mounted in the secondary combustion combustor, is shown in Figure 32.

(U) The data ranging equipment which accepts the multiplier phototube output signal from the spectrometer, provides four output signals having gains of 1, 10, 100 and 1000. Each of these signals is recorded on 5KH_z galvanometers set for a maximum undirectional swing of four inches. In addition to these signals, there is one channel for monitoring the spectrometer scan signal (sinusoidal swing of 2 inches, peak to peak) and three channels for the reference source intensity monitors (four inch maximum undirectional swing).

(U) A procedure for the conduct of the spectrometric measurements was prepared and the electronics arrangement for the acquisition and recording of the spectrometric data at four levels of gain was developed. Gains from 1 to 1000 are required to permit the precise recording of the wide range of temperatures and emittances which exist along the axis of the secondary chamber.

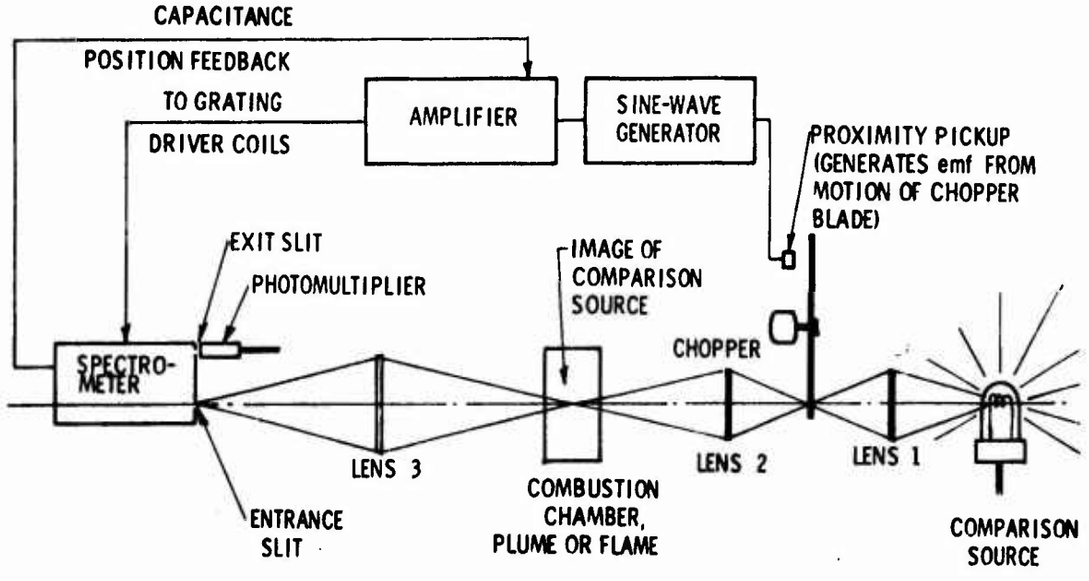

Figure 25. Optics and Electromechanical Schematic of Spectral Comparison Pyrometer

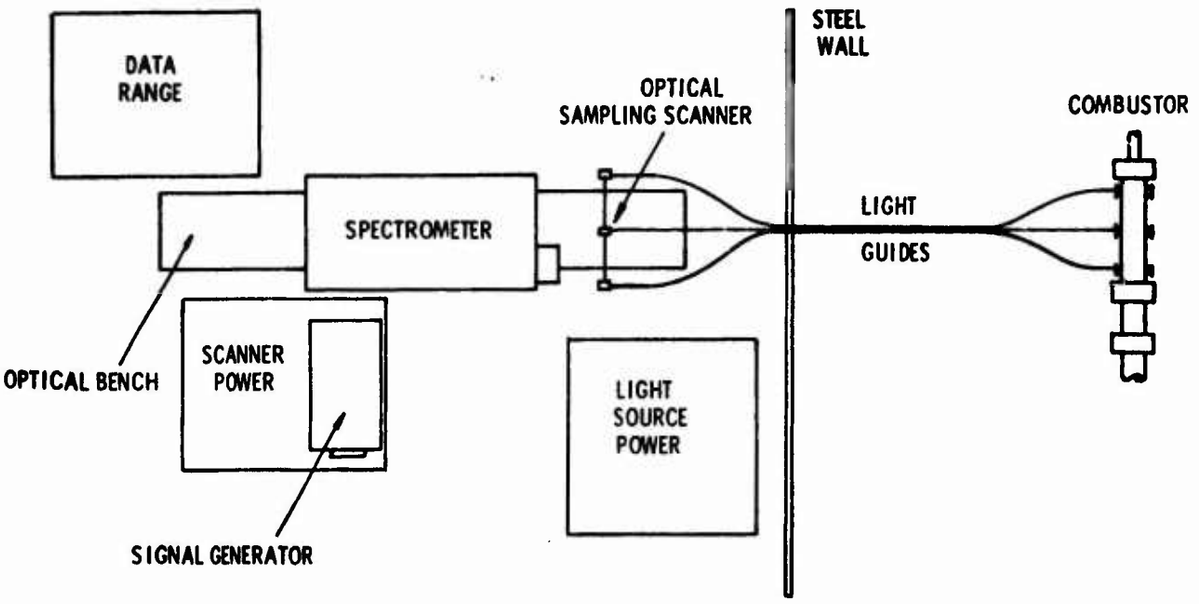

Figure 26. Spectral Equipment Layout

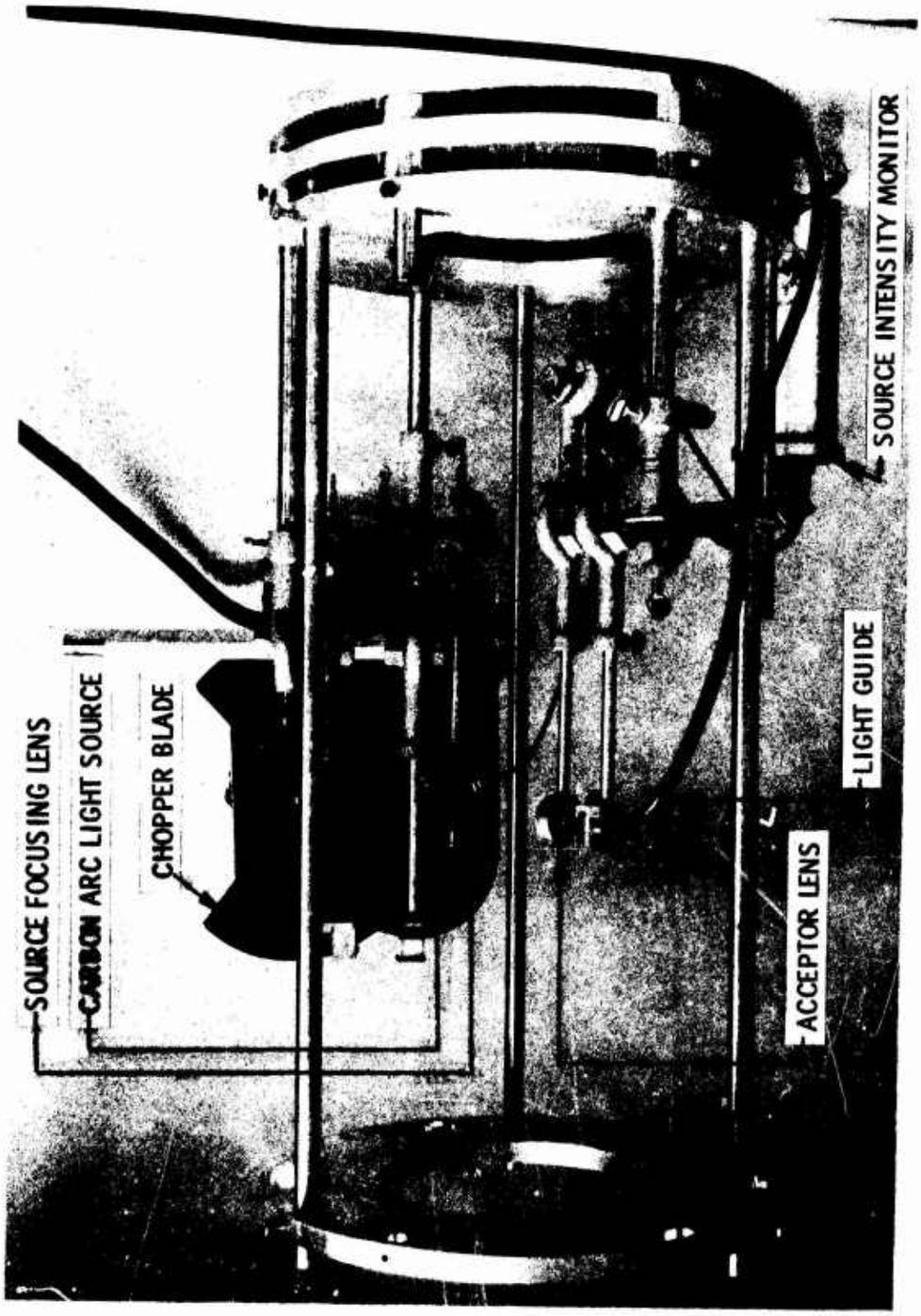

Figure 27. Optical Light Source Mounting Ring Assembly

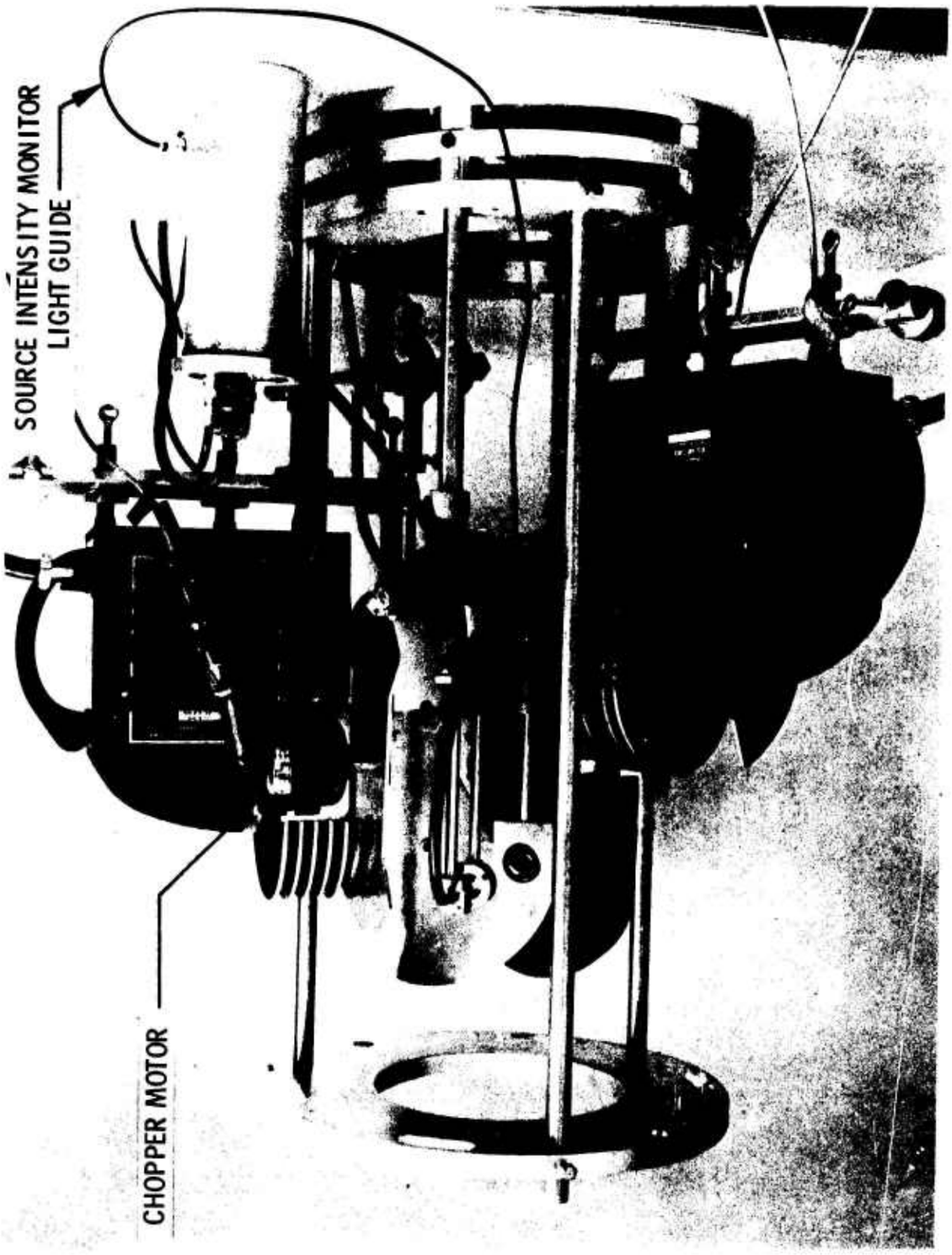

Figure 28. Spectral Comparison Pyrometer Light Source Assembly

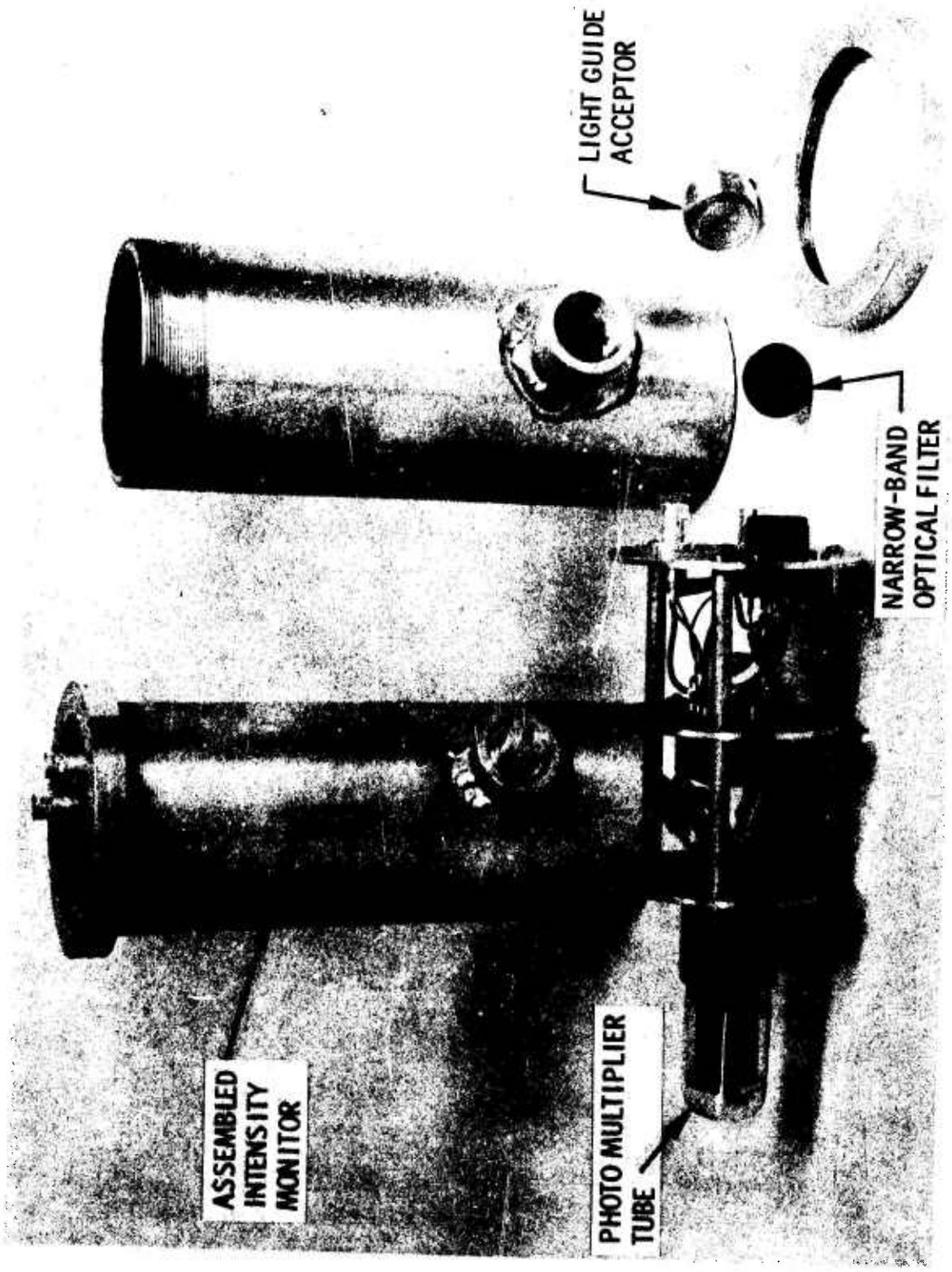

Figure 29. Light Source Intensity Monitor Assembly

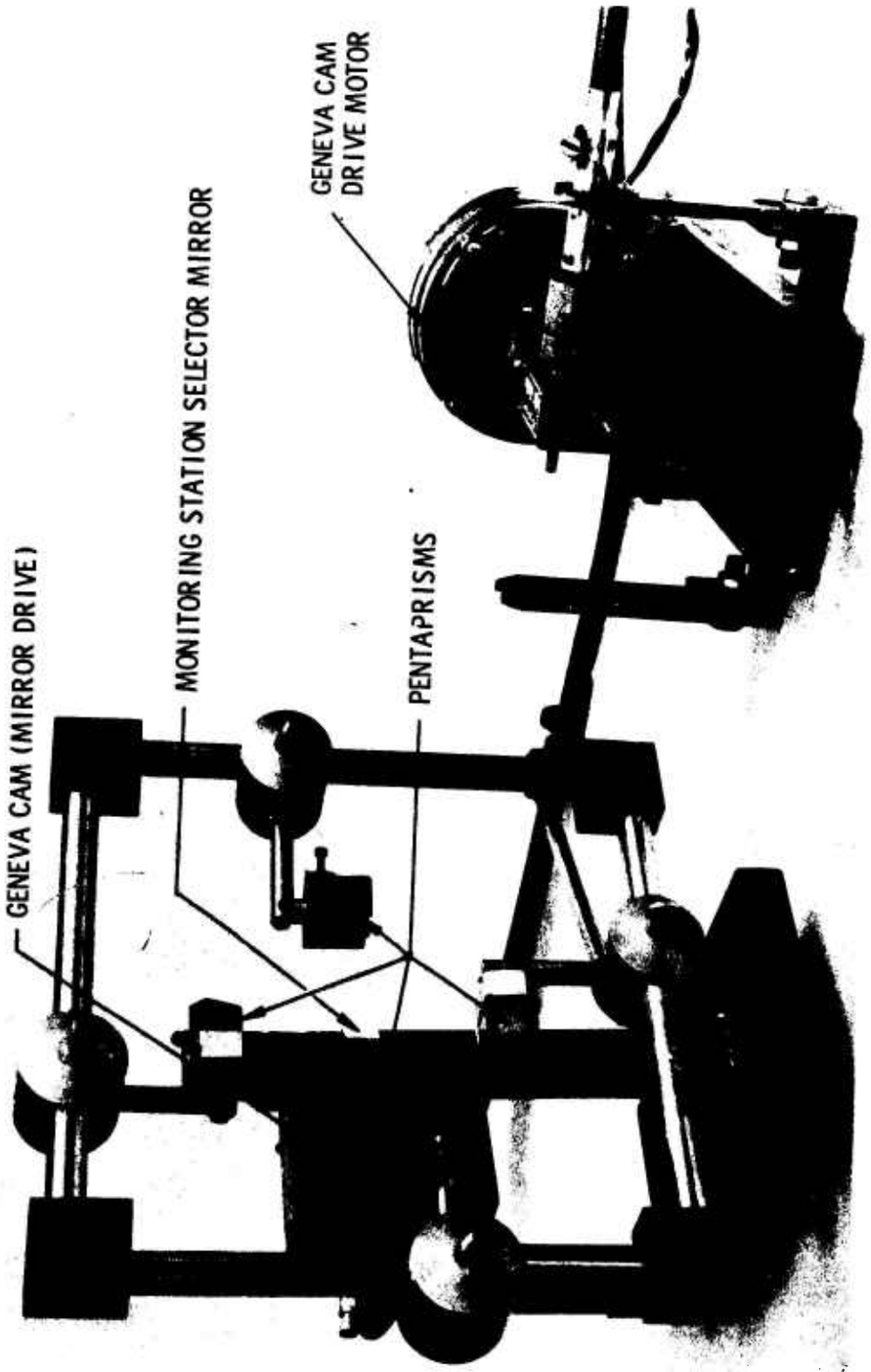

Figure 30. Optical Sampling Scanner

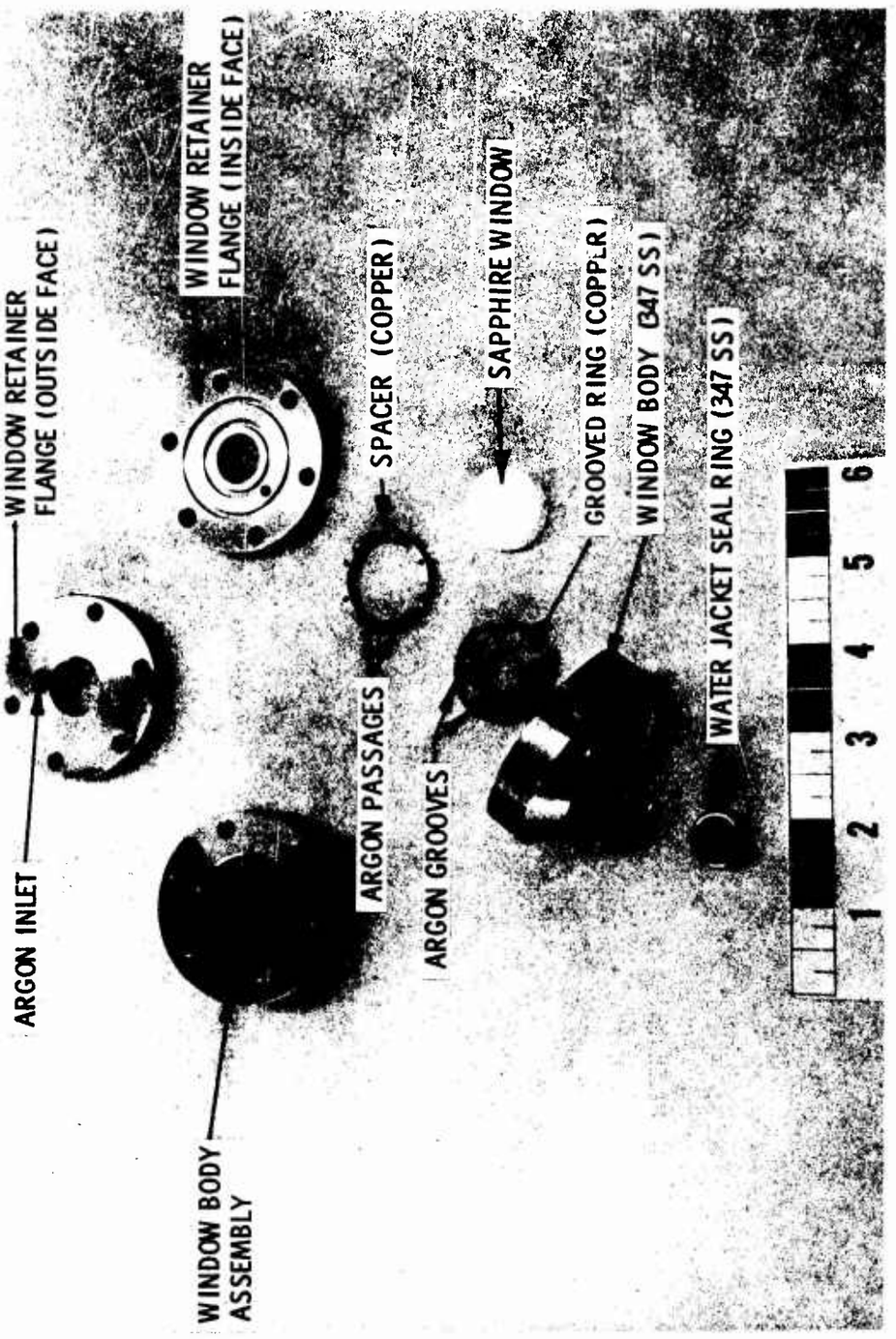

Figure 31. Secondary Chamber Optical Window Components

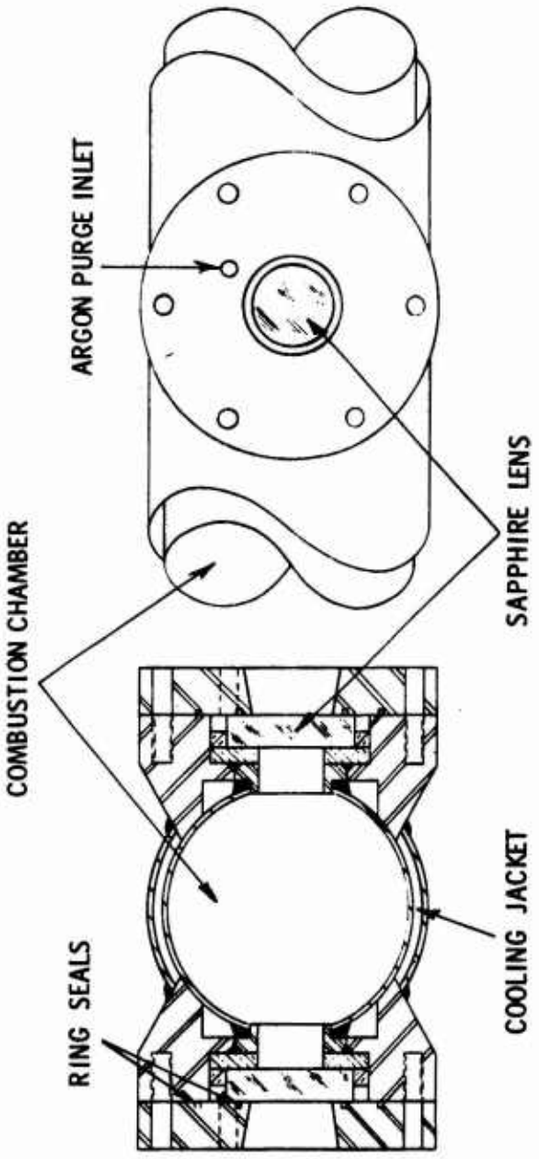

Figure 32. Optical Ports in the Secondary Chamber

(U) Special components which were required to complete the apparatus included (1) three reference source beam intensity monitors for recording the radiance of each of the carbon arc lamps throughout a run, (2) the scanner power supply to drive the grating within the spectrometer, and (3) the impedance couplers and data ranging equipment to provide signals of low impedance and a range of gains for coupling of all equipment to the data recording equipment.

IV. DATA REDUCTION

(U) The computer program employed to reduce the experimental spectral data to the desired temperature was written for use on the IBM 1130 computer. A description of the program (PROGRAM TEMP) is presented in this section.

A. GENERAL DESCRIPTION

(U) Program TEMP is a machine program written in Fortran IV language for use either with the IBM 360, 7094 or 1130 machines. Input data is placed on 80 column punched cards. Output is adaptable to 8-1/2 x 11 in. paper.

(U) The program receives calibration data related to the spectral response of some sort of detector used for the spectrometric measurements. Detector constants (called "TUBE CONSTANT") are determined over any spectral range and signal strength, the number of total data points being limited to 100, at a maximum of 10 wavelengths.

(U) From spectrometric data taken within the continuum of the flame and at specific spectrum line centers, the temperature of both the gas and particle cloud within the flame is calculated from Planck's Law.

B. COMPUTATIONAL SCHEMES

(U) The main program is divided into several computational schemes, which are identified by comment cards which correspond to the following headings.

1. Calculation of Detector Constants

(U) After having read into storage the emissivity tables for the reference source being used in the calibration, the program accepts data which relates signal strength (e.g., galvanometer deflection, inches) to reference source intensity (e.g., brightness temperature). After having calculated the detector constants which relate measured signal strength to radiance (or temperature), the program prints out an equation for the relationship together with statistical indicators for assessing the validity of the relationship.

2. Calculation of Reference Source and Window Conditions

(U) The reference souce temperature is determined from the measured signal from the reference source just prior to flame introduction. Data on reference source intensity just after flame extinguishment is also introduced as input at this point in the routine, together with the run time. To account for any spectral nonuniformity in window transmissivity, the post-test data can include up to 10 wavelength data, each being associated with a corresponding source of intensity. Any transient change in window transmissivity or reference source radiation is accounted for subsequently in the calculations of temperature from the spectrometric data, with the assumption that such changes occurred linearly with time between the pre- and post-run data points (i.e., during the "run time").

3. Calculation of Gas and Particle Cloud Temperatures and Spectral Emittance

(U) The spectrometric data, in the form of galvanometer deflections, are introduced here. Data on gas and condensed phase density are used together with previously stored data on particle absorption and scattering cross sections to calculate the particle number density (or concentration) and other physical properties of the particle cloud as required. If no particulates are present in the flame, the mass fraction of particles, CHI, is set equal to zero on the input.

(U) Several computational options are used to calculate temperatures. The first of these treats the problem of radiation scattering by the particle cloud for the "optically thin"* condition. This treatment is valid for most common flames having particulate mass fractions up to 0.4 together with a thickness up to 7 centimeters. When conditions on condensed phase mass fraction or thickness simultaneously exceed these values, the results may be invalid. At this condition on optical depth in a direction parallel to the optical axis, two conditions on transverse optical thickness are considered. In the first of these, termed the "TRANSVERSE-OPTICALLY THICK" case, the temperatures are computed for the condition where scattering losses from the flame radiation equal scattering gains, within the optical path. This condition is most frequently valid. In the second condition, termed "TRANSVERSE-OPTICALLY THIN" (see Table XII), the results are based on the assumption that there is a net scattering loss of radiation from the flame within the optical path, either because the flame's transverse dimension is extremely small or because there is extreme thermal disequilibrium. In both of the above cases, it is assumed that all the radiation from the reference source, scattered out of the optical path, is permanently lost.

*This refers to optical characteristic of the cloud for scattering of radiation along the "line of sight;" this case is shown directly under "SCATTERING EFFECTS CONSIDERED," Table XII.

TABLE XII

SAMPLE OUTPUT, PROGRAM TEMP

```
RUN NUMBER N-2, NITROGEN, TIME APPROXIMATE
  SODIUM SOLUTION USED TO COAT WALLS ON DOWNSTREAM END OF MIX CHAMBER

  EQUATION FOR TUBE CONSTANT AT 0.5890 MICRONS

      K(E) = 0.73433F-03 + -0.43587E-04 (E - 0.11233E 01)

      WITH VARIANCE OF ESTIMATE = 0.49151E-10
           POPULATION VARIANCE = 0.41460E-09
      FTEST = 8.435 HAVING 12 DEG OF FRDM.
      GAIN RATIO, RUN/CAL. = 1.00369

  SOURCE TEMPERATURE = 2792.472

  RUN TIME = 55.000 SECS

1  ELD(I)       TW2(I)
1  0.5880     0.96636F 00
2  0.5890     0.96705F 00
3  0.5900     0.96067F 00

  MEAN PARTICLE VOLUME = 0.10000E-11 CU CM

  NUMBER CONCENTRATION = 0.26666E-02 PER CU CM
--------------------------------------------------------------------------------
----------------------------------CASE 1----------------------------------------

  TIME = 0.000 SECS

----------------------SCATTERING EFFECTS CONSIDERED-----------------------

  FLAME THICKNESS = 0.12406E  06  CM

  PARTICLE EMISS. = 0.0033, REF = 0.0325 AT 0.5880 MICRONS
  PARTICLE EMISS. = 0.0033, REF = 0.0325 AT 0.5890 MICRONS
  GAS EMISSIVITY  = 0.3031 AT 0.5890 MICRONS

  TRANSVERSE - OPTICALLY THICK

 *PARTICLE TEMP. = 2828.01, GAS TEMP. = 2817.15

  TRANSVERSE - OPTICALLY THIN

 *PARTICLE TEMP. = 2833.41, GAS TEMP. = 2822.24
```

computed from EIOP, ELP all temperatures in °K

where particle effects are important, this qty must agree with actual thickness

considered to be most valid under normal conditions

TABLE XII (cont.)

```
*****EFFECTIVE FLAME THICKNESS USED (MULT. SCATTERING)*****
     XNO*OST*ST  = 0.33084E-01

 FLAME THICKNESS  = 0.41047E-04 CM

 PARTICLE EMISS.  = 0.0001, REF = 0.0010 AT 0.5880 MICRONS
 PARTICLE EMISS.  = 0.0001, REF = 0.0010 AT 0.5890 MICRONS
 GAS EMISSIVITY   = 0.0118 AT 0.5890 MICRONS

 TRANSVERSE - OPTICALLY THICK

*PARTICLE TEMP.   = 4660.34, GAS TEMP. = 4491.25

 TRANSVERSE - OPTICALLY THIN

*PARTICLE TEMP. = 4660.87, GAS TEMP. = 4491.71


 ------------------------SCATTERING EFFECTS NEGLECTED----------------------

 PARTICLE EMISS.  = 0.0357 AT 0.5880 MICRONS
 PARTICLE EMISS.  = 0.0357, GAS EMISS. = 0.3031 AT 0.5890 MICRONS

 PARTICLE TEMP.   = 2217.68, GAS TEMP. = 2822.18
```

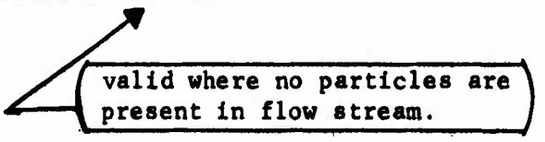

(U) The above computations are repeated, using an effective flame thickness to account for multiple scattering. The validity of this treatment has not been verified but it is used to serve as a basis of comparison.

(U) Lastly, the data are reduced and temperatures calculated with the assumption that there is no scattering of radiation by the particles. This case leads to an accurate determination of temperature where the particles are pure absorbers or where there are no particles.

(U) Under conditions ordinarily encountered in flames and small rocket motors, either the output directly under the heading "SCATTERING EFFECTS CONSIDERED. . . TRANSVERSE-OPTICALLY THICK" or under the heading "SCATTERING EFFECTS NEGLECTED," (Table XII) will be most valid.

4. Subroutines or Functions Used

(U) Subordinate to the main program deck are four subroutines which are used by the main program to perform intermediate calculations and interpolate tabulated information. They are described in the following paragraphs.

a. Function RI(EL, T)

(U) This subroutine calculates the value of the Planck function.

$$R_i(\lambda, T) = \frac{1}{\lambda^5 \exp\left(\frac{C_2}{\lambda T}\right) - 1}$$

b. Function EPS (EL, T)

(U) This subroutine is used to perform the interpolation of the tabulated reference light source emissivitiy, $\epsilon(\lambda, T)$.

c. Function TWF1 (EL)

(U) This subroutine interpolates tabulated pre-run window transmissivity data to obtain the window transmissivity at any specified wavelength.

d. Subroutine TRANS (T,S,U,A,B,X,T)

(U) This subroutine calculates the window transmissivity at the specified time, based upon pre- and post-test transmissivity data. It is assumed that window deposits build up linearly with time.

V. OPTICAL ABSORPTION AND SCATTERING CROSS-SECTIONS

(U) The primary exhaust consists chiefly of submicron boron nitride particles, surrounded by gaseous combustion products. The temperatures of both phases are measured by the spectral comparison method (Reference 2 of Appendix I) which utilizes measurements of spectrum line emission from the gas and continuum emission from the particle cloud. To determine the particle cloud emittance from light extinction measurements, it is necessary to delineate the effects of scattering and absorption by particles in the cloud.

(U) The optical absorption and scattering cross-sections of the particulate exhaust products are required for the determination of particle temperature. Calculations of these properties for spherical particles of boron nitride have been made using the Mie theory computer program SCAT. The program allows the calculation of the effective absorption and scattering cross-sections for polydispersions of spherical particles having any selected size distribution. The calculations for particle number-mean-diameters in the range 0.04 to 1.8 and criteria describing the size distributions used are contained in this section.

A. DESCRIPTION OF THE ANALYSIS

(U) For an optically thin cloud of particles, it can be shown (Reference 1 of Appendix I) that a light beam passed through a particle cloud in a spectral region isolated from spectrum lines or bands is extinguished according to the relation

$$\frac{I}{I_o} = \exp(-\delta) \tag{1}$$

where δ, the optical depth of the cloud, is given by

$$\delta = \tilde{N} (\bar{\gamma}_a + \bar{\gamma}_s)t \tag{2}$$

where $\tilde{N}$ is the number density of particles in the cloud,

$\bar{\gamma}_a$, $\bar{\gamma}_s$ are the absorption and scattering cross sections of the particles,

t is the actual thickness of the cloud.

(U) Equation 2 can be rewritten in terms of the physical properties of the cloud, to become

$$\delta = \left(\frac{\rho_g \chi}{\rho_s(1-\chi)L_u}\right) \left(\frac{\bar{\gamma}_a + \bar{\gamma}_s}{\bar{v}}\right) t \tag{3}$$

where ρ_g is the gas density,

ρ_s is the density of the solid comprising the particles,

L_u is the velocity lag, u_p/u_g,

χ is the condensed phase mass fraction.

(U) The second factor, which is a function only of the particle-size distribution and refractive index, is determined from Equation (4):

$$\frac{\bar{\gamma}_t}{\bar{V}} = \frac{\bar{\gamma}_a + \bar{\gamma}_s}{\bar{V}} = \frac{\int_0^\infty (\gamma_a(m,D) + \gamma_s(m,D))\ f_N(D)dD}{\int_0^\infty \frac{\pi D^3}{6} f_N(D)dD} \tag{4}$$

where $\gamma_a(m,D)$, $\gamma_s(m,D)$ are the absorption and scattering cross sections calculated from the Mie theory (Reference 3 of Appendix I) for the particle diameter D,

$f_N(D)$ is the frequency function which describes the particle size distribution, normalized such that

$$\int_0^\infty f_N(D)\ dD = 1.0, \tag{5}$$

and m is the refractive index, given by

$$m = n - in' \ . \tag{6}$$

(U) The emittance of the particle cloud is related to the effective absorption cross section for the polydispersion and to the particle number density. For an optically thin cloud, the relationship is particularly simple:

$$\epsilon_p = 1 - \exp(-\tilde{N}\ \bar{\gamma}_a\ t) \tag{7}$$

which can be recast into a form similar to Equation (3):

$$\epsilon_p = 1 - \exp\left[\left(\frac{\rho_g\ \chi}{\rho_s\ (1-\chi)L_u}\right)\left(\frac{\bar{\gamma}_t}{\bar{V}}\right)\left(\frac{\bar{\gamma}_a}{\bar{\gamma}_t}\right) t\right] \tag{8}$$

(U) It can be seen from Equations (1), (2) and (3) that, with an estimate of the condensed phase mass fraction, it is possible to determine the extinction parameter for the cloud, $\bar{\gamma}_t/\bar{V}$, from an optical extinction measurement. This parameter can then be used to determine the particle size distribution function from Equation (4). Finally, the ratio $(\bar{\gamma}_a/\bar{\gamma}_t)$ can be determined from the defined variables according to the relationship

$$\frac{\bar{\gamma}_a}{\bar{\gamma}_t} = \frac{\int_0^\infty \gamma_a(m,D)\, f_N(D)dD}{\int_0^\infty (\gamma_a(m,D) + \gamma_s(m,D))\, f_N(D)dD} \tag{9}$$

and used in Equation (8) to determine the desired value of particle cloud emittance.

B. RESULTS

(U) Calculations of the optical properties of a boron nitride cloud have been performed utilizing a high-speed computational scheme, Program SCAT (Reference 4 of Appendix I). The results are presented in Table XIII as a function of number-mean-particle diameter,

$$\bar{D} = \int_0^\infty D f_N(D)dD. \tag{10}$$

The frequency function, $f_N(D)$, used in the calculations was based on the typical unimodal distribution of particle sizes which is characteristic of particles generated randomly through mechanisms of agglomeration and fracture. This distribution is indicated in Figure 33, together with those associated with active combustion (the so-called "bimodal" distributions, Reference 1 of Appendix I).

(U) The refractive index for the boron nitride was determined from data of W. W. Lozier (Reference 5 of Appendix I) and of Basche and Schiff (Reference 6 of Appendix I) and is given by

$$m = 2.118 - 0.00086\, i, \quad \lambda = 0.6\mu. \tag{11}$$

(U) Corrections to the value for the effect of higher temperature were determined from reflectance measurements of Null and Lozier (Reference 5 of Appendix I), and were found to be extremely small.

TABLE XIII

OPTICAL PROPERTIES OF BORON NITRIDE POLYDISPERSIONS

$m = 2.118 - 0.00086i$

$\lambda = 0.6\mu$

Typical unimodal distribution (Figure 33)

Number Mean Diameter, microns	Absorption cm^2	Scattering, cm^2	$\bar{\gamma}_a/\bar{\gamma}_t$ (Eq 9)	$\bar{\gamma}_t/\bar{V}$ (Eq 4)	$4\bar{\gamma}_t/\overline{\pi D^2}$
0.0382	*0.7074(-14)	0.4832(-12)	0.1443(-1)	0.7127(4)	0.4093(-1)
0.0764	0.1233(-12)	0.3542(-10)	0.3470(-2)	0.6458(5)	0.7418
0.0993	0.3938(-12)	0.1347(-9)	0.2915(-2)	0.1117(6)	0.1669(1)
0.1508	0.1971(-11)	0.6298(-9)	0.3120(-2)	0.1490(6)	0.3380(1)
0.2009	0.5703(-11)	0.1358(-8)	0.4181(-2)	0.1362(6)	0.4115(1)
0.3017	0.2761(-10)	0.3155(-8)	0.8678(-2)	0.9382(5)	0.4256(1)
0.4010	0.3411(-10)	0.4838(-8)	0.7000(-2)	0.6117(5)	0.3689(1)
0.6033	0.2098(-9)	0.1043(-7)	0.1973(-1)	0.3919(5)	0.3556(1)
0.8018	0.2977(-9)	0.1709(-7)	0.1712(-1)	0.2730(5)	0.3292(1)
0.9928	0.5398(-9)	0.2607(-7)	0.2028(-1)	0.2201(5)	0.3286(1)
1.2067	0.1047(-8)	0.3802(-7)	0.2680(-1)	0.1800(5)	0.3267(1)
1.4052	0.1324(-8)	0.4836(-7)	0.2665(-1)	0.1449(5)	0.3063(1)
1.8138	0.2738(-8)	0.8056(-7)	0.3287(-1)	0.1130(5)	0.3082(1)

* $A(B) = A \times 10^B$

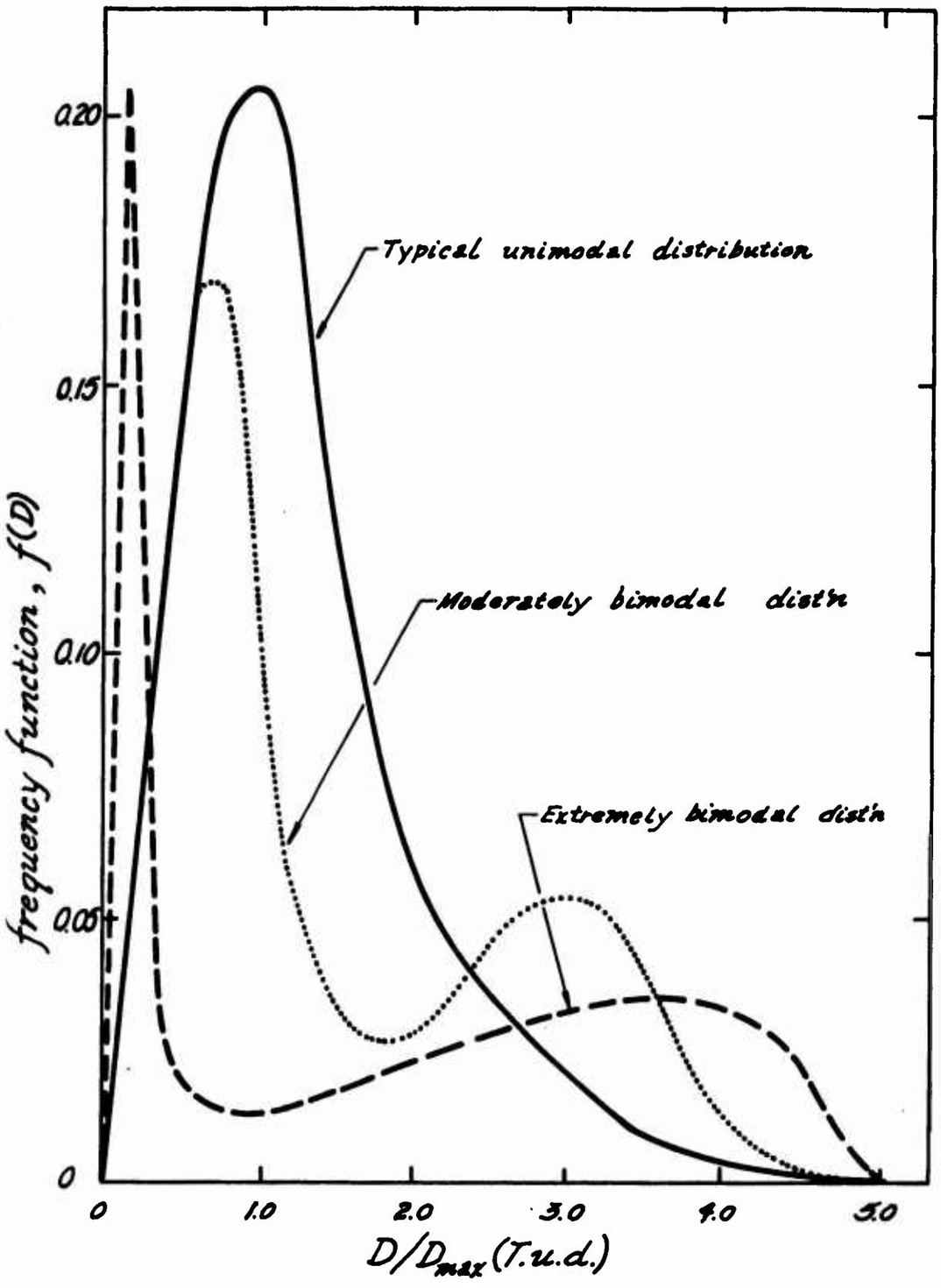

Figure 33. Particle Size Distributions Used in Generating Curves of Extinction Parameter vs Mean Particle Diameter

REFERENCES, APPENDIX I

1. Colucci, S. E. and Adams, J. M., Flame Temperature Measurement in Metalized Propellant Combustion, Technical Report AFRPL-TR-66-203, September 1966.

2. Adams, J. M., "The Measurement of Gas and Particle Temperatures in Rocket Motor Chambers and Exhaust Plumes," AGC T.P. 11, presented at AFRPL Two-Phase Flow Conference, San Bernardino, California, March 1967. To be published in Pyrodynamics.

3. Van de Hulst, H. C., Light Scattering by Small Particles, Wiley, New York (1957), Chapter 9.

4. Adams, J. M., "Program SCAT - A Computational Scheme in Fortran IV for Determination of Optical Absorption and Scattering Cross Sections for Polydispersions of Spherical Particles," AGC Internal Report, 10 October 1967.

5. Lozier, W. W., private communication, 17 July 1967.

6. Basche, M. and Schiff, D., "New Pyrolytic Boron Nitride," Materials in Design Engineering, pp 78-81, February 1964.

APPENDIX II

ANALYSIS OF ERRORS IN CHARACTERISTIC VELOCITY, c*, PERFORMANCE MEASUREMENTS

I. INTRODUCTION

(U) The analysis of errors contained in this report was conducted chiefly to determine the reliability of the c* performance data obtained in this study of the air-augmented hydrazine/pentaborane system. In addition, an analysis of this type provides an understanding of the problems involved in the accurate determination of c* performance in an air-augmented system and isolates those areas where improved methods of measurement are needed.

II. BACKGROUND

(U) In the treatment which follows, the standard deviation, σ_x, has been used as the indicator of the "error" in the measurement of the variable, x. The quantity, 100 σ_x/x, is the "percentage error" in the measurement of the variable, x. From the standpoint of arithmetic manipulation, it is more convenient to use the variance, σ^2; therefore, the variance has been used in the mathematical manipulation and the final result reduced to the "percentage error."

(U) The equation for c* is:

$$c^* = k\, PD^2/\dot{w} \qquad (1)$$

where P = chamber pressure, psia
D = throat diameter, in.
$\dot{w}$ = total propellant flow-rate, g/sec
and k = 45830 g-ft/sec^2-lbf, a constant.

For this expression the percentage error in c* is obtained from Equation (2).

$$\sigma_{c^*}/c^* = \pm \sqrt{(\sigma_P/P)^2 + 4(\sigma_D/D)^2 + (\sigma_w/w)^2} \qquad (2)$$

Thus, the desired error analysis required the evaluation of $(\sigma_P/P)^2$, $(\sigma_D/D)^2$, and $(\sigma_w/w)^2$ for these tests.

III. CALIBRATION DATA

A. PRESSURE MEASUREMENT

(U) The pressure transducers employed in the micromotor testing of the air-augmented hydrazine/pentaborane system were Taber Model 176,

employing 350-ohm bonded strain gages in a fully active, four arm bridge configuration. These transducers, available from stock in a variety of pressure ranges, are calibrated and standardized in the Aerojet Transducer Laboratory. The transducers used in these tests, 0-1000 psia, have an "error factor" of 0.251% of full scale; i.e., $\sigma_P = 2.51$ psia.

B. DIAMETER MEASUREMENT

(U) The measurement of throat diameter was made by means of a set of precision micrometers with 0.001 in. divisions. Repeated measurements of throat diameters with these instruments demonstrated reproducibility well within a variation of 0.001 in. Therefore, a reasonable estimate would be $\sigma_D \leq 0.001$ in.

C. PROPELLANT AND AIR FLOW MEASUREMENT

(U) The flow-rates of the hydrazine, pentaborane, and air were measured by several methods. In the case of hydrazine, the flow-rates were determined from the upstream pressure on one of the cavitating venturis, one for each of the flow ranges required. The flow-rates of pentaborane were measured by means of a paddle-wheel flowmeter. Air and nitrogen flow-rates were determined from the measurements of pressure and temperature of the gas on the upstream side of one of two sonic orifices.

(U) These flow devices were calibrated specifically for the measurements made in this study. The cavitating venturis were calibrated by measuring the flow-rate of hydrazine as a function of pressure. The flow-rate/pressure relationships and its variance were determined from a least-square threatment of the data.

(U) The pentaborane flowmeter calibrations were made using hexane as the fluid, because of the toxic and pyrophoric character of pentaborane. Hexane was selected because of the similarity of its physical properties to those of pentaborane. The flow-rate/flowmeter reading (cycles/sec) relationship and its variance was determined by the method of least-squares.

(U) The sonic orifices used to determine the air and nitrogen flow-rates were calibrated against standard sonic orifices in the pressure and temperature ranges of the tests. The mass flow-rates, as determined from the standard orifice data, were measured as a function of upstream pressure and temperature. Least-squares treatment of these data provided the relationships of mass flow-rate of gas vs $P/T^{\frac{1}{2}}$ and the variances of each set.

(U) The calibration data for the hydrazine venturis and the air orifices were obtained using instrumentation identical to that used in the tests. Consequently, the intrensic errors involved in the instrumentation were inherent in the variances obtained from the calibration data.

(U) The variances determined from these calibration data are presented in Table XIV. In general, the flow-rates involved in the tests fell into relatively narrow ranges; thus, the average value of the flow-rates in these various ranges have been used to determine the value of $(\sigma_w/w)^2$.

TABLE XIV

σ_w^2 AND $(\sigma_w/\bar{w})^2$ FOR PROPELLANTS (U)

Propellant	Instrument	Flow Rate Variance σ_w^2 (g/sec)^2	Average Flow Rate, $\bar{w}$, (g/sec)	$(\sigma_w/\bar{w})^2$	% Error in Flow Rate $100\sigma_w/\bar{w}$
Hydrazine	Venturi #1	0.01134	8.50	1.570×10^{-4}	1.25
Hydrazine	Venturi #2	0.01790	11.85	1.275×10^{-4}	1.13
Pentaborane	Flowmeter	0.02304	7.25	3.862×10^{-4}	1.97
Air	Sonic Orifice #1	0.835	127	0.518×10^{-4}	0.72
Air	Sonic Orifice #2[a]	6.63	252	1.044×10^{-4}	1.02
Air	Sonic Orifice #2[a]	35.18	607	0.953×10^{-4}	0.97

[a] Different calibrations were obtained for sonic orifice #2 in the ranges 0-1000 psia and 1000-2000 psia.

IV. ERROR IN PRIMARY c*

(U) The primary c* performances were calculated from the data using Equation (1) and the measured values of primary chamber pressure, throat diameter, and flow-rates of hydrazine and pentaborane. The average primary chamber pressures for all tests was 372 psia. Therefore, using the σ_p = 2.51 psia, the percentage error in the measurement of primary chamber pressure was:

$$100\ \sigma_p/P = 0.675;\ (\sigma_p/P)^2 = 0.455 \times 10^{-4}$$

(U) The throat diameter of the primary nozzle in these tests was 0.125 in.; thus the percentage error in the measurement of throat diameter, using σ_D = 0.001 in., was:

$$100\ \sigma_D/D = 0.800;\ (\sigma_D/D)^2 = 0.640 \times 10^{-4}$$

(U) In the largest group of tests, Tests 102-119, the flow-rates of hydrazine and pentaborane totalled approximately 15 g/sec and in Tests 120-122 these flow-rates totalled approximately 20.75 g/sec. To find the value of the variance of the total primary propellant flow-rate, Equation (3) was used.

$$\sigma_{w1}^2 = \sigma_{w_o}^2 + \sigma_{w_f}^2 \qquad (3)$$

The percentage error in the measurement of total flow-rate, determined from the data in Table XIV, were:

For Tests 102-119 $\quad 100\ \sigma_{w1}/\bar{w}_1 = 1.218 \quad (\sigma_{w1}/w_1)^2 = 1.484 \times 10^{-4}$

For Tests 120-122 $\quad 100\ \sigma_{w1}/\bar{w}_1 = 0.972 \quad (\sigma_{w1}/w_1)^2 = 0.945 \times 10^{-4}$

(U) Table XV presents a summary of the errors in the measured values of the primary c* performance. The percentage error in c* were calculated using Equation (2).

TABLE XV

SUMMARY OF ERRORS IN PRIMARY c* DETERMINATION (U)

Test Group	% Error in Chamber Pressure $100\ \sigma_p/P$	% Error in Throat Dia $100\ \sigma_D/D$	% Error in Flow Rate $100\ \sigma_w/w$	% Error in Measured c* $100\ \sigma_{c*}/c*$
102-119	0.68	0.80	1.218	2.12
120-122	0.68	0.80	0.972	1.99

(U) The largest contribution to the error in the primary c* measurement was the measurement of the throat diameter. Because of the small size of the throat, compounded by the fact that the c* value requires the squaring of the diameter, the error in this measurement causes a 1.5% error in the value of c*.

V. ERROR IN SECONDARY c*

(U) The secondary c* performances were calculated using Equation (1) and measured values of secondary chamber pressures, throat diameters, and flow-rates of primary propellants and air (or nitrogen). Two ranges of secondary chamber pressures were employed, simulating flight at two altitudes. The average values of these secondary chamber pressure ranges were 217 psia and 64.7 psia. The standard deviation of the pressure transducer is:

$$\sigma_P = 2.51 \text{ psia}$$

Expressed as percentage error:

at 217 psia chamber pressure, $100\ \sigma_P/P = 1.157$

at 64.7 psia chamber pressure, $100\ \sigma_P/P = 3.880$

(U) A wide variety of nozzles were used in the secondary chamber. The percentage error in the measurement of thro[illegible]ameter varied also, because the measuring accuracy remained fixed, i.e., $\sigma_D = 0.001$ in., while the throat diameter varied. Table XVI presents the individual values of $100\ \sigma_D/D$ for each throat.

TABLE XVI

PERCENT ERROR IN SECONDARY THROAT DIAMETER (U)

Throat Dia. (in.)	Percent Error in Throat Dia. $100\ \sigma_D/D$	$(\sigma_D/D)^2 \times 10^4$
0.315	0.317	0.1008
0.390	0.256	0.0658
0.463	0.216	0.0467
0.500	0.200	0.0400
0.562	0.178	0.0316
0.677	0.148	0.0218
0.994	0.100	0.0100
1.150	0.087	0.0076
1.260	0.079	0.0063

(U) Three ranges of gas flow-rates and two ranges of primary propellant flow-rates were employed in the tests. The variances in total secondary propellant flow-rates, $\sigma_{w_2}^2$, were determined for the various combinations and are presented in Table XVII.

TABLE XVII

VARIANCES OF TOTAL FLOW-RATE (U)

Hydrazine Flow Rate $\sigma_{w_o}^2$	Pentaborane Flow Rate $\sigma_{w_f}^2$	Air or Nitrogen Flow Rate $\sigma_{w_A}^2$	Total Secondary Propellant Flow Rate $\sigma_{w_2}^2$
0.01134	0.02304	0.835	0.869
0.01134	0.02304	6.63	6.66
0.01134	0.02304	35.18	35.21
0.01790	0,02304	0.835	0.876
0.01790	0.02304	6.63	6.67

(U) The error data for secondary chamber pressure, throat diameter, and total propellant flow-rates were combined, according to Equation (2), to determine the percentage error in the measured values of the secondary c*. The results of this analysis are presented in Table XVIII.

TABLE XVIII

SUMMARY OF ERRORS IN SECONDARY c* DETERMINATION (U)

Test Group	% Error in Chamber Pressure $100\ \sigma_P/P$	% Error in Throat Diameter $100\ \sigma_D/D$	% Error in Total Flow-Rate $100\ \sigma_{w2}/w_2$	% Error in Measured c* $100\ \sigma_{c*}/c*$
, 102, 105, 106, 112, 113, 120, 121	1.16	0.24	0.67	1.36
107, 115	1.16	0.16	1.10	1.58
108, 111	1.16	0.14	0.95	1.47
118, 119	3.88	0.15	0.70	3.95
117, 122	3.88	0.05	0.82	3.95

(U) Note that in these final calculations, the error in throat diameter was obtained from the average values of $4(\sigma_D/D)^2$ within each group of tests. The magnitude of the error in diameter measurement is very small and introduces only a very small error in c*.

(U) This analysis leads to the conclusion that the values of c* determined in the test program are quite reliable. The results of the tests in the 200 psia chamber pressure regime are somewhat more reliable than those at 50 psia chamber pressure. Furthermore, the large potential errors appearing in the latter cases originated in the fact that low chamber pressures were measured by means of high range transducers.

VI. ERROR IN HEAT LOSS CORRECTION

(U) The theoretical c* performance values, used for comparison with the measured values, were corrected for the heat-losses experienced in the system. The heat-rejection rates were determined for each test from the measured variables: Mass flow-rate of water, temperature rise of the water, and the mass flow-rates of the propellants. Therefore, the corrected theoretical c* values are subject to the errors involved in the heat-rejection rate measurements. The magnitude of these errors and their effect on the theoretical c* values were determined.

(U) The heat-rejection rate, expressed in cal/g of propellant, were determined using Equation (4).

$$H = b\, w_c t / w_p \qquad (4)$$

where w_c = flow-rate of cooling water, lb/sec

t = temperature rise of water, °F

w_p = flow-rate of propellant, g/sec

and b = 252 cal/°F-lb, a constant

The percent error in H is obtained from Equation (5).

$$\sigma_H/H = \pm \sqrt{(\sigma_{wc}/w_c)^2 + (\sigma_t/t)^2 + (\sigma_{wp}/w_p)^2} \qquad (5)$$

(U) The two turbine flowmeters used to measure water flow-rates, one in the primary cooling-water circuit and one in the secondary cooling-water circuit, were calibrated by the Transducer Laboratory using a time-weight calibration system. The overall system error for the flowmeters was;

$$100\ \sigma_{wc}/w_c = 0.5\%.$$

(U) Three copper-constantan thermocouples were used to measure the temperature rise in the cooling-water circuit. Thermocouple calibrations, conducted in the Transducer Laboratory, indicate that, in the range 32-200°F the error in each thermocouple is:

$$\sigma = 0.75°F$$

Thus, the variance of the temperature rise is given by;

$$\sigma_t = \pm\sqrt{2\,\sigma^2} = 1.06°F$$

(U) The measurement of propellant flow-rates has been described in Section III,C of this appendix.

(U) The heat-rejection rates in the primary system were low and relatively constant, while the magnitudes of the heat rejection rates in the secondary chamber were found to vary over a relatively broad range of values. The heat-rejection rates in the secondary chamber were found to bear a rough relationship with air-to-propellant ratio.

(U) Table XIX presents the data for the error in the measurement of the primary heat-rejection rate. It is seen that the error in the heat-rejection rate to the primary cooling-jacket amounted to approximately 2.5%, i.e., $100\ \sigma_H/H = 2.5\%$.

TABLE XIX

MAGNITUDE OF ERROR IN HEAT-REJECTION RATE
PRIMARY COMBUSTION CHAMBER (U)

Source of Error	Range	Average	% Error
Coolant flow-rate	0.110-0.208 lb/sec	0.150 lb/sec	0.50
Temperature rise	26-73°F	50°F	2.12
Propellant flow-rate	11.6-20.8 g/sec	16.0 g/sec	1.21
	Error in Heat-Rejection Rate (Eqn. 5)		±2.50

(U) The errors in heat-rejection rate in the secondary chamber were calculated in a similar manner. However, these data were grouped on the basis of air-to-propellant ratio, because the magnitudes of the heat-rejection rates varied over such a broad range and because each group was internally consistent. The results are summarized in Table XX.

TABLE XX

MAGNITUDE OF ERROR IN HEAT-REJECTION RATE
SECONDARY COMBUSTION CHAMBER (U)

Test No.	% Error in water flow-rate	% Error in temp. rise	% Error in propellant flow-rate	% Error in heat-rejection rate
102, 112, 119, 121	0.50	2.43	0.67	2.57
105, 106, 113, 118, 120	0.50	0.61	0.67	1.03
107, 115, 117	0.50	0.73	1.10	1.41
108, 111	0.50	1.27	0.95	1.66

(U) Two sets of theoretical c* calculations were made for both the primary bipropellant system and the secondary combustion of the primary exhaust; one set was not corrected for heat-loss, while the other set included these corrections. The differences between the two values showed the magnitude of the heat-loss corrections. Table XXI shows these values for both the primary and the secondary systems.

(U) The error analysis indicates that the error in heat-rejection rate measurements has no significant effect on the theoretical c* value. The maximum heat-loss correction in the primary c* calculation was 3% for Test No. 107; if we assumed as much as 3% error in heat rejection measurement, the error introduced into the corrected theoretical c* would be less than 0.1%. Similarly, the greatest heat-loss correction in the secondary c* calculation was about 10%; a maximum error of 2.5% in the heat-rejection measurement would introduce an error of only 0.25% in the c* value. Thus, it is concluded that the error in measuring the heat-rejection rate has no significant effect on the theoretical c* calculation.

TABLE XXI

MAGNITUDE OF HEAT-LOSS CORRECTION TO THEORETICAL c* PERFORMANCE (U)

Test No.	Primary			Secondary		
	Theor. c*, ft/sec		Magnitude of Correction	Theor. c*, ft/sec		Magnitude of Correction
	Uncorr.	Corr.	% of Uncorr. c*	Uncorr.	Corr.	% of Uncorr. c*
102N	6103	5992	1.82	3223	3021	6.27
112N	6212	6117	1.53	3323	3146	5.33
119N	6050	5912	2.28	3479	3267	6.09
121N	6020	5927	1.54	3166	2974	6.06
105	----	5589	----	4419	4041	8.55
106	6064	5949	1.90	4739	4317	8.90
113	6073	5961	1.84	4747	4264	10.17
118	6050	5976	1.22	4840	4469	7.67
120	6010	5859	2.51	4695	4344	7.48
107	5944	5766	2.99	3790	3580	5.54
115	6152	6029	2.00	4052	2880	4.24
117	6056	5904	2.51	4109	3852	6.25
108	----	5303	----	2794	2705	3.19
111	6020	5869	2.51	3132	3035	3.10

CONFIDENTIAL

CONFIDENTIAL

Security Classification

DOCUMENT CONTROL DATA - R&D

(Security classification of title, body of abstract and indexing annotation must be entered when the overall report is classified)

1 ORIGINATING ACTIVITY (Corporate author) Aerojet-General Corporation P.O. Box 15847 Sacramento, Calif.	2a REPORT SECURITY CLASSIFICATION CONFIDENTIAL 2b GROUP 4

3 REPORT TITLE

Secondary Combustion of Pentaborane-Hydrazine Exhaust in Air

4 DESCRIPTIVE NOTES (Type of report and inclusive dates)

Final Report, 1 May 1967 through 30 April 1968

5 AUTHOR(S) (Last name, first name, initial)

Rosenberg, Sanders D.; Yates, Robert E.; Adrian, Robert C.

6 REPORT DATE	7a TOTAL NO OF PAGES	7b NO OF REFS
June 1968	111	13

8a CONTRACT OR GRANT NO. F04611-67-C-0106 b PROJECT NO c d	9a ORIGINATOR'S REPORT NUMBER(S) AFRPL-TR-68-98 9b OTHER REPORT NO(S) (Any other numbers that may be assigned this report) Aerojet Report No. 1134-81-F

10 AVAILABILITY/LIMITATION NOTICES In addition to security requirements which must be met, this document is subject to special export controls and each transmittal to foreign governments or foreign nationals may be made only with prior approval of AFRPL (RPPR/STINFO), Edwards, California 93523

11 SUPPLEMENTARY NOTES	12 SPONSORING MILITARY ACTIVITY Rocket Propulsion Laboratory Air Force Systems Command Edwards, California

13 ABSTRACT CONFIDENTIAL ABSTRACT - The determination of c* performance of the air-augmented hydrazine/pentaborane system was conducted in a permanent micromotor test facility. The newly-constructed facility employs electrically-heated, clean secondary air and includes equipment for collection of solid and gaseous secondary exhaust products. The c* performance of the air-augmentation stage was determined in two flight simulation regimes. In the sea level/Mach 2.5 regime (200 psia chamber pressure/800°F air-temperature), the c* performance efficiencies were 96-99% of theoretical at air-to-propellant ratios of 8:1, 16:1, and 50:1. Chemical analysis indicated complete combustion of all primary exhaust products, including boron nitride and elemental boron. In the 40,000 ft/Mach 4.0 regime (50 psia chamber pressure/1500°F air-temperature), the c* performance was 91-92% of theoretical at air-to-propellant ratios of 8:1 and 16:1. Chemical analysis indicated high boron nitride combustion efficiency but very low elemental boron combustion efficiency. Low chamber pressure and low residence time (L*) were concluded to be major contributing factors to the low elemental boron combustion efficiency and reduced c* performance efficiency. A high water concentration in the secondary chamber, resulting from secondary hydrogen combustion, appears to contribute significantly to the high combustion efficiency of the boron and boron nitride. In addition, chamber pressures in excess of 50-75 psia appear to be required to ensure efficient elemental boron combustion. A model describing the secondary combustion process has been developed. The model reflects the importance of water vapor and high chamber pressure in promoting high combustion efficiency and high performance efficiency of boron-containing propellants.

DD FORM 1 JAN 64 1473

CONFIDENTIAL

Security Classification

14. KEY WORDS	LINK A		LINK B		LINK C	
	ROLE	WT	ROLE	WT	ROLE	WT
- Air Augmentation - Boron - Boron Nitride - Characteristic Exhaust Velocity - Combustion Characteristics - Combustion Model - Exhaust Sampling - Micromotor - Pentaborane/Hydrazine - Secondary Combustion - Temperature Profiles						

INSTRUCTIONS

1. **ORIGINATING ACTIVITY:** Enter the name and address of the contractor, subcontractor, grantee, Department of Defense activity or other organization *(corporate author)* issuing the report.

2*a*. **REPORT SECURITY CLASSIFICATION:** Enter the overall security classification of the report. Indicate whether "Restricted Data" is included. Marking is to be in accordance with appropriate security regulations.

2*b*. **GROUP:** Automatic downgrading is specified in DoD Directive 5200.10 and Armed Forces Industrial Manual. Enter the group number. Also, when applicable, show that optional markings have been used for Group 3 and Group 4 as authorized.

3. **REPORT TITLE:** Enter the complete report title in all capital letters. Titles in all cases should be unclassified. If a meaningful title cannot be selected without classification, show title classification in all capitals in parenthesis immediately following the title.

4. **DESCRIPTIVE NOTES:** If appropriate, enter the type of report, e.g., interim, progress, summary, annual, or final. Give the inclusive dates when a specific reporting period is covered.

5. **AUTHOR(S):** Enter the name(s) of author(s) as shown on or in the report. Enter last name, first name, middle initial. If military, show rank and branch of service. The name of the principal author is an absolute minimum requirement.

6. **REPORT DATE:** Enter the date of the report as day, month, year; or month, year. If more than one date appears on the report, use date of publication.

7*a*. **TOTAL NUMBER OF PAGES:** The total page count should follow normal pagination procedures, i.e., enter the number of pages containing information.

7*b*. **NUMBER OF REFERENCES:** Enter the total number of references cited in the report.

8*a*. **CONTRACT OR GRANT NUMBER:** If appropriate, enter the applicable number of the contract or grant under which the report was written.

8*b*, &*c*, & 8*d*. **PROJECT NUMBER:** Enter the appropriate military department identification, such as project number, subproject number, system numbers, task number, etc.

9*a*. **ORIGINATOR'S REPORT NUMBER(S):** Enter the official report number by which the document will be identified and controlled by the originating activity. This number must be unique to this report.

9*b*. **OTHER REPORT NUMBER(S):** If the report has been assigned any other report numbers *(either by the originator or by the sponsor)*, also enter this number(s).

10. **AVAILABILITY/LIMITATION NOTICES:** Enter any limitations on further dissemination of the report, other than those imposed by security classification, using standard statements such as:

(1) "Qualified requesters may obtain copies of this report from DDC."

(2) "Foreign announcement and dissemination of this report by DDC is not authorized."

(3) "U. S. Government agencies may obtain copies of this report directly from DDC. Other qualified DDC users shall request through _____."

(4) "U. S. military agencies may obtain copies of this report directly from DDC. Other qualified users shall request through _____."

(5) "All distribution of this report is controlled. Qualified DDC users shall request through _____."

If the report has been furnished to the Office of Technical Services, Department of Commerce, for sale to the public, indicate this fact and enter the price, if known.

11. **SUPPLEMENTARY NOTES:** Use for additional explanatory notes.

12. **SPONSORING MILITARY ACTIVITY:** Enter the name of the departmental project office or laboratory sponsoring *(paying for)* the research and development. Include address.

13 **ABSTRACT:** Enter an abstract giving a brief and factual summary of the document indicative of the report, even though it may also appear elsewhere in the body of the technical report. If additional space is required, a continuation sheet shall be attached.

It is highly desirable that the abstract of classified reports be unclassified. Each paragraph of the abstract shall end with an indication of the military security classification of the information in the paragraph, represented as *(TS)*, *(S)*, *(C)* or *(U)*

There is no limitation on the length of the abstract. However, the suggested length is from 150 to 225 words.

14. **KEY WORDS:** Key words are technically meaningful terms or short phrases that characterize a report and may be used as index entries for cataloging the report. Key words must be selected so that no security classification is required. Identifiers, such as equipment model designation, trade name, military project code name, geographic location, may be used as key words but will be followed by an indication of technical context. The assignment of links, rules, and weights is optional